Martin Maximilian Schütz

The role of NIMA-like kinase Nek9 in mitosis

TESI DOCTORAL UPF – 2011

Thesis supervisor: Dr Isabelle Vernos

Cell and Developmental Biology Program

Microtubule Dynamics Unit

CRG (Centre for Genomic Regulation)

Für meine Eltern und meine Brüder

Dank Euch fühle ich dass ich alles erreichen kann!

Summary

The role of NIMA-like kinase Nek9 in mitosis

Mitosis is the essential process during which a cell divides into two viable daughter cells. To allow a faithful segregation of the chromosomes into each daughter, the cell forms the bipolar spindle. The bipolar spindle is a macromolecular structure based on microtubules that connect the chromosomes to each spindle pole. Spindle assembly requires highly dynamic microtubules emanating from the centrosomes and from the chromatin. The regulation of microtubule dynamics and organisation involves hundreds of proteins including motor proteins that contribute to the assembly of the bipolar spindle and to generate the forces that are essential for chromosome segregation.

The NIMA-like kinase family member Nek9 has been previously proposed to play a role in bipolar spindle assembly and in the chromosomal pathway of microtubule assembly. We aimed at gaining a better understanding of Nek9 function by characterizing *Xenopus* Nek9, xNek9, using the *Xenopus* egg extract system.

We have shown that xNek9 may not act through the kinase cascade xNek9 – xNek6 in meiosis as described for human Nek9 in somatic cells and therefore may have different substrates. Furthermore, we have demonstrated by depletion, increased addition of Flag-hNek9 and a dominant-negative approach that xNek9 is important for bipolar spindle formation. In addition, we have shown that xNek9 depletion causes decreased microtubule density in bipolar spindles and slower RanGTP induced aster formation. We identified xNedd1, the adaptor protein for the γTuRC, as a novel interactor and substrate of xNek9. xNek9 depletion

reduces the recruitment of xNedd1 to sperm nuclei induced aster and decreases the number and length of nucleated microtubules. These data suggest that one role of xNek9 in spindle assembly is exerted through xNedd1 regulation. We propose a model for xNek9 – xNedd1 interaction and a putative mechanism for the regulation of xNek9 – xNedd1 explaining how they fulfil their role in bipolar spindle assembly.

Resumen

El papel de la quinasa NIMA-like kinase Nek9 en la mitosis

La mitosis es el proceso esencial durante el cual una célula se divide en dos células hijas viables. Para permitir una segregación fiable de los cromosomas en cada hija, la célula forma el huso bipolar. El huso bipolar es una estructura macromolecular basada sobre los microtúbulos que unen los cromosomas a cada polo del huso. La formación del huso requiere microtúbulos muy dinámicos que emanan de los centrosomas y de la cromatina. La regulación de la dinámica de los microtúbulos y la organización implica a cientos de proteínas como proteínas motoras que contribuyen a la asamblea del huso bipolar y al generar de las fuerzas que son esenciales para la segregación de los cromosomas.

Nek9, el miembro de la familia de quinasas NIMA-like ha sido propuesto para desempeñar un papel en el la asamblea del huso bipolar y en la vía cromosómica de ensamblaje de los microtúbulos. Nuestro objetivo era lograr una mejor comprensión de la función Nek9 caracterizando Nek9 de *Xenopus*, xNek9, utilizando el sistema de extracto de huevos de *Xenopus*.

Hemos demostrado que xNek9 probablemente no actuará a través de la cascada de las quinasas xNek9 - xNek6 en la meiosis como se describe para Nek9 humano en células somáticas y por lo tanto pueden tener diferentes sustratos. Además, hemos demostrado por el agotamiento, la adición incrementada de Flag-hNek9 y un enfoque dominante-negativas que xNek9 es importante para la formación del huso bipolar. Además, hemos demostrado que el agotamiento xNek9 causa una disminución de la densidad de los microtúbulos en los husos bipolares y una formación más lenta de asteres inducidos por RanGTP. Se identificó xNedd1, la proteína adaptadora para el γTuRC, como un interactor y sustrato novedoso de xNek9. El agotamiento de xNek9 reduce la contratación de xNedd1 a los asteres inducidas por núcleos de espermatozoides y disminuye el número y longitud de microtúbulos nucleados. Estos datos sugieren que un papel de xNek9 en el conjunto del huso se husorce a través de la regulación de xNedd1. Proponemos un modelo para la interacción xNek9 – xNedd1 y un supuesto mecanismo para la regulación de xNek9 – xNedd1 explicando cómo cumplen su papel en la asamblea del huso bipolar.

Preface

The work presented in this thesis was carried out in the Cell and Developmental Biology Program at the Centre for Genomic Regulation (CRG) and was supervised by Dr Isabelle Vernos (ICREA, CRG).

The presented work provides novel insight and a putative mechanism of the contribution of a mitotically active kinase in bipolar spindle assembly

Abbreviations

aa	amino acid
ATP	Adenosine triphosphate
AurA	Aurora A
ºC	Celsius grade
Cdk	Cyclin dependent kinase
CSF	cytostatic factor
C-terminal	carboxy-end of protein
Ct	carboxy-end of protein
Da	Dalton
DNA	deoxyribonucleic acid
DTT	dithiothreitol
EDTA	ethylenediaminetetraacetic acid
EE	CSF-arrested egg extract
EGTA tetraacetic acid	ethylene glycol-bis(b-aminoethyl ether) N,N,N',N'
FCS	Fetal Calf Serum
Fh9	Flag-hNek9
GCP	Gamma-Tubulin Complex Protein
γTuRC	Gamma-Tubulin Ring Complex
γTuSC	Gamma-Tubulin Small Complex
GDP	green fluorescent protein
GEF	GTP exchange factor
GST	glutathione-S-transferase

GTP	guanosine triphosphate
HCG	human chorionic gonadotropin
HEPES	N-(2-hydoxyethyl) pipierizine-N'-(2-ethano
hNek9	human Nek9
Human	*Homo sapiens*
ID	Immunodepletion
IF	Immunofluorescence
IgG	Immunoglobulin G
IP	Immunoprecipitation
IPTG	isopropyl b-D-thiogalactopyranoside
KD	Kinase domain
kDa	kilo Dalton
LB	Luria Browth
M	Molar
MAP	Microtubule associated protein
MBP	Maltose binding protein
MPF	Mitosis Promoting Factor
mg	milligram
min	minute
ml	millilitre
mM	millimolar
µg	microgram
µl	microliter
MTOC	Microtubule organising centre
NIMA	Never In Mitosis A

NLS	Nuclear localisation signal
nM	nanomolar
nm	nanometer
N-terminus	Amino-terminal end of protein
Nt	Amino-terminal end of protein
PCM	Pericentriolar material
PCR	Polymerase Chain reaction
PBS	Phosphate Buffered Saline
PIPES	Piperazine-N,N'-bis(2-ethanesulfonic acid)
PMSG	Pregnant mare serum gonadotropin
RanGAP	RanGTPase activating protein
RCC1	Regulator of Chromosome Condensation
RNA	Ribonucleic acid
RNAi	RNA interference
rpm	rotations per minute
SDS	Sodium dodecyl sulphate
SDS-PAGE	SDS-polyacrylamide gel electrophoresis
sec	second
Tris	Tris (Hydroxymethyl) aminomethane
Xenopus	*Xenopus laevis*
V	Voltage
WB	Western blotting
xNek9	*Xenopus* Nek9

Table of Contents

Introduction

I. Introduction

1. The cell and its cytoskeleton

It was in 1665 that Robert Hooke first found structures in cork which 174 years later in 1839 were proposed by Schwann to be the elementary structural and functional unit of every living organism. Since then we have acquired great knowledge about the organisation of a typical eukaryotic cell. Within the cell membrane, organelles and the cytoskeleton cooperate in all cellular processes to finally enable the cell to self reproduce by cell division.

The cytoskeleton is a network of different types of filaments that defines the shape and also the motility of a given cell type. Each of the filament types may differ in function and localisation. There are three types of filaments. Intermediate filaments are for example made of keratin, desmin or vimentin proteins and serve mostly for cell stability. They form protein strings which then build triple helices through disulfide bonds and thereby a strong filament. Actin filaments consist of two actin strings that form a helix similar to the intermediate filaments. Their function is vast throughout the cell and is implicated in many processes such as cell motility and stability, muscle contraction, and also in cytokinesis. Microtubules, similar to actin, have a broad range of functions. They are implicated among others in organelle positioning, intracellular transport and cell polarity. In mitosis they have a major role by building up a bipolar spindle to segregate the chromosomes.

1.1. Microtubules

Microtubules are hollow tubes with a diameter of around 25nm. They consist of α-β-Tubulin heterodimers that pile up to form protofilaments

with alternating αTubulin and βTubulin. Generally it is thought that 13 laterally associated protofilaments form a fully closed microtubule, however in vivo and in vitro studies have also shown divergent microtubule lattices reaching from 12-15 protofilaments. (Amos and Schlieper, 2005; Janosi et al., 2002)

αTubulin and βTubulin can both bind GTP. The microtubule lattice forms due to incorporation of new α-β-Tubulin dimers bound to GTP which is hydrolysed shortly after incorporation. GTP hydrolysis happens only at the βTubulin subunit (Desai and Mitchison, 1997). This hydrolysis to GDP - α-β-Tubulin induces a curvature in the protein complex and therefore in the protofilament. As a consequence, the microtubule lattice remains stable but under tension. At the moment of microtubule disassembly, protofilaments peel back rapidly from the lattice due to the tension previously induced by hydrolysis of GTP bound α-β-Tubulin (Chretien et al., 1995; Janosi et al., 2002).

Microtubules undergo constant polymerisation and depolymerisation. This cycle of growth and shrinkage of the microtubule is called “dynamic instability” (Mitchison and Kirschner, 1984). Thereby the microtubule undergoes “catastrophe” when changing from growth to shrinkage or “rescue” when changing from shrinkage to growth (Figure 1).

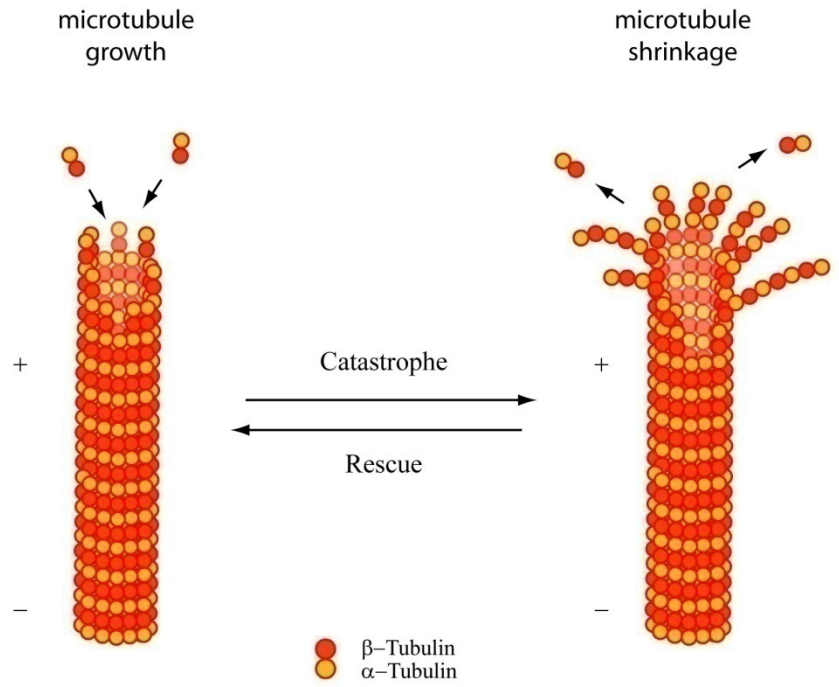

Figure 1: Dynamic instability of microtubules
Microtubules are intrinsically unstable due to tension within the microtubule lattice. When a microtubule undergoes a catastrophe event, the intrinsic tension within the microtubule lattice helps protofilaments to peel back rapidly and the microtubule shrinks. The microtubule undergoes rescue when changing from shrinkage to growth. Then, tubulin dimers become incorporated at the growing "+" end.

Growth, or α-β-Tubulin dimer incorporation occurs by "head-to-tail" binding. Thereby, the αTubulin subunit of one dimer interacts with the βTubulin subunit of the last dimer. As a consequence, microtubules exhibit a polarity with a minus end and a plus end. The rate of association is bigger at the plus end, whereas the rate of dissociation is bigger at minus end. Association and dissociation rates can be equal so that a steady state of kinetics establishes. Tubulin dimers then flux from the proximal end to the distal end without changing the overall length of the

microtubule. This process has been named “treadmilling” (Margolis and Wilson, 1978).

At the entry into mitosis microtubule dynamics increases strongly. Besides the intrinsic dynamic instability of the microtubule, microtubule associated proteins and motors influence the stabilization or destabilization of microtubules. Stabilizing proteins such as the families of end-binding proteins (EB) or Clip-associated proteins (Clasp) stabilize microtubules by accumulating at the plus end and favouring the entry of tubulin dimers (Akhmanova and Steinmetz, 2008). Destabilizing proteins such as the motor protein XKCM1/MCAK use their activity rather to remove tubulin dimers at microtubule ends than to walk along the microtubule (Walczak et al., 1996). Op18/Stathmin increases microtubule catastrophe events by sequestering tubulin dimers (Maiato et al., 2004).

In cells, growth of microtubules is not randomly distributed throughout the cell but arises usually from a specific location, the microtubule organising centre (MTOC). In most eukaryotes, the major MTOC is the centrosome.

1.2. Centrosomes

The centrosome, named by Theodor Boveri in 1888 for its central localisation close to the nucleus, is the main microtubule nucleation point of the cell. From there microtubules nucleate in a radial pattern with their minus end located at the centrosome and the plus end pointing towards the cytoplasm.

1.2.1. Centrioles and pericentriolar material

The focal point of centrosomal microtubule nucleation is achieved by anchoring the minus ends in a fibrous matrix called the pericentriolar material (PCM). This electron-dense cloud consists of over a hundred proteins including high molecular weight proteins that function as binding platform for microtubule nucleation (Andersen et al., 2003; Delgehyr et al., 2005; Zhu et al., 2008). The pericentriolar material is organised by two barrel-like shaped structures, the centrioles. They lie within the proteineous matrix of the pericentriolar material and are connected with each other through centriole associated filaments. The centrioles are cylinders with around 0,2µm radius and around 0,5µm length and are made of microtubule triplets organised in a nine-fold symmetrical configuration (Bornens, 2002; Paintrand et al., 1992). Both centrioles differ from each other by age and to some extent by protein composition. The older centriole, also called mother centriole, exposes sub-distal and distal appendages whereas the younger centriole, also called daughter centriole, remains immature without appendages. Those appendages enable the mother centriole to concentrate platform proteins and therefore anchor microtubules similar to the PCM (Piel et al., 2000). In fact, centrioles are organising the PCM, shown by a dispersal of the PCM after centriole loss (Basto et al., 2006; Bobinnec et al., 1998). Both, centriole and PCM enable the docking of γTubulin, the key protein for microtubule nucleation.

1.2.2. γTubulin Ring Complex

Within the cell, γTubulin is found in a specific complex: the γTubulin Small Complex (γTuSC). Several γTuSC form a ring shaped structure, the γTubulin Ring Complex (γTuRC). The γTubulin Ring Complex (γTuRC)

was first purified in 1995 from *Xenopus* CSF – arrested egg extract. Electron microscopy pictures suggested that it may form an open ring structure with a diameter close to the one of a microtubule. Furthermore it was found to nucleate microtubules in vitro and to bind to one microtubule end (Zheng et al., 1995). Therefore it was proposed that the γTuRC may act as a microtubule minus end capping structure (Wiese and Zheng, 2000). Further analysis of the complex revealed that the ring complex consists of around 13 γTubulin molecules and at least six additional proteins, the Gamma-Tubulin Complex Proteins (GCP) (Zheng et al., 1995). Growing evidence however suggests that the core complex may consist of additional proteins (Hutchins et al., 2010; Teixido-Travesa et al., 2010). Two models are currently discussed to explain how the γTuRC may trigger microtubule nucleation. The "protofilament model" proposes γTubulin to act as a starting protofilament where α-β-Tubulin dimers can attach laterally. Together they form a sheet that finally closes to form the hollow tube of the microtubule (Erickson, 2000; Erickson and Stoffler, 1996). The currently more accepted model is the "template model" with the γTubulin ring serving as a template where each γTubulin contacts one α-β-Tubulin dimer that bind longitudinally (Figure 2) (Keating and Borisy, 2000; Kollman et al., 2010; Moritz and Agard, 2001; Moritz et al., 2000; Zheng et al., 1995). Microtubule nucleation is necessary throughout the lifecycle of a cell and essential when the cell undergoes cell division.

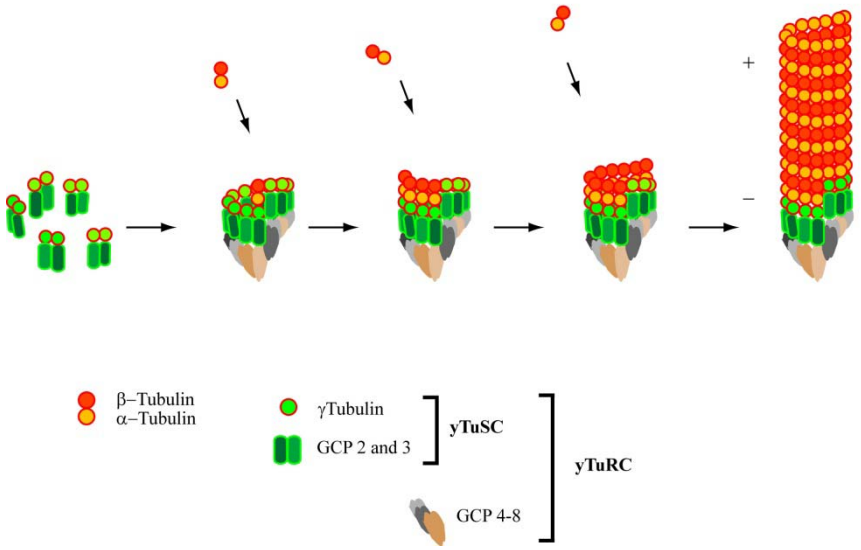

Figure 2: The "template model" of microtubule nucleation
γTubulin, the key protein for microtubule nucleation, and Gamma-Tubulin Complex Proteins (GCP) 2 and 3 form the γTubulin Small Complex (γTuSC). Several γTuSC in addition to further GCP proteins form the γTubulin Ring Complex (γTuRC). The γTuRC serves as "template" for α-β-Tubulin dimers that associate longitudinally with γTubulin. The incorporation of new tubulin dimers establishes the polarity of the nascent microtubule with the γTuRC capping the microtubule minus end.

2. The cell cycle

Every cell undergoes a sequence of events with the objective to reproduce. This sequence of events is called the cell cycle and implicates the duplication of its content prior to division. These events happen in the four different phases of the cell cycle being M, G1, S and G2 phase (Figure 3). During M-phase, the cell divides its DNA (mitosis) and cytoplasm (cytokinesis) and forms two daughter cells. In the following, recently divided cells grow in size and mass (G1), duplicate DNA and centrosomes (S) and prepare for the next cell division (G2). G1, S and G2

phases are also named Interphase. Depending on the environment the cell can exit the cell cycle and enter G0 phase. There, the cell stops cell division but maintains its function until it dies or returns into the cell cycle.

The entry and the exit from each phase to the next are tightly controlled. The family of cyclin dependent kinases (Cdk) plays a major role in the control of cell cycle progression. The binding of Cdks with its regulatory subunits, the cyclins, activates the kinases which then phosphorylate their substrates and allow further progression of the cell cycle. Whereas Cdk levels are relatively constant throughout the cell cycle, cyclins undergo specific expression or degradation at each cell cycle state. Therefore they can act as cell cycle switches (Figure 3). One of the best known complexes is cyclin B – Cyclin dependent kinase 1 (Cdk1), also called Mitosis promoting factor (MPF) that upon activation, triggers the entry into M phase (Doree and Galas, 1994; Murray et al., 1989). The degradation of cyclin B by the proteasome upon targeting by the APC (Anaphase-promoting complex) is the signal for mitotic exit. To avoid mistakes during cell division so-called checkpoints function as error sensors throughout the cell cycle. Thus, for instance the mitotic checkpoint allows cyclin B degradation, and therefore mitotic exit, only after each kinetochore is properly attached to microtubules to ensure faithful chromosome segregation.

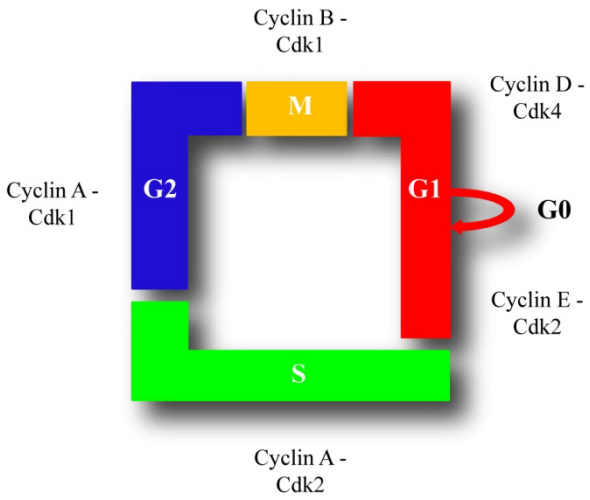

Figure 3: The cell cycle
The cell cycle consists of two main parts. ***M-phase***: the cell divides its genetic material (mitosis) and cytoplasm (cytokinesis) into two daughter cells. ***Interphase***: the daughter cells grow in size and mass (G1), replicate the DNA and duplicate the centrosomes (S), and prepare for the next cell division (G2). Cells can exit the cell cycle into a resting phase (G0). Each phase is controlled by specific biochemical switches, the Cyclin-dependent kinases (Cdk) and their regulators, the cyclins.

3. M – phase

M-phase is the cell cycle process during which a cell divides into two identical daughter cells by equally distributing the previously duplicated genetic information (mitosis) and the cytoplasm (cytokinesis).

To segregate chromosomes into the two daughter cells, cells engineer a macromolecular machinery, the mitotic spindle. The spindle consists of microtubules that connect two opposite poles with the condensed chromosomes to form a symmetric and fusiform structure (Compton,

2000). Hundreds of proteins are involved in the formation of the bipolar spindle and its maintenance until chromosomes are segregated.

During mitosis the cell passes through distinct steps, called prophase, prometaphase, metaphase, anaphase and telophase before finally entering cytokinesis.

During prophase, the replicated DNA molecules start to condense and to form chromosomes, each consisting of two sister chromatids that are still connected at the centromeres. Meanwhile, the duplicated centrosomes already move along the nuclear envelope due to pushing forces generated by microtubule associated motors on centrosomal nucleated microtubules. Thus, the centrosomes approach opposite sides of the nucleus where they will form the mitotic spindle poles.

Prometaphase starts when the nuclear envelope breaks down. Thus, pole microtubules are able to reach the condensed chromosomes and to bind to specific structures assembled at the centromeres, the kinetochores. Each kinetochore fibre consists of around 20-40 microtubules to ensure a strong connection between spindle poles and kinetochores (Walczak and Heald, 2008). Once connected to both poles, the bioriented chromosomes oscillate and finally congress to the centre of the spindle.

There, a balance of pulling and pushing forces lead to the alignment of all chromosomes and therefore the formation of the metaphase plate, characteristic for metaphase.

Once aligned and with each chromosome properly connected to the poles, the spindle assembly checkpoint is satisfied. This is the signal for degradation of Cyclin B – Cdk1, the mitosis promoting factor and the onset of anaphase.

Anaphase starts with the loss of chromatid cohesion, kinetochore microtubules shorten and each chromatid segregates towards its respective spindle pole (Anaphase A). The distance between both chromatid groups grows by elongation of the spindle itself (Anaphase B).

During telophase, the chromatids reach the pole and the kinetochore microtubules disassemble. The nuclear envelope rebuilds and surrounds the decondensing chromosomes.

Cytokinesis occurs by the formation of a contractile ring of actin filaments perpendicular to the spindle. By contracting, a furrow forms and the ring constricts the space in between by converging the plasma membrane. Finally the plasma membrane fuses, the cytoplasm is divided and two identical daughter cells form.

4. Spindle assembly

At the onset of mitosis the cell undergoes crucial changes at the molecular level. Microtubules totally change their dynamic behaviour. The relatively long and stable interphase microtubules become shorter and highly unstable. Their half-life decreases from around 10 minutes to around 60 seconds (Compton, 2000). Also the number of microtubules that are nucleated from the centrosome highly increases based on the maturation of the centrosome. Thereby, microtubule nucleation factors concentrate at the centrosome allowing microtubule nucleation towards the kinetochores to form kinetochore fibers, towards the distant pole to form interpolar microtubules and towards the cell cortex to form astral microtubules (Figure 4) (Walczak and Heald, 2008). These three types of microtubules as well as microtubule stabilizing and destabilizing proteins and many

different motors contribute to bipolar spindle assembly. There are two models that were proposed to explain this complex process.

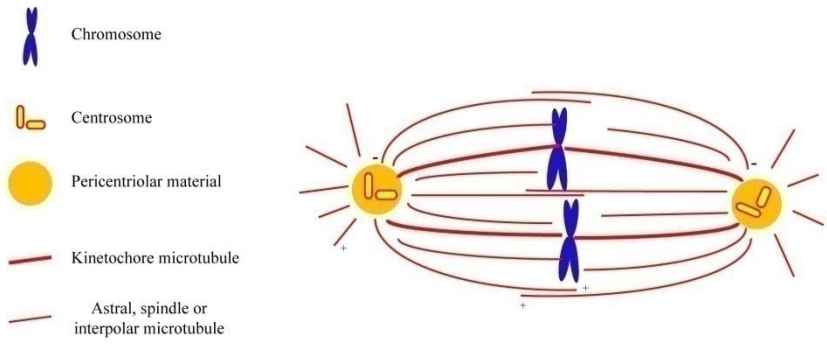

Figure 4: Model for a bipolar spindle
Key components of a bipolar spindle in metaphase are shown. Chromosomes are aligned in the metaphase plate and two centrosomes form the poles. The centrosomes are surrounded by an electron-dense matrix, the pericentriolar material which concentrates spindle assembly factors. The main body of the bipolar spindle consists of microtubules, composed of antiparallel spindle microtubules, microtubule bundles connected to the kinetochores (K-fibres), and astral microtubules that emanate away from the spindle. Microtubules have an intrinsic polarity, with the minus ends anchored at the poles and the plus ends pointing outwards.

4.1. "Search and capture" model

Kirschner and Mitchison proposed the "search and capture" model in 1986. The model is based on the behavioural change of centrosomes and microtubules in mitosis. Mitotic centrosomes increase in size by recruiting centrosomal proteins such as Ninein or Cep152 (Casenghi et al., 2003; Dzhindzhev et al., 2010). Subsequently, microtubule nucleation factors such as γTubulin and the γTuRC attach and allow increased nucleation of microtubules. At the same time microtubule dynamics change. Increased rescue and catastrophe events result in short and unstable microtubules

(Compton, 2000). These dynamic microtubules search the space, grow and shrink in all directions pointing with their plus ends towards the cytoplasm until they find a kinetochore. When microtubules capture kinetochores, local stabilisation of the microtubule occurs and they form a strong kinetochore fibre together with additional microtubules. Thus, a bipolar spindle assembles due to the presence of two centrosomes and two sister kinetochores, one on each side of the chromosomes.

4.2. "Self – assembly" model

The "search and capture" model however could not define, how a random "search and capture" of microtubules accounts for a timely process like spindle assembly (Wollman et al., 2005). In addition, it lacked the explanation how a spindle forms in systems where centrosomes are absent such as in higher plants or in the female meiosis of some vertebrates. First hints for the "self – assembly model" appeared in 1984 based on the observation that chromatin can generate a favourable environment for microtubule nucleation and that spindle formation is not dependent on centrosomes. Karyoplasts which are nuclei surrounded by a plasma membrane and therefore free of centrosomes, or plasmid DNA injected into *Xenopus* eggs formed spindle like structures (Karsenti et al., 1984). Furthermore, DNA-coated beads nucleated microtubules that eventually organised into a bipolar array, strongly resembling bipolar spindles (Heald et al., 1996). Further proof for centrosome independent spindle assembly came from vertebrate cells that segregated chromosomes correctly although centrosomes were previously laser ablated (Khodjakov et al., 2000). Moreover, it was shown that "centrosome-free" mutant flies are viable (Basto et al., 2006).

Up to now, various proteins have been identified that play a role in the process of spindle self-assembly. One basic component is the small GTPase Ran.

The GTPase Ran exists in two forms: GDP or GTP bound. Its binding state is regulated by RanGTPase activating protein 1 (RanGAP) which induces GTP hydrolysis and by its guanine exchange factor (GEF) RCC1. Ran was previously known as a regulator of nucleocytoplasmic transport during interphase. There, cells take advantage of the compartmentalisation of the cell into cytoplasm and nucleus. RCC1 localises in the nucleus and RanGAP1 in the cytoplasm.

During interphase, proteins targeted to the nucleus contain nuclear localisation signals (NLS) and can therefore bind to importin α – importin β protein complexes as a "cargo". The ternary complexes enter into the nucleus through nuclear pores where RanGTP induces the dissociation of the complex due to the high affinity of RanGTP for importin β. Subsequently, the newly formed importin – RanGTP complex forms a new ternary complex with proteins exhibiting a nuclear export signal (NES) and trespass again the nuclear envelope into the cytoplasm. There, RanGAP1 activates the GTPase activity of Ran for GTP hydrolysis, causing the dissociation of Ran from Importin β and the release of the cargo (Figure 5).

During mitosis, RanGTP acts similar, even though the compartmentalisation in nucleus and cytoplasm is lost due to nuclear envelope breakdown. RanGTP enriches in close vicinity to the chromosomes due to the chromatin association of its GEF RCC1. In the cytoplasm further away from the chromatin the presence of RanGAP1 stimulates GTP hydrolysis lowering the concentration of RanGTP.

Thereby, a gradient is generated with a high concentration of active RanGTP close to the chromosomes with decreasing concentrations away in the cytoplasm. The high RanGTP concentration induces the release of cargo proteins bound by importins. Some of the importin bound cargo proteins are spindle assembly factors and proteins that favour microtubule nucleation. Therefore an environment forms that enables the assembly of microtubules (Figure 5).

This intriguing model is based on several observations that have been made over time. For instance, Kalab et al showed that the role of Ran in spindle assembly is independent of nucleocytoplasmic transport (Kalab et al., 1999). Microtubule asters assembled after addition of RanGTP mimicking mutants to the egg extract (Zhang et al., 1999) Remarkably, both in *Xenopus* egg extract and in HeLa cells the existence of the RanGTP gradient has been visualized using FRET microscopy (Caudron et al., 2005; Kalab et al., 2006; Kalab et al., 2002).

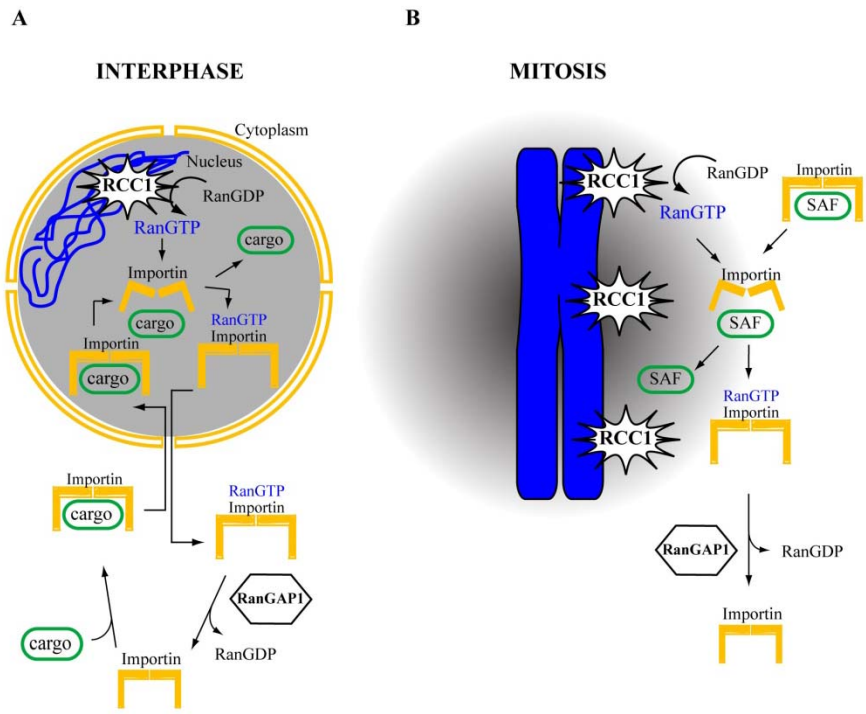

Figure 5: Function of the GTPase Ran in interphase and mitosis
(A) ***Nucleocytoplasmic transport***: During interphase, Ran remains in the nucleus in a GTP associated form due to chromatin bound RCC1, the GTP-exchange factor (GEF) and in the cytoplasm bound to GDP due to the Ran-GTPase-activating enzyme 1 (RanGAP1). The importin complex (importin α and importin β) sequesters NLS-containing proteins in the cytoplasm as cargo and passes the nuclear envelope. There, RanGTP releases the cargo protein due to its higher affinity to the importin complex. **(B)** ***RanGTP gradient***: In mitosis, chromatin bound RCC1 creates a high RanGTP concentration close to the chromosomes that decreases with increasing distance due to RanGAP1 activity. The high concentration of RanGTP around the chromosomes dissociates spindle assembly factors (SAF) from the importin complex and therefore favours microtubule nucleation and stabilization around the chromosomes.

4.3. The current model: an integrated model of spindle assembly

Currently, a combination of both models "search and capture" and "self-assembly" is widely accepted (Figure 6). Centrosomal microtubules grow

and shrink to eventually interact with microtubules derived from the chromosomes. Their interaction gets stabilised and the chromosomal microtubules are guided along the centrosomal microtubules towards the pole. Similarly, chromosomal microtubules that grow directly from the kinetochore are captured and their distal ends then transported poleward along the astral microtubules by dynein motors (Rusan et al., 2002; Tulu et al., 2006). The combination of both models allows a timely bipolar spindle formation. It is noteworthy that the integrated model cannot account for bipolar spindle assembly in all systems and that one or the other pathway may contribute stronger. Therefore, when present, centrosomes serve as "attraction point" for the recruitment of spindle components and microtubules and thus foment bipolar spindle formation (O'Connell and Khodjakov, 2007). Recently, further mechanisms have been proposed that may contribute to bipolar spindle assembly. The "cut and run" mechanism implicates severing proteins such as katanin, that cut centrosomal microtubules which then move along existing spindle microtubules by dynein and integrate into the bipolar spindle and amplify the number of microtubules (Baas et al., 2005; Keating et al., 1997). Similarly, the recently discovered augmin complex reinforces the spindle by microtubule based microtubule nucleation (Goshima et al., 2008).

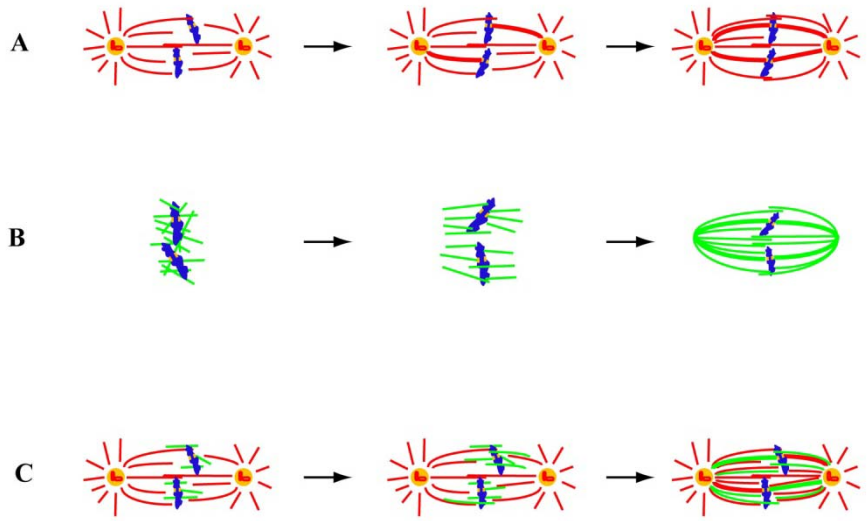

Figure 6: From the early models to the current integrated model of bipolar spindle assembly

(A) "Search and Capture" model: microtubules from the centrosomes grow and shrink while searching the space. Eventually they encounter the chromatin and kinetochores and are stabilised to form the spindle. **(B)** "Self-assembly": microtubules nucleate from the vicinity of the chromosomes. Motor proteins organise the microtubules that are eventually focussed to form two poles in absence of centrosomes. **(C)** "Integrated Model": microtubules are nucleated from the centrosome and from the chromatin. Microtubules get captured, integrated in the centrosomal pathway and guided towards the centrosome. Together all microtubules form the bipolar spindle. Red, centrosomal microtubules; green, chromosomal microtubules; yellow, centrosomes; blue, DNA. Figure modified from Gadde et al. 2004 (Gadde and Heald, 2004)

5. NIMA

Spindle assembly is highly regulated by kinases such as Aurora or Polo-like kinase families. Another family of kinases which is recently emerging as an important family for spindle assembly is the NIMA-like kinase family.

Genetic screens for cell cycle mutants performed by Ron Morris in 1975 in the multicellular filamentous fungus *Aspergillus nidulans*, revealed

several candidates that never entered in mitosis but were blocked in interphase (Morris, 1975). "**N**ever **i**n **m**itosis" mutant **A**, therefore NIMA, arrested late in G2 with duplicated spindle pole bodies, the fungal equivalent of the centrosome (Oakley and Morris, 1983). This arrest could be bypassed with a second mutation allowing the entry into mitosis, but resulted in an aberrant mitotic state characterized by abnormalities of the nuclear envelope and a failure to form a bipolar spindle (Osmani et al., 1991). NIMA protein itself is nuclear during mitosis and associated with the chromosomes, spindle and spindle pole bodies (De Souza et al., 2000). Moreover, NIMA overexpression causes condensed chromosomes and aberrant spindles (Osmani et al., 1988).

fin1 is the NIMA ortholog in fission yeast and shares many characteristics with Aspergillus NIMA. It encodes for a kinase whose protein level fluctuates during the cell cycle with a peak in mitosis. Overexpression of fin1 promotes premature chromatin condensation at any point of the cell cycle independent of Cdc2 function. Fin1 protein localises to the spindle pole body in late G2 and remains there throughout mitosis. In addition, fin1 deleted cells are hypersensitive to anti-microtubule drugs and show unusual and extensive elaborations of the nuclear envelope (Krien, Bugg et al. 1998; Krien, West et al. 2002).

6. NIMA – like kinases

In mammals, 11 different NIMA-like kinases, the Nek kinases, have been identified based on sequence identity within the N-terminal kinase domains. None of these kinases unifies all functions of the founder kinase NIMA but those seem rather distributed among the different Nek kinases.

The diversity of function was related to their highly divergent C-terminal non-catalytic regions (Figure 7) (O'Connell et al., 2003).

Nek kinases were found to be involved in cilia formation and to be essential for proper expression of cilia proteins and therefore cilia functioning (Nek1 and Nek8). Impairment of kinase function was related to cilia dependent diseases such as polycystic kidney disease (Otto et al., 2008; Shalom et al., 2008; Sohara et al., 2008; White and Quarmby, 2008).

Furthermore, Nek kinases were also found part of signalling cascades at the G2 / M transition (Nek1, Nek10, Nek11). They were reported to participate in ERK and MEK1 signalling, and also upstream and downstream of the DNA damage checkpoint kinases Chk1 and Chk2 (Chen et al., 2011; Melixetian et al., 2009; Moniz and Stambolic, 2011; Sorensen et al., 2010). Therefore, Nek kinases may have a very important role in proper cell cycle progression.

In addition, Nek kinases were shown to be implicated in cytoskeleton organisation (Nek3 and Nek4). Impairing Nek kinases, the cytoskeleton reorganised within the cell and induced changes in cell morphology, polarity and sensitivity against microtubule drugs (Chang et al., 2009; Doles and Hemann, 2010; Miller et al., 2007).

Nek2 is well studied for its role in centrosome disjunction at the onset of mitosis. By phosphorylation, Nek2 induces the disassembly of the molecular linker C-Nap1 and Rootletin at the proximal end of duplicated centrosomes and enables them to separate at mitotic entry (Faragher and Fry, 2003; Mardin et al., 2010). Nek2 has recently also been implicated in kinetochore – microtubule attachment through regulation of kinetochore associated proteins (Du et al., 2008).

Besides Nek2, three other Nek kinases have been associated with mitotic progression and spindle assembly: Nek9, Nek6 and Nek7.

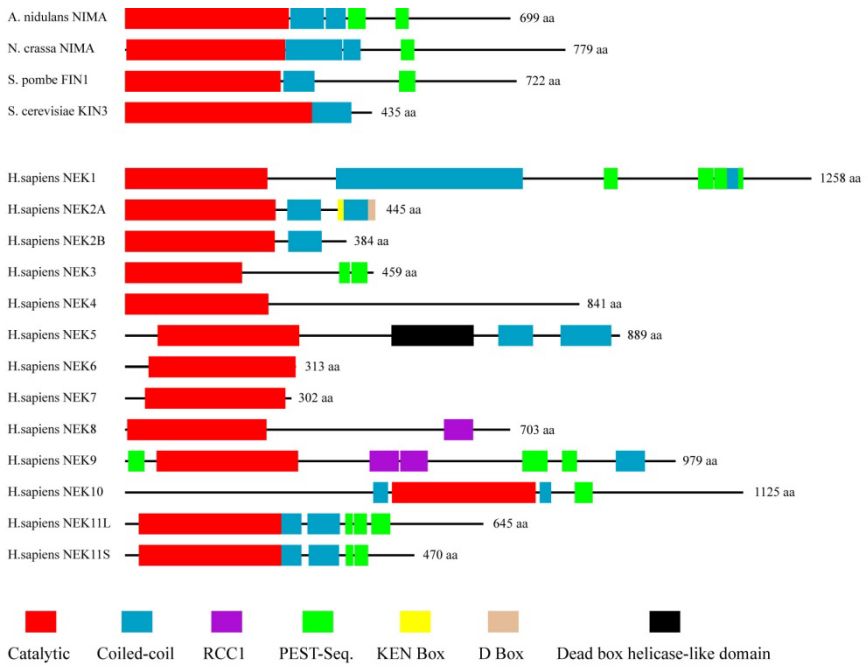

Figure 7: Structural organisation of NIMA and NIMA-like kinases
Structural features and domains of NIMA and NIMA-like kinases are depicted. Aspergillus nidulans NIMA, the founder of the NIMA-like kinase family is shown at the top with the characteristic kinase domain at the N-terminus, coiled-coil regions and PEST sequences. Related kinases exhibit a very similar domain structure. In mammals, 11 NIMA-like kinases have been identified. All exhibit the conserved kinase domain at the N-terminus. The C-terminus is very divergent and may account for different cellular functions. Abbreviations: A.nidulans, Aspergillus nidulans; N.crassa, Neurospora crassa; S.pombe, Schizosaccaromyces pombe; S.cerevisiae, Saccaromyces cerevisiae; H.sapiens, Homo sapiens; RCC1, Regulator of Chromosome Condensation 1; Figure modified from O'Connell, Krien et al. 2003 (O'Connell et al., 2003)

7. NIMA – like kinases Nek9, Nek6 and Nek7

Previously xNek9, xNek6 and xNek7 have been shown to interact and to form a signalling module (Belham et al., 2003; Roig et al., 2002).

Besides the characteristic NIMA-like kinase domain, Nek9 exhibits furthermore an RCC1-like domain and a coiled-coil domain in the C-terminus. Nek9 protein levels do not fluctuate during the cell cycle as reported for both NIMA and Fin1 protein. However, similar to NIMA, Nek9 kinase activity peaks in mitosis based on phosphorylation at threonine 210 (T210). Moreover, this kinase activity increases in Nek9 mutants that lack the RCC1-like domain suggesting an autoinhibition by this domain. The coiled-coil domain at the C-terminus allows dimerization, which allows autophosphorylation and autoactivation of the kinase. Nek9 localisation is cytoplasmic throughout the cell cycle; however a phospho-specific anti-P-T210 antibody against active Nek9 revealed localisation at the spindle poles during mitosis. Also in *Xenopus* egg extract spindles Nek9 has been found at the spindle poles (Roig et al., 2005; Roig et al., 2002).

Functional experiments have provided evidence for a role of Nek9 in mitotic progression. Injection of anti-Nek9 antibodies in human cells blocked mitotic entry. In addition, Nek9 expression of wild-type and kinase-inactive mutants in cells caused a reduction in the mitotic index and an increase in apoptosis. Functional experiments in the *Xenopus* egg extract system and in human cells suggested also a role for Nek9 in spindle assembly. Injection of anti-Nek9 antibodies in cells after mitotic entry caused defects in mitotic spindle formation and chromosome segregation. In addition bipolar spindle formation as well as microtubule aster formation upon RanGTP addition was impaired in Nek9 depleted *Xenopus* egg extract (Roig et al., 2005; Roig et al., 2002).

Nek6 and Nek7 are also implicated in mitotic progression. Their kinase domains exhibit 87% amino acid identity. Only the short N-termini are different from each other (O'Connell et al., 2003). Both kinases are activated in mitosis and have essential functions in mitotic progression. Their depletion by RNAi induces a metaphase delay with fragile mitotic spindles. Recently it has been shown that both Nek6 and Nek7 localise to the spindle poles and the midbody, but only Nek6 localises as well to spindle microtubules in metaphase and anaphase (Kim et al., 2007; O'Regan and Fry, 2009). Mitotic progression defects were the outcome of either RNAi Nek6 or Nek7 indicating that their functions are not redundant (O'Regan and Fry, 2009).

As mentioned above, both Nek6 and Nek7 have been shown to be interaction partners and substrates of Nek9. Indeed, Nek9 and Nek6 form a signalling module which phosphorylates the kinesin Eg5, an essential protein for the establishment of spindle bipolarity (Rapley et al., 2008). Nek6 binding to Nek9 has been located at the C-terminus of Nek9 and, as shown recently, to be controlled by Dynein light chain 8 / LC8. LC8 binding to Nek9 interferes with Nek6 binding. Nek9 autophosphorylation at a specific site releases LC8, thus allowing Nek6 binding and activation (Regue et al., 2011; Richards et al., 2009).

More recently, the mitotically active NIMA-like kinases have been related to nuclear envelope breakdown at mitotic entry due to phosphorylation of Nup98 and thus its dissociation from nuclear pore complexes (Laurell et al., 2011).

8. The *Xenopus* egg extract as the system of choice

The meiotic *Xenopus* egg extract is a widely recognized system for cell cycle research, especially for cell division.

After oogenesis, *Xenopus* oocytes grow and remain in a natural arrest in prophase of meiosis I. Stimulation by progesterone induces oocyte maturation until the second natural arrest in metaphase of meiosis II due to the activity of the cytostatic factor (CSF). Arrested in metaphase of meiosis II, the *Xenopus* egg is a single large cell of around 1mm in diameter ready for fertilisation. Fertilisation induces the inactivation of the CSF by calcium, the pronuclei of egg and sperm fuse followed by a series of cell divisions that last around 30 minutes each and alternate between S and M phase. The cytoplasm of the *Xenopus* egg contains enough reserves of RNA, protein, membranes and other materials for the first 12 divisions. Then genome transcription starts (Alberts, 2008).

Centrifugation of a large number of *Xenopus* eggs allows a separation of the cytoplasm from other egg components such as lipids and membranes. The cytoplasm remains arrested in metaphase of meiosis II which is one great advantage of this system as it is a natural arrest which then can be released at will. Furthermore, the separation of the cytoplasm from membranes makes the egg extract an open system that can be manipulated by retrieval or addition of proteins. Therefore various processes, especially bipolar spindle assembly and microtubule dynamics can be tested under different conditions.

Bipolar spindle assembly can be monitored after the addition of purified sperm nuclei. These contain chromatin and an immature centrosome which upon addition starts the recruitment of microtubule nucleation factors. Together with microtubule nucleation from the chromatin, a half

spindle forms with the centrosome at the pole and radially emanating microtubules attached to the chromatin. Fusion of two half spindles results in a bipolar spindle (Figure 8).

To monitor bipolar spindle assembly with higher similarity to mitotic spindle assembly, CSF-arrested egg extract can by “cycled”. Calcium addition sends the CSF – extract into interphase inducing the replication of chromosomes and centrosome duplication. Addition of CSF – extract drives the interphase extract back again into mitosis by restoring Cdk1 activity.

Another advantage of the *Xenopus* egg extract system is the possibility to visualize the two pathways of microtubule assembly separately. By addition of centrosomes, purified from human cells, to the extract, microtubule aster formation can be visualized from the centrosome. To address the effect on the chromosomal pathway of microtubule formation, the extract can be supplemented with constitutively active mutants of the GTPase Ran. Thus, the presence of chromatin is mimicked and triggers the release of microtubule nucleation factors that ultimately assemble microtubule asters or minispindles. Otherwise, chromatin coated beads can be added and microtubule nucleation visualized that eventually forms into bipolar spindles-like structures.

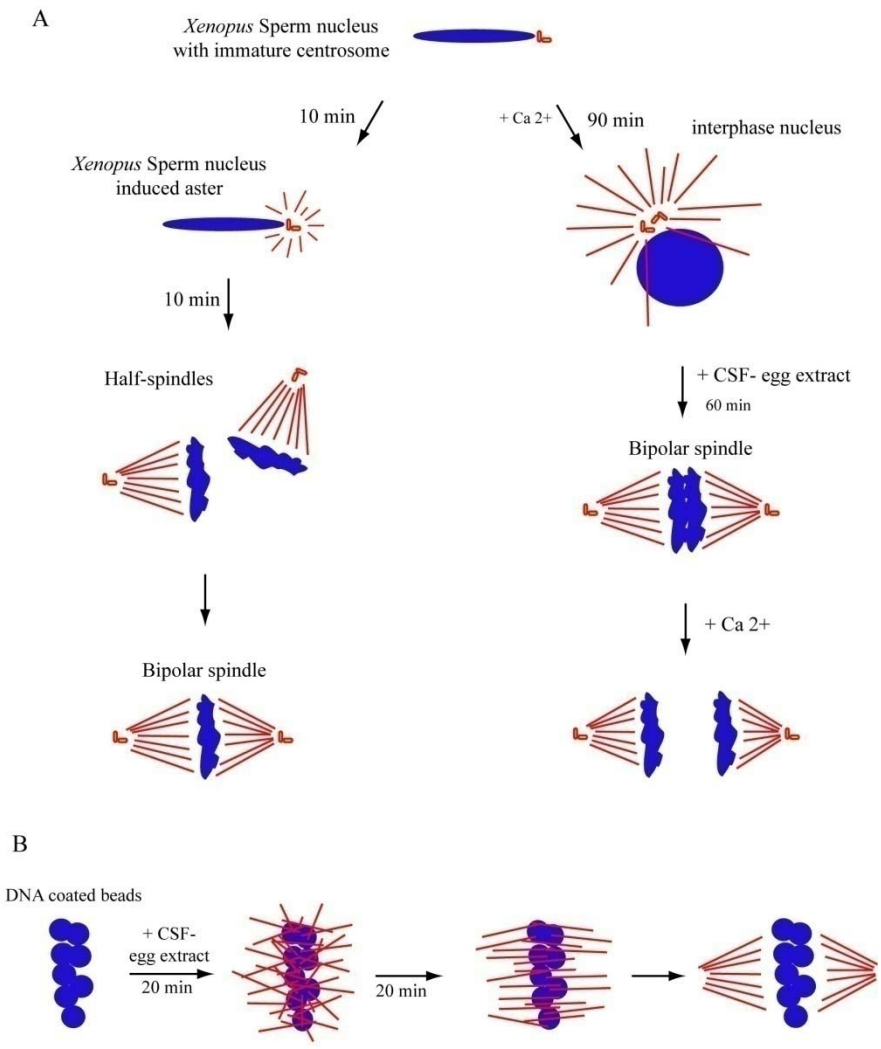

Figure 8: Spindle assembly in *Xenopus* egg extract
(A) *Xenopus* sperm nuclei consist of chromatin and an immature centrosome which recruits proteins essential for microtubule assembly and enables microtubule aster formation. Those asters assemble half spindles after around 30 minutes which may eventually meet and fuse to form bipolar spindles. Otherwise, Ca^{2+} addition to mitotic extract releases the CSF - arrest and induces interphase allowing DNA replication and centrosome duplication. After 90 minutes addition of CSF-arrested egg extract causes bipolar spindle formation by restoring Cyclin B - Cdk1 activity. Metaphase spindles appear after around 60 minutes. Upon addition of Ca^{2+}, anaphase starts and chromosomes segregate. **(B)** DNA coated

beads, previously incubated in interphasic extract, nucleate microtubules when added to mitotic egg extract. After 30-45 minutes, microtubules organise due to the activity of motors (”coalescence”). After 60 minutes and onwards, bipolar spindles appear increasingly.

Objectives

II. Objectives

The aim of the work presented in this thesis was to determine the exact role of *Xenopus* Nek9, xNek9, in bipolar spindle assembly. The *Xenopus* egg extract system is the ideal system to study the contribution of xNek9 kinase in the different pathways of bipolar spindle formation.

The objectives of this thesis were:

1) Determine whether in *Xenopus* egg extract xNek9 acts as upstream kinase in a kinase cascade with Nek6 or Nek7 as reported in human cells

2) Study the role of xNek9 and its mechanism in bipolar spindle assembly

3) Determine the role of xNek9 in microtubule assembly

4) Find novel interaction partners that may give hints on xNek9 function during mitosis

Material and Methods

III. Materials and Methods

1. Tools

1.1. Plasmid constructions

The following plasmid constructions were produced for the project. All constructions were checked for correct insertion and mutations by sequencing

GST-xEg5 Ct: wild-type Eg5 construction (gift from Thomas Surrey; Vernos construct database #426) was subjected to PCR using specific primers for the C-terminus of xEg5 (aa 789-1068; primers xEg5; see below); the amplified fragment was cloned into the vector pGEX-6P-1 using BamHI and SalI as restriction enzymes;

MBP-xEg5 Ct: xEg5 Ct was subcloned from the construction GST-xEg5 Ct (see above) into the vector pMal-C2 using BamHI and SalI as restriction enzymes

GST-xNek6: full length xNek6 cloned in pGEX-KG using EcoRI and XhoI (gift from Joan Roig, IRB)

MBP-xNek6: full length xNek6 was subcloned from the construct GST-xNek6 (see above) into the vector pMal-C2 using BamH1 and HindIII as restriction enzymes.

GST-xNek9 Ct: C-terminal aa707-944 cloned into pGEX; gift from Joan Roig,IRB)

MBP-xNek9 Ct: pCMV5 – xNek9 (gift from Joan Roig, IRB) was subjected to PCR using specific primers for the C-terminus of xNek9 (aa

707-944; primers xNek9 Ct; see below); the fragment was cloned into the pMal-C2 vector using EcoRI and SalI as restriction enzymes;

GST-xNek9 Nt: pCMV5 – xNek9 (gift from Joan Roig, IRB) was subjected to PCR using specific primers for the N-terminus of xNek9 (aa 1-33; primers xNek9 Nt; see below); fragment was cloned in the vector pGEX-6P-1 using EcoRI and SalI as restriction enzymes

MBP-xNek9 Nt: xNek9 Nt was subcloned from the construct GST-xNek9 Nt into the vector pMal-C2 using EcoRI and SalI as restriction enzymes

1.2. Primers

The following primers were used during the project to prepare plasmid constructions (see point 1.1)

xEg5	Fd	5' CGATGGATCCGTAGCAGTGGACATC 3'
xEg5	Rv	5' TCGTGTCGACTCAGTTCTGCATTCGCA 3'
xNek9 Ct	Fd	5' GCGAATTCGAGAAAGTTCTGAACTCCAAAACC 3'
xNek9 Ct	Rv	5' CGGTCGACTTCACATTGGTGTCCCAGAGGAAGA 3'
xNek9 Nt	Fd	5' GTGCGAATTCATGTCCGCCCTCGGC 3'
xNek9 Nt	Rv	5' ATGTCGACTTAATGCAGCTCCTCCTG

1.3. Recombinant protein purification

All fusion proteins were expressed using *Escherichia coli* (*E. coli*) BL21 (DE3). Therefore, small-scale cultures were inoculated with a single colony in Luria broth (LB)-medium supplemented with 100 µg/ml of ampicillin and grown overnight at 37ºC. The next morning, the overnight culture was diluted 1:10 to one liter of antibiotic supplemented LB-medium and grown at 37ºC until optical density 0.4-0.6. Then protein expression was induced by addition of 0.5 mM IPTG for three hours.

Finally, bacteria were centrifuged at 3000 rpm (JA.8.1000) for 20 minutes at 4ºC and resuspended in 30ml of ice-cold PBS. The suspension was centrifuged again, supernatant discarded, the bacterial pellet frozen in liquid nitrogen and stored at -80ºC in case of no immediate protein purification.

Recombinant proteins were purified using affinity chromatography techniques. To purify recombinant proteins, the cells were resuspended in 30ml of PBS supplemented with protease inhibitors complex "mini" (Sigma, 1 tablet in 10ml buffer) followed by lysis using 3 cycles of French Press. The suspension was centrifuged at 15000 rpm (JA25.50), for 30 minutes at 4ºC and the pellet discarded. The supernatant was used for protein purification. GST-fusion proteins were purified using standard protocols for glutathione affinity chromatography (Amersham). MBP-fusion proteins were purified using standard protocols for amylase affinity chromatography (Amersham). The elution of recombinant protein was done in a PD10 column by incubation of the resin with 0.5ml of elution buffer for 10min followed by draining into a test tube. This was repeated 5 times. Therefore the protein peak could be followed by Bradford. Amicon columns (Millipore) were used for buffer exchange to PBS or CSF-XB. The concentration of protein was estimated by Coomassie blue staining, using BSA as a standard. The proteins were stored in small aliquots at -80ºC.

Flag-hNek9 or Flag-xNek9 protein purification from transfected Hek293T cells (see 2.2) was performed using of anti-Flag M1 resin and Flag-peptide (Ref F3290) following the manufacturers instruction. Shortly, 500µl unpacked Flag-resin was washed three times with PBS and finally with cell lysis buffer for equilibration. The resin was incubated with 1ml cell lysate of transfected Hek293T cells for 1h at 4ºC.

Subsequently the resin was washed three times with cell lysis buffer and then incubated twice during 30 minutes with 2.5 resin volumes of CSF-XB containing 100mg/ml of Flag-peptide for competition. Bead were then centrifuged and discarded. The supernatant was concentrated using Amicon columns (Millipore). The concentration of purified recombinant Flag-tagged protein was then check by Western Blotting and Coomassie stain SDS-Page against BSA. Furthermore, the activity was tested in an in vitro kinase assay.

1.4. Antibodies

During the project the following antibodies were raised: anti-xEg5, anti-xNek6, anti-xNek9 (Nt 1-33), anti-xNek9 (Ct 707-944). GST-tagged proteins were produced for injection into rabbits and MBP-tagged proteins for affinity chromatography purification.

Recombinant proteins were expressed and purified as described above. Specific antibodies were raised by injection into rabbits. Sera from sacrificed rabbits were then passed over previously prepared Hi-trap NHS-activated HP (GE healthcare, preparation following the manufacturer's instructions) affinity column with a covalently bound MBP-tagged version of the protein of interest. The eluted antibodies were dialysed against PBS buffer. Purified antibodies were tested by Western Blot and immunofluorescence in XL177 cells.

1.5. List of solutions

ATP mix	0.15 mM ATP, 30 mM $MgCl_2$
Aster fixation solution	BRB80, 10 % glycerol, 0.25 % glutaraldehyde

	and 0.1 % Triton X-100
Aster cushion	25 % glycerol in BRB80
Bead fixing solution	BRB80, 1% glutaraldehyde, heat to 37ºC before use
BRB80	80 mM Pipes pH 6.8 , 1 mM $MgCl_2$ and 1 mM EGTA
Coomassie solution	Coomassie Brilliant Blue R250, 50 % Methanol, 10 % acetic acid
10X Calcium	1 mM $MgCl_2$, 4 mM $CaCl_2$ and 100 mM KCl
Cell lysis buffer	50 mM Tris pH 7.4, 100 mM NaCl, 50 mM NaF, 1 mM DTT, 1% Triton X-100, 1 mM EDTA, 1 mM EGTA, 0.5 mM PMSF, 2 mM Na_3VO_3, 10 mM bGlycerophosphate, 1 tablette complete EDTA free protease inhibitor complex (Sigma)
CSF-XB	XB containing of 2 mM $MgCl_2$ and 5 mM EGTA, pH to 7.7 with KOH
Destain solution	10 % methanol, 10 % acetic acid
Dejellying solution	2 % Cystein in water pH 7.8 with NaOH
GST-wash buffer	PBS, 0,5 % Triton X-100, 200 Mm KCl,1 mM DTT, and protease inhibitor

GST-elution buffer	50 mM Tris pH 8.1, 200 mM KCl, 1 mM DTT, 10 mM reduced Glutathione (Sigma)
GST-dialysis buffer	CSF-XB
Kinase assay buffer	50 mM MOPS pH 7.4, 5 mM $MgCl_2$, 1 mM EGTA, 10 mM b-Glycerophosphate, 100 μM ATP (add just before use)
Kinase assay buffer pull-down	50 mM Hepes pH 7.5, 0.1 mM EGTA, 0.015 % Tween-20 in kinase assay buffer pull-down
Kinase Dilution buffer pull-down	0.1 mg/ml BSA, 0.2 % β-mercaptoethanol in kinase buffer
Kinase Wash buffer	PBS, 0.5 % Triton X-100, 0.25 mM Na_3VO_3, 10 mM NaF
IF buffer	PBS, 0.1 % Triton X-100, 2 % BSA, 0.02 % sodium azide
Mowiol	0.1 M Tris pH 8.5, 10 % Mowiol 4-88 (Hoechst), 25 % Glycerol
MMR	5 mM Hepes, 100 mM NaCl, 2 mM KCl, 1 mM $MgCl_2$, 2 mM $CaCl_2$ and 0.1 mM EDTA, pH to 7.8 with NaOH
PBS 10X	80.6 mM sodium phosphate, 19.4 mM potassium phosphate, 27 mM KCl and 1.37 M

	NaCl in high purity dH_2O, pH 7.4
PBS-Tween	PBS, 0.1 % Tween-20
PBS-T	PBS, 0.1% Triton X-100
Purification buffer 2X	50 mM K-Hepes pH 7, 660 mM KCl, 10 mM $MgCl_2$
Protease inhibitors solution	one tablet of complete EDTA free (Roche) in 0.5 ml of water
Running buffer	25 mM Tris base, 200 mM glycine, 0.1% SDS
SDS sample buffer	10 % glycerol, 3 % SDS, 10 mM Tris-HCl pH 6.8, 5 mM DTT 0.2 % Bromophenolblue
Stacking gel	4 % acrylamide (30% acrylamide BioRad), 125 mM Tris-HCl pH 6.8, 0.1 % SDS and 0.07% ammonium persulfate
Spindle fixation solution	BRB80, 30 % glycerol, 0.25 % glutaraldehyde and 0.1 % Triton X-100
Spindle cushion	40 % glycerol in BRB80
Semi-dry transfer buffer	25 mM Tris-Base, 18 % MeOH, 0.15 % SDS
Tubulin solution	1mM GTP, BRB80, pure tubulin at 20μM
XB buffer	10 mM Hepes, 100 mM KCl, 0.1 mM $CaCl_2$, 1

	mM $MgCl_2$, 50 mM Sucrose, pH to 7.7 with KOH

2. Tissue cell culture

2.1. Tissue culture

XL-177 cells (Miller and Daniel, 1977) were maintained in 70% Leibovitz L-15 Medium (Gibco) supplemented with 15% Fetal Calf Serum (FCS, Gibco), 100 U/ml of 100 µg/ml Penicillin-Streptomycin (Gibco) and 2 mM of L-Glutamine (Gibco). The growth conditions were in a humidified incubator at 22°C.

Hek293T cells were maintained in Dulbecco's modified Eagle's medium (DMEM) supplemented with 10% Fetal Calf Serum (FCS, Gibco), 100 U/ml of 100 µg/ml Penicillin-Streptomycin (Gibco) and 2 mM of L-Glutamine in an atmosphere of 5% CO2 in air.

2.2. Transfection

For transfection of Hek293T cells, Hek293T cells were grown to 50% confluency. Cells were transfected the following day in the absence of antibiotics in the culture medium using Flag-Nek9 - Lipofectamine 2000 (Invitrogen) ratios as suggested by the manufacturer. After 48h, the cells were washed once with medium followed by one wash with cold PBS cells, and then were lysed using cell lysis buffer. Lysis occurred for 20min on ice, then the lysed cells were centrifuged and the supernatant subjected to protein purification or stored in 100µl aliquots for kinases assays.

2.3. Cell fixation and immunofluorescence

Cells were grown on coverslips in tissue culture plates. Before fixation, coverslips were washed once with PBS (70%); excess of liquid was carefully removed from the coverslips using soft paper tissues; cells were then fixed for 10 minutes in cold methanol (-20°C) and for rehydration transferred into PBS. Extracts from *Xenopus* XL-177 were prepared as described previously in Le Bot et al, 1998 (Le Bot et al., 1998).

For immunofluorescence, fixed cells were incubated for 20 minutes with IF buffer for blocking, followed by 20 minutes incubation times for primary and secondary antibodies, both previously diluted in IF buffer. After antibody incubation the slides were washed three times for five minutes with PBS-Triton 0.1%. Primary antibodies were used at 1µg/ml if not otherwise stated. Secondary antibodies were diluted according to the indications of the supplier. For DNA staining, coverslips were incubated together with the secondary antibody at a final concentration of 5 µg/ml of Hoechst (33342). The coverslips were mounted on glass slide with 5 µl of Mowiol.

3. *Xenopus* egg extract

3.1. *Xenopus* egg extract preparation

CSF-arrested *Xenopus* egg extracts were prepared according to Murray (Murray, 1991). Unfertilized eggs were obtained from *Xenopus laevis* female frogs. Ovulation was induced by a first injection with 100 units of pregnant mare serum gonadotropin (PMSG, Calbiochem), followed by another injection with 500-1000 units of human chorionic gonadotropin hormone (HCG, Sigma Chemical Co.) four to eleven days later. Injected frogs were kept overnight in MMR at 16°C. Around 16 hours later, eggs

were collected and rinsed a twice with MMR to remove skin and other detritus. The eggs were dejellied with cystein solution until the eggs were tightly packed (after around 5 minutes). Dejellied eggs were washed twice with XB buffer, twice with CSF-XB buffer and finally left in CSF-XB buffer supplemented with protease inhibitors. Eggs were then transferred through a cut Pasteur pipette into Beckman SW50 centrifuge tubes containing 0.5 ml CSF-XB supplemented with protease inhibitors and 20µg/ml Cytochalasin D (10mg/ml stock). Then, eggs were packed by low speed centrifugation at 200g for 1 minute, followed by 400g for 30 seconds at 16°C in a Beckman centrifuge. Liquid supernatant was removed. Then, packed eggs were crushed spinning at 16°C in a JS 13.1 (Beckman) rotor at 17500g for 18 minutes with slow brake. The cytoplasmic layer was collected by piercing the tube wall with an 18-gauge needle and aspirated in a syringe from the side of the tube. The extract was then transferred into a test tube and supplemented with 1:1000 protease inhibitors solution and 20µg/ml Cytochalasin D (10mg/ml stock). The CSF-extracts were then stored on ice until further use.

3.2. Spindle assembly formation

Mitotic spindle assembly was carried out following the method of Sawin and Mitchison (Sawin and Mitchison, 1991). To visualize microtubules and follow spindle formation, tetramethylrhodamine (rhodamine) labeled bovine brain tubulin was added to the CSF-arrested egg extract at 0.2mg/ml. The extract was then divided into two aliquots, one of which remained on ice, while the other was supplemented by demembranated sperm nuclei (500 nuclei/µl of final volume of extract reaction). Then the extract was released from the CSF-arrest by addition of 0.4 mM (final

concentration) of calcium and incubated for 70 minutes at 20°C. During the cycling through interphase the extract synthesizes proteins from stored mRNA's and replicates DNA and centrosome. Consequently, S-phase extract contains round shaped nuclei with decondensed DNA and relatively stable long microtubules. To drive the extract back to mitosis the second aliquot of CSF-arrested ice cold extract was then added, well mixed with the interphasic egg extract to restore the CyclinB-Cdk1 activity and therefore mitotic environment. The reaction mixture was further incubated at 20°C for 60 minutes. During the incubation time, flat bottom tubes (Greiner Bio-one Company) were prepared with a glass cover slip (12 mm in diameter) and 3 ml of spindle cushion to spin down the mitotic structures for further visualization. After 60 minutes of incubation time at 20ºC the reaction mixture was diluted in 1 ml of Spindle fixation buffer. The samples were carefully loaded on the cushion with a cut Pasteur pipette and centrifuged at 4000g for 20 minutes at 20ºC. The cushion was then removed by aspiration and the coverslip fixed for 10 minutes in cold methanol (-20°C). Slides were then prepared for immunofluorescence.

3.3. RanGTP induced aster formation

Microtubule asters were assembled in 20µl of egg extract by addition of centrosomes purified from KE-37 lymphoid cells or 15µM of RanQ69L-GTP (Carazo-Salas et al., 1999) in the presence of 0.2 mg/ml rhodamine-labeled tubulin. The reactions were incubated for 20 minutes at 20°C, fixed with 1ml of aster fixing solution and centrifuged through 3ml aster cushion onto coverslips, as it was described for spindle assembly assays.

3.4. Centrosome aster formation

Centrosomes, purified from KE-37 lymphoid cells were added to 20µl of CSF-arrested egg extract in the presence of 0.2 mg/ml rhodamine-labeled tubulin. After incubation for 20 minutes at 20ºC, asters were fixed using 1ml aster fixing solution and centrifuged through 3ml aster cushion onto coverslips as described for spindle assembly assays.

3.5. Sperm nuclei induced aster formation

Sperm nuclei induced asters were assembled in 20µl of egg extract by addition of demembranated sperm nuclei (500 nuclei/µl of final volume of extract reaction) in the presence of 0.2 mg/ml rhodamine-labeled tubulin. The reactions were incubated for 20 minutes at 20°C, fixed with 1ml of aster fixing solution and centrifuged through 3ml aster cushion onto coverslips as described for spindle assembly assays.

3.6. Immunoprecipitation

Protein immunoprecipitation experiments on egg extract or XL177 cell lysate were performed with Protein A magnetic beads (Dynal) coated with appropriate antibodies. Therefore, beads were washed three times with 1 ml of PBS-T. Then, beads were incubated in a final volume of 0.25-0.5 ml of PBS-T with antibody solution (5 µg of antibodies per 20 µl of beads) during 30 minutes at room temperature on a rotating wheel. After the binding of the antibodies, coated beads were washed twice in 1 ml of PBS-T and twice with 1 ml of CFS-XB buffer (in egg extract) or with 1ml of cell lysis buffer. Antibody-coated beads were incubated in 50µl of *Xenopus* egg extract on ice and mixed each 10 minutes by tipping the test tube. After 1h the beads were retrieved on a magnet for 10 minutes and washed twice with 0.5 ml of CSF-XB and twice with 0.5 ml of PBS-T, both containing phosphatase inhibitors (100 mM NaF, 80 mM β-

Glycerophosphate and 1 mM Na_3VO_3). Proteins were eluted from the beads by incubation in 1x SDS sample buffer for 10 minutes at room temperature. The samples were then subjected to SDS-PAGE and analyzed by Western blotting.

3.7. Depletion and addback experiments

ProteinA magnetic beads were coated with anti-xNek9 (Ct 707-944) antibodies to remove xNek9 from the *Xenopus* egg extract. To efficiently deplete xNek9 from one volume of extract, half volume of beads was washed twice with PBS-T and then incubated 30 minutes at room temperature on a rotating wheel with anti-xNek9 antibody (20µl beads can bind 5µg of antibody). Afterwards, bead-antibody complexes were washed again twice with PBS-T and twice with CSF-XB prior to addition to the egg extract. This mix was incubated for 20 minutes on ice with mixing steps every 5 minutes by tipping at the bottom of the tube to avoid bead sedimentation. Subsequently beads were retrieved using a magnetic suport. The egg extract was further used as xNek9 depleted egg extract for functional studies whereas the beads were further treated as shown in point 3.5. Addback experiments were performed by addition of recombinant protein Flag-hNek9/Flag-xNek9 at different concentrations (10nM – 150nM) just after depletion. The protein level was analyzed by Western blot.

3.8. Immunofluorescence and quantification

For quantifications, non-saturated images of randomly selected spindles and asters were taken using the same camera settings (more than 30 for each condition). Measurements of spindle length and of total tubulin

fluorescence intensity were carried out using ImageJ. The average aster length and average tubulin content was measured using a custom made macro running on Matlab software (Math Works) as described in Gruss et al, 2002 (Gruss et al., 2002). Population of values were compared using the Student T-test, with 2 tail.

4. In vitro experiments

4.1. Pull-down

ProteinA magnetic beads were coated with anti-GST antibodies (20µl beads can bind 5µg antibody) as described previously (see point 3.5). Subsequently, GST or GST-tagged recombinant proteins were incubated with the beads for 1h on ice, gently shaking the tube every 10 minutes to avoid sedimentation of the beads. After washing twice with CSF-XB, the beads were incubated in CSF-arrested egg extract to allow binding. After 1h on ice, beads were retrieved, washed twice with CSF-XB and twice with PBS-T. Then bound proteins were eluted by addition of 20µl sample buffer. Samples were separated by SDS-PAGE and subjected to Western blotting or stained with CoomassieBlue for further mass spectrometry analysis.

4.2. Bead assay

ProteinA magnetic beads were coated with anti-XMAP215 or anti-xNek9 (Ct 707-944) or anti-xNek9 (Nt 1-33) antibodies (20µl beads can bind 5µg antibody) as described previously (see point 3.5). Subsequently, beads were incubated for 1h at 4ºC in CSF-arrested egg extract. Subsequently, beads were washed twice with CSF-XB and twice with BRB80. 1µl of

these beads was then incubated in 30µl tubulin solution for 15 minutes at 37ºC, then samples were fixed in bead fixing solution and spun down onto coverslips through a cushion of 15% glycerol in BRB80. Samples were then fixed in MeOH and subjected to immunofluorescence.

4.3. Kinase assay

100µl lysate of Flag-Nek9 transfected Hek293T cells were mixed with 20µl previously with cell lysis buffer washed anti-Flag antibody coated beads (Sigma; Ref A2220). Upon 1h incubation at 4ºC on the rotating wheel bead-Flag-hNek9 complexes were washed twice with cell lysis buffer and twice with kinase assay buffer at 4ºC. Then bead-Flag-xNek9 complex were incubated for 30min in 20µl kinase assay buffer at room temperature for preactivation. Subsequently, the mixture was centrifuged, the supernatant discarded. 10µl of a meanwhile prepared mixture of phosphorylation buffer with10 µM ATP^{32} and 10µM substrate was added to the beads. After 30 minutes incubation at 30ºC the reaction was stopped by addition of 10µl sample buffer (2x). Samples were then loaded onto a SDS-PAGE and Coomassie blue stained. The phosphorylated protein levels were detected by autoradiography.

5. Additional experiments

5.1. Antibodies

The following antibodies were used during the project for Western blotting, immunoprecipitation (IP) or immunodepletion (ID).

Name	Origin	Recognition	IP	ID	Reference
xEg5	Rb	*Xenopus*	Yes	No	Home made
xNek6	Rb	*Xenopus*	Yes	No	Home made
hNek6	Rb	*Human*	No	No	(Roig et al., 2002)
xNek7	Rb	*Xenopus*	Yes	No	(Roig et al., 2002)
hNek9	Rb	*Human*	No	No	(Roig et al., 2002)
xNek9 (Nt 3-18)	Rb	*Xenopus*	Yes	Yes	(Roig et al., 2002)
xNek9 (Nt 1-33)	Rb	*Xenopus*	Yes	Yes	Home made
xNek9 (Ct 707-944)	Rb	*Xenopus*	Yes	Yes	Home made
xNedd1	Rb	*Xenopus*	Yes	Yes	Home made
GST	Rb		Yes	No	Home made
αTubulin	M		No	No	DM1A (Sigma)
γTubulin	M		No	No	GTU88 (Sigma)
IgG (C-)	Rb		yes	yes	I-5006 (Sigma)

Table 2: Table of antibodies

The table summarizes the antibodies used during the project. If not otherwise stated the antibodies were used in Western blot at a concentration of 1µg/ml and in immunofluorescence at a concentration of 2µg/ml.

5.2. SDS-Page, Coomassie blue staining and Western blotting

Protein analysis of equivalent amounts of treated and untreated egg- or cell-extracts were resolved on SDS-PAGE according to Laemmli (Laemmli, 1970). The separating gel contained 8-12% acrylamide (BioRad, 30% acrylamide stock containing 0.8% bisacrylamide). The polymerization was started with 1µl of N,N,N´N´-tetramethylenediamine per ml gel solution. The stacking gel contained 4% acrylamide. The gels were usually 1-1.5 millimetre thick minigels and were run in a Running buffer at 150V. Gel staining was performed with Coomassie brilliant blue (R250) staining solution for 10-20 minutes and then destained in destaining solution. Molecular weight markers were from Bio-Rad Laboratories or Fermentas.

For Western blot analysis, gels were transferred onto a nitrocellulose membrane (Protran) under semidry conditions. The semidry transfer was performed using the Semidry transfer buffer for 90minutes at 1mA per square cm of nitrocellulose membrane, in a Amersham system or fast transfer using the iBlot transfer system (Invitrogen, standard protocol 3).

The membrane was blocking from unspecific binding by incubating the membrane in Odyssey blocking solution (Li-Cor) for 1 hour at room temperature or overnight at 4ºC.

Antibodies were diluted in Odyssey blocking solution and added to the membrane for 1 hour at room temperature. After antibody incubation the membrane was washed 3 times with PBS-Triton 0.1% for a total of

30 minutes. The membrane was probed with secondary antibody Alexa fluor 680 or 780 (Molecular Probes and Rockland, respectively). Blots were developed using the Odyssey Infrared imaging system (Li-Cor).

Results

IV. Results

1. Preparation of tools

Nek9 has recently emerged as an important player in spindle assembly but its precise role in this process has not been fully addressed yet (Roig et al., 2005; Roig et al., 2002). To get further insight into Nek9 function in spindle assembly we decided to use the *Xenopus* egg extract system to perform functional studies on the *Xenopus* ortholog, xNek9. We therefore raised antibodies against xNek9.

1.1. Anti-xNek9 antibodies recognise xNek9 specifically in CSF – arrested egg extract

To obtain specific antibodies against xNek9, two fragments of the kinase, the N-terminus (aa 1-33) and the C-terminus (aa 707-944) were cloned and expressed in bacteria as recombinant proteins fused with GST. The purified proteins were injected into rabbits. We then purified the immune sera using columns of MBP-xNek9 N-terminus (aa 1-33) and C-terminus (aa 707-944), respectively, obtaining the anti-xNek9 (Nt 1-33) and anti-xNek9 (Ct 707-944) antibodies. In addition, we obtained an anti-xNek9 (Nt 3-18) raised against a peptide corresponding to xNek9 N-terminus (aa 3-18), in the context of a collaboration with Joan Roig (IRB, Barcelona) (Roig et al., 2005).

The specificity of the three antibodies was first determined on Western blot of CSF – arrested egg extracts. Both anti-xNek9 Nt antibodies recognized a single band at around 120 kDa whereas the anti-xNek9 (Ct 707-944) antibody recognized a single band at around 130 kDa. To determine whether the different antibodies recognized specifically xNek9 despite the different size of the bands, each was used for

immunoprecipitation experiments in CSF – arrested egg extracts. Mass spectrometry analysis showed that xNek9 was immunoprecipitated by all the antibodies indicating their specificity (Figure 9).

1.2. Anti-xNek9 specific antibodies deplete xNek9 efficiently from CSF – arrested egg extract

We then examined whether the anti-xNek9 antibodies were able to deplete the endogenous protein from CSF – arrested egg extracts. Protein A magnetic beads coated with each of the anti-xNek9 antibodies were incubated in egg extracts and retrieved. All three antibodies were able to deplete efficiently xNek9 (Figure 9). Interestingly, both anti-xNek9 N-terminal antibodies required 4 successive rounds of bead incubation to efficiently deplete xNek9 whereas the C-terminal antibody was able to fully deplete it in a single incubation. These results suggest that the anti-xNek9 (Ct 707-944) may have a higher affinity for xNek9 than the N-terminal antibodies.

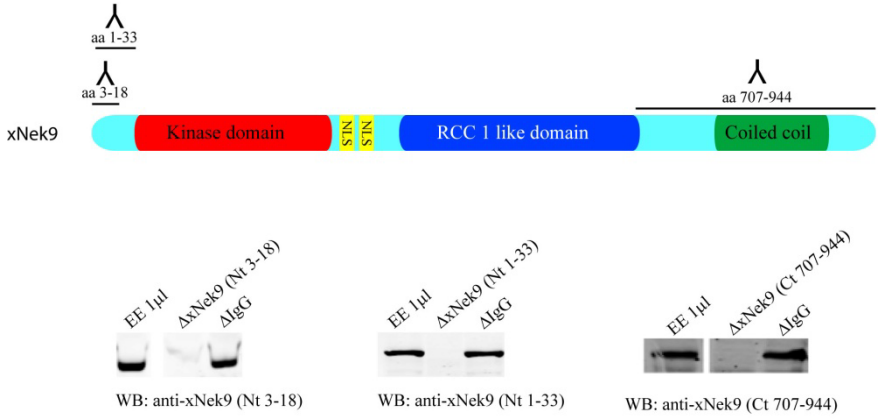

Figure 9: Anti-xNek9 specific antibodies deplete xNek9 efficiently from *Xenopus* meiotic egg extract

Schematic representation of xNek9 kinase. NLS, Nuclear Localisation Signal; RCC1, Regulator of Chromosome Condensation 1; aa, amino acid. Three

different antibodies deplete xNek9 efficiently: anti-xNek9 peptide antibodies were raised against the N-terminus (aa 3-18), gift of Joan Roig (IRB, Barcelona). Polyclonal anti-xNek9 N-terminus and C-terminus antibodies were raised against GST-xNek9 constructs containing aa 1-33 and 707-944, respectively.

2. Localisation of xNek9

The localisation of Nek9 in human cells was previously reported as cytoplasmic (Roig et al., 2002). In addition, using a phospho-specific antibody active Nek9 was found to localise at the centrosome upon mitotic entry, peaking in metaphase and with decreasing signal towards mitotic exit. We aimed at determining the specific localisation of unphosphorylated xNek9 by using the anti-xNek9 antibodies that we produced.

2.1. Subcellular localisation of xNek9 in XL177 cells

To determine the localisation of xNek9 in *Xenopus* XL177 cells, cells were grown to 80% confluency, fixed and stained with anti-xNek9 antibodies. Different fixation methods (methanol, paraformaldehyde, glutaraldehyde), anti-xNek9 antibodies (anti-xNek9 Nt3-18 or 1-33; or anti-Nek9 Ct 707-944) at various concentrations (1-10µg/ml) gave the same results. Confocal microscopy on methanol fixed cells stained with the anti-Nek9 (Ct 707-944) antibodies revealed a faint and diffuse signal in the cytoplasm of both interphase and mitotic cells. To reduce the cytoplasmic staining soluble proteins in XL177 cells were preextracted by incubation in PBS-0.1% Triton for 3 seconds previous to fixation. Preextraction reduced the overall fluorescent signal, but no specific localisation could be observed in interphase cells. However, preextraction allowed to detect a faint centrosomal localisation of xNek9 a minority of prophase (Figure 10A) and metaphase cells (Figure 10B). In addition, a signal for xNek9 was also observed around the metaphase plate close to

the chromatin (Figure 10A). In anaphase and telophase no xNek9 signal was detectable anymore. Therefore, xNek9 may localise to prophase and metaphase centrosomes as well as around the chromatin at the metaphase plate.

These results, similar to the reported localisation of Nek9 in human cells, suggest that the anti-xNek9 (Ct 707-944) antibody recognizes specifically total Nek9. Interestingly, there are no previous reports on a putative enrichment of Nek9 around the chromosomes.

2.2. xNek9 localisation in CSF – arrested egg extract

2.2.1. xNek9 localisation in bipolar spindles and centrosome asters

We next analysed xNek9 localisation in spindles assembled in *Xenopus* egg extract. Immunofluorescence analysis of bipolar spindles assembled in cycled egg extract did not show any specific localisation for xNek9 (Figure 10C). This is in contrast to a previous report on xNek9 accumulation at the centrosome in egg extract derived spindles (Roig et al., 2005). We then examined whether Nek9 localised to centrosome induced asters in egg extract. A faint anti-xNek9 signal was detectable at some asters (Figure 10D).

2.2.2. GST-xNek9 Ct localisation in bipolar spindles and centrosome asters

As a complementary approach, we looked at the potential localisation of a fragment of Nek9, GST-xNek9 Ct that was previously used to raise anti-xNek9 antibodies. GST-xNek9 Ct was added to the egg extract followed

by immunofluorescence analysis of bipolar spindles and asters using anti-GST antibodies. We did not observe any specific localisation of this recombinant protein on bipolar spindles (Figure 10E) or centrosome asters (Figure 10F).

Altogether, these results suggest that xNek9 may localise to the centrosome in prophase and metaphase in XL177 cells as well as to centrosome asters formed in egg extract. In addition, xNek9 is enriched around the chromatin in XL177 metaphase cells. No specific localisation was observed at any other cell cycle stage. GST-xNek9 Ct does not localise to any structure in egg extracts suggesting that the C-terminal tail of xNek9 is not involved in its localisation.

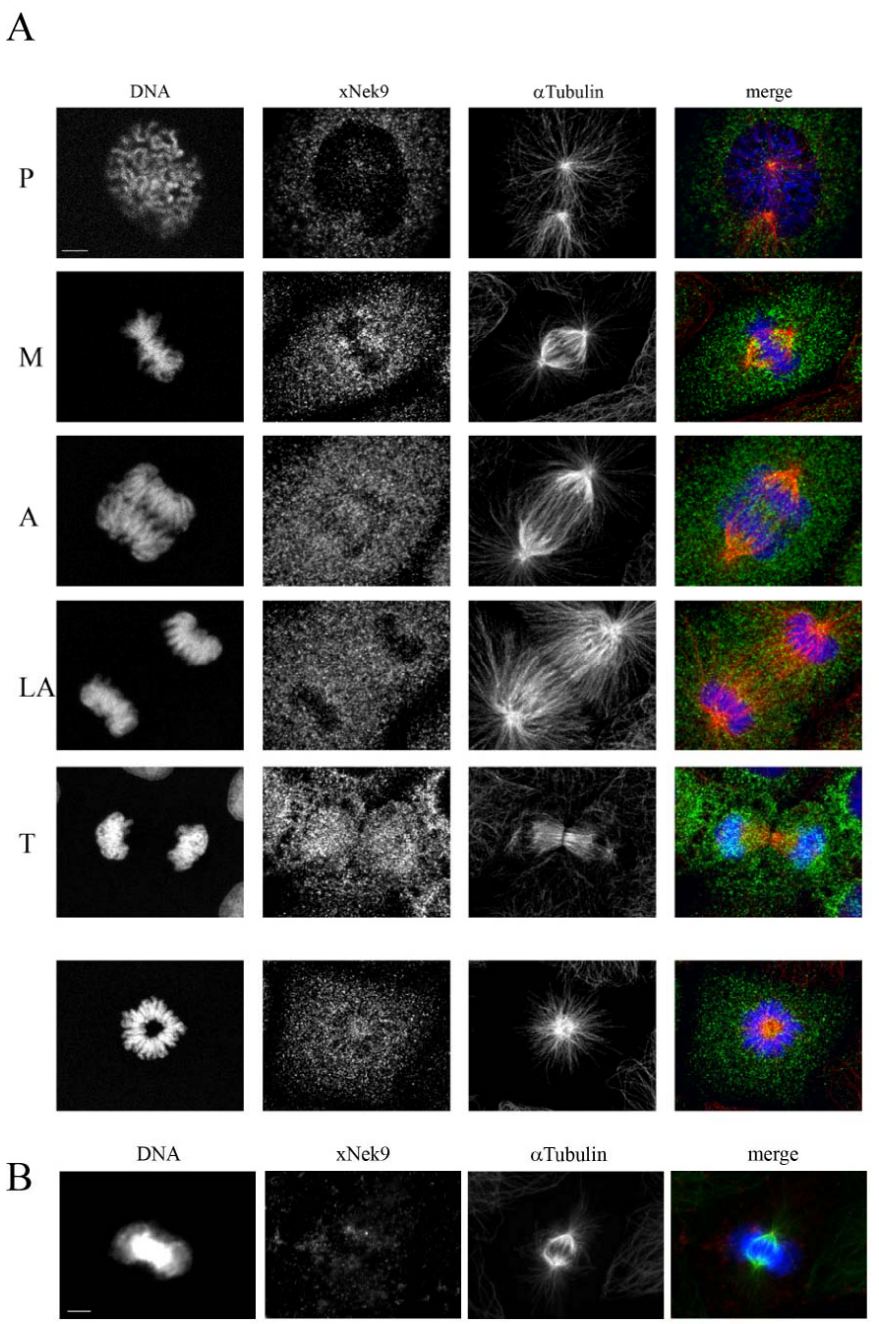

Figure 10: Localisation of xNek9

(A) Confocal microscopy pictures showing xNek9 localisation in different mitotic phases of methanol fixed XL177 cells. Prophase (P); Metaphase (M); Anaphase

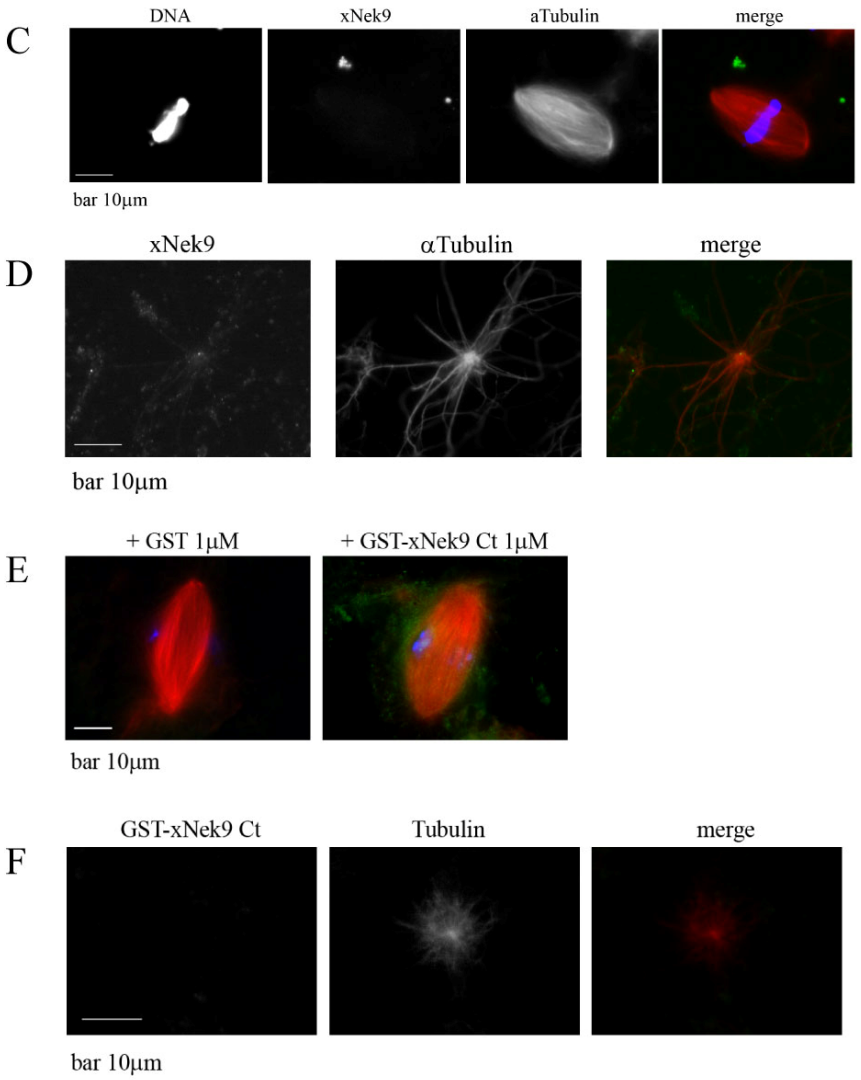

(A); Late Anaphase (LA); Telophase (T); Tubulin, red; xNek9, green; DNA, blue; bar 5µm. **(B)** Fluorescence microscopy picture showing xNek9 localisation in a XL177 cell in metaphase. Tubulin, green; xNek9, red; DNA, blue; bar 5µm. **(C)** xNek9 localisation in bipolar mitotic spindles formed in cycling egg extract. Tubulin, red; xNek9, green; DNA, blue. **(D)** xNek9 localisation in centrosomal asters formed in cycling egg extract. Tubulin, red; xNek9, green. **(E)** GST-xNek9 Ct localisation in bipolar mitotic spindles formed in cycling egg extract. Tubulin, red; GST-xNek9 Ct, green; DNA, blue. **(F)** GST-xNek9 Ct localisation in centrosomal asters formed in cycling egg extract; tubulin, red; GST-xNek9 Ct, green.

3. xNek9 may not interact with xNek6 or xNek7 in CSF – arrested egg extract nor with the Nek6 substrate Eg5

In human cells, NIMA-like kinase Nek9 is the upstream kinase of a kinase cascade involving either Nek7 or Nek6 (Belham et al., 2003). Nek6 then acts on downstream substrates such as the kinesin Eg5 (Rapley et al., 2008). We sought to determine whether a similar kinase cascade exists in *Xenopus* eggs.

3.1. There is no evidence for xNek6 presence in CSF – arrested egg extract

We first produced a polyclonal anti-xNek6 antibody. Full length *Xenopus* Nek6 (xNek6) was cloned for expression as a GST-tagged recombinant protein. GST-xNek6 was expressed in bacteria, purified and injected into rabbits to raise polyclonal antibodies (Figure 11A). We then purified the immune sera using columns of MBP-xNek6 obtaining anti-xNek6 antibodies. Western blot analysis showed that the affinity purified anti-xNek6 antibody recognised a band at the expected size of 36kDa in XL177 cell lysate, but not in CSF – arrested egg extract (Figure 11B). One possibility was that xNek6 is present in small quantities in CSF – arrested egg extract and therefore may be hard to detect by Western blot. We therefore performed immunoprecipitation experiments with anti-xNek6 antibodies in CSF – arrested egg extract. Western blot analysis of the immunoprecipitated samples did not reveal any band at the expected size of xNek6 (Figure 11C). A 60kDa protein that was efficiently immunoprecipitated instead was found to be pyruvate kinase by mass spectrometry (data not shown). By contrast, xNek6 was efficiently immunoprecipitated from XL177 cell lysate as confirmed by Western blot analysis and mass spectrometry (Figure 11C).

3.2. xNek9 does not interact with xNek6 or xEg5

Nek6 is known to interact with Nek9. Thus, as another approach to check whether xNek6 is present in CSF – arrested egg extract, we immunoprecipitated xNek9 and tested by Western blot whether Nek6 was co-immunoprecipitated. Western blot analysis did not reveal the presence of xNek6 in the xNek9 immunoprecipitation (Figure 11D).

Eg5 has been recently shown to be an interaction partner and downstream target of the kinase cascade hNek9 – hNek6 in human cells (Rapley et al., 2008). To check whether in CSF – arrested egg extract xNek9 may be the kinase that interacts and phosphorylates Eg5, we immunoprecipitated xNek9 and checked for xEg5 in the immunoprecipitate. xNek9 was not able to co-immunoprecipitate xEg5 in CSF – arrested egg extract (Figure 11E). Similarly, an immunoprecipitation using anti-xEg5 antibodies did not co-immunoprecipitate xNek9 suggesting that both proteins do not interact in CSF – arrested egg extract (data not shown).

3.3. There is no evidence for xNek7 presence in CSF – arrested egg extract

In human cells, Nek9 also interacts and activates Nek7, another NIMA kinase family member highly similar to Nek6 with an amino acid sequence identity of 77%. We therefore tested whether *Xenopus* eggs and XL177 cells express xNek7 using an anti-xNek7 peptide antibody (gift from Joan Roig, IRB, Barcelona). Immunoprecipitation experiments indicated that xNek7 is absent from both CSF – arrested egg extract and XL177 cell lysate (Figure 11F). However, this antibody only recognized

faintly recombinant GST-xNek7 suggesting that the negative results should be re-examined (Figure 11G).

Altogether, these results suggest that unfertilized *Xenopus* eggs may not contain xNek6 nor xNek7. Therefore xNek9 may not function through a kinase cascade involving xNek6 during meiosis and it may not regulate the same substrates as in mitotic cells.

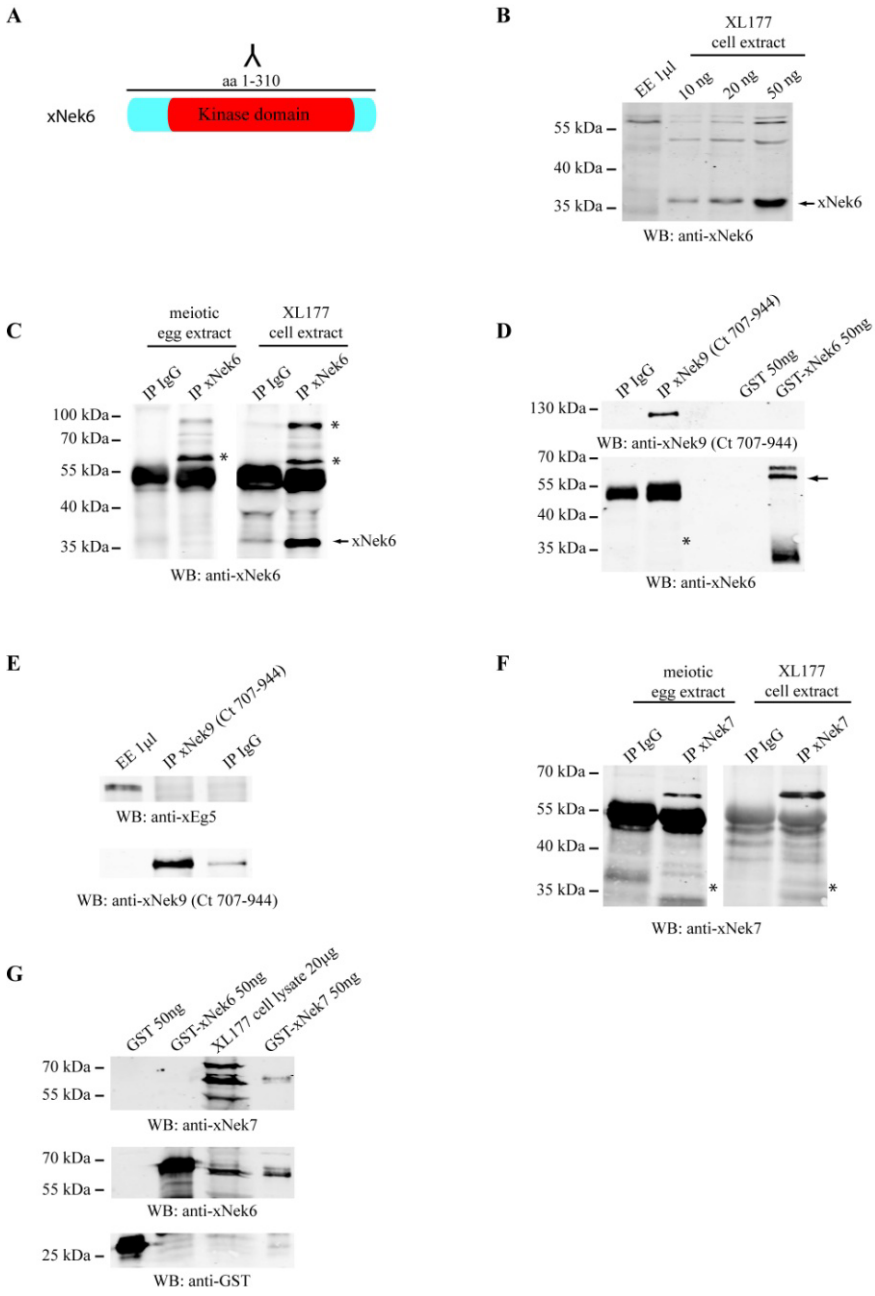

Figure 11: There is no evidence for xNek6 and xNek7 presence in *Xenopus* meiotic egg extract

(A) Schematic representation of xNek6 kinase. Polyclonal anti-xNek6 antibodies were raised against a GST construct with full-length xNek6 (aa 1-310). **(B)**

Immunoblot analysis for the presence of xNek6 in egg extract and *Xenopus* XL177 cell lysate. **(C)** xNek6 immunoprecipitation from egg extract or *Xenopus* XL177 cell lysate. Immunoblot is shown after incubation with anti-xNek6 antibodies. Asterisks mark unspecific bands. **(D)** xNek9 immunoprecipitation from egg extract and immunoblotting with anti-xNek9 (Ct 707-944) and anti-xNek6 antibodies. Asterisk marks the expected size of endogenous xNek6 in the immunoprecipitation. Arrow marks recombinant GST-xNek6. **(E)** xNek9 immunoprecipitation from egg extract and immunoblotting with anti-xNek9 (Ct 707-944) and anti-xEg5 antibodies. **(F)** xNek7 immunoprecipitation from egg extract and XL177 cell lysate. Immunoblot is shown after incubation with anti-xNek7 antibodies. Asterisk marks the expected size of endogenous xNek7. **(G)** Immunoblot analysis for a possible crossreaction of anti-xNek6 and anti-xNek7 antibodies on respective recombinant protein GST-xNek6 and GST-xNek7.

4. The role of xNek9 in bipolar spindle assembly

To determine the role of xNek9 in spindle assembly, we used the *Xenopus* egg extract system. xNek9 was efficiently depleted from CSF – arrested egg extract as reported above (Figure 9). The depleted extract was sent to interphase by calcium addition and sent back to mitosis by addition of a volume of the initially depleted egg extract kept on ice. After 60 minutes of incubation, mitotic structures were fixed and processed for immunofluorescence.

4.1. xNek9 depletion impairs bipolar spindle assembly

4.1.1. xNek9 depletion causes decrease of bipolarity and increase of monopolarity and aberrant structures

We first examined spindle assembly upon addition of sperm nuclei to the extract. Figure 12A shows some representative structures formed in control and xNek9 depleted extracts and the corresponding quantifications (Figure 12A). xNek9 depletion caused a substantial decrease in spindle bipolarity (33,3% versus 52,6% in the control) and an increase of

monopolar structures (44% versus 31,3% in the control). The number of multipolar structures or structures with split poles was similar in control and xNek9 depleted extracts. However the number of aberrant structures was higher in the absence of xNek9 (9,3% versus 4% in the control). These abnormal structures had a very condensed chromatin, surrounded by few and very short microtubules. These results strongly suggested that xNek9 is important for bipolar spindle formation.

4.1.2. xNek9 depletion affects microtubule density in bipolar spindles but not spindle length or width

The increase in monopolar and aberrant structures suggested that xNek9 is required for microtubule assembly. To test this idea, we compared the microtubule density of bipolar spindles in control and xNek9 depleted extract. Using ImageJ, we measured the integrated αTubulin fluorescence intensity of individual bipolar spindles and their areas. By dividing these values we obtained the microtubule density value. We found that xNek9 depletion indeed caused a significant 19% decrease of microtubule density (Figure 12B), suggesting that xNek9 is required for microtubule assembly.

We then quantified the length and width of the bipolar spindles formed in the different experimental conditions. We found that the average spindle length, measured by pole-pole distance, was similar in both conditions (32,9 μm versus 33,2 μm in control) and to published data (Goshima and Scholey, 2010; Hannak and Heald, 2006) (Figure 12C). Furthermore, the spindle width was not significantly altered in xNek9 depleted extract (17,3 μm versus 15,8 μm in control) (Figure 12D). Also these values were in the range of published data (Cha et al., 1999).

Altogether these results suggest that xNek9 is important for bipolar spindle assembly and that its function may be in the regulation of microtubule assembly.

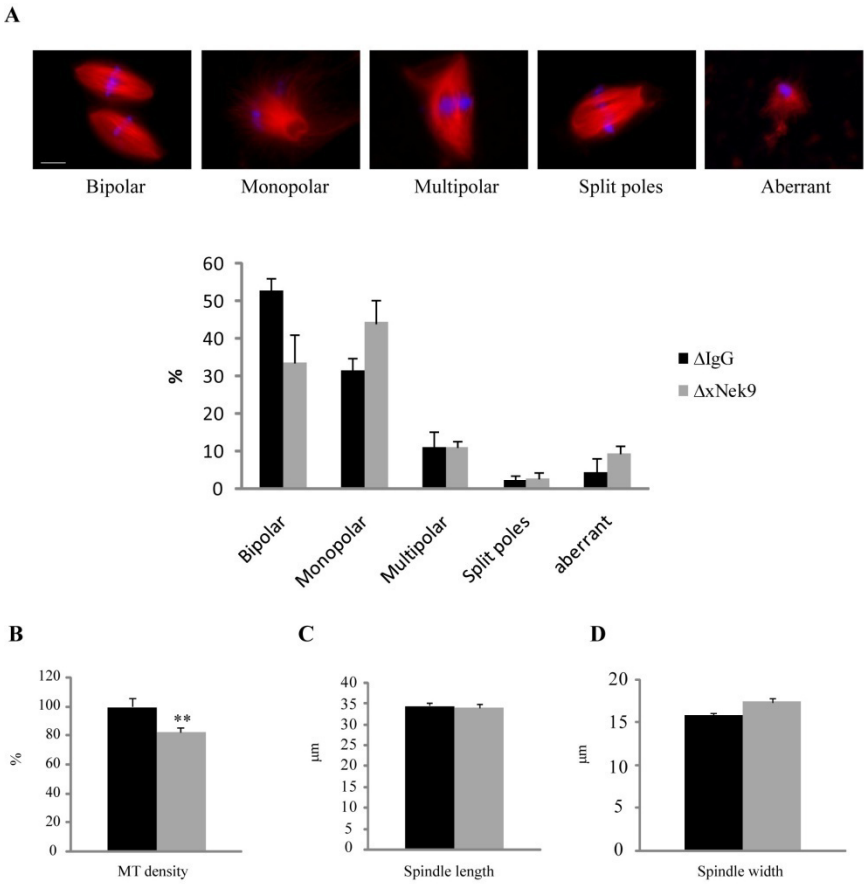

Figure 12: Depletion of xNek9 impairs bipolar spindle assembly
(A) Representative images showing the different phenotypes formed in control and xNek9 depleted extract. Graph representing the average percentage of phenotypes in control and xNek9 depleted cycled mitotic egg extract from 3 independent experiments. 50 structures were analyzed in each experiment. Immunodepletion was performed using rabbit IgG and anti-xNek9 (Ct 707-944) antibodies. Bar, 10µm. **(B)**,**(C)**,**(D)** Graphs representing the average microtubule (MT) density (in %), spindle length and spindle width (in µm) of bipolar spindles

under control and xNek9 depleted conditions; results are means from 3 independent experiments.

4.2. Flag-hNek9 rescues spindle assembly defects upon xNek9 depletion

To determine whether the phenotypes observed in xNek9 depleted extracts were specific for xNek9 and not due to co-immunoprecipitated proteins we performed add-back experiments using Flag-tagged Nek9 protein.

4.2.1. xNek9 molarity in CSF – arrested egg extract is around 150 nM

We first estimated the endogenous xNek9 concentration in CSF – arrested egg extract. Therefore, Flag-xNek9 was expressed in human Hek293T cells for 48h and after cell lysis concentrated on anti-Flag affinity resin. Several washing steps later, Flag-xNek9 was eluted by competition with Flag peptide and then dialyzed against CSF-XB buffer. The concentration was estimated against a BSA protein curve in Coomassie blue stained SDS-PAGE. Western blot analysis of different volumes of CSF – arrested egg extract and purified Flag-xNek9 protein allowed an estimation of xNek9 protein concentration in CSF – arrested egg extract to around 150nM. This concentration is in the range of other microtubule related proteins e.g. Maskin (Peset et al., 2005).

4.2.2. Flag-xNek9 addback at endogenous levels causes dominant-negative effects

Adding Flag-xNek9 to 150nM final concentration in xNek9 depleted extract failed to rescue the spindle phenotypes of the xNek9 depletion.

Moreover, it induced a dominant-negative effect decreasing furthermore the number of bipolar spindles and increasing the number of monopolar structures (results not shown). As Flag-xNek9 purified from transfected Hek293T cells also contained two major contaminant proteins (Figure 13A) we aimed at improving the preparation by increasing the salt concentration during the washing steps and performing a faster bead elution step. However this new preparation did not clearly change the previous results. We then tried the rescue experiment with Flag-tagged human Nek9 that is 69% identical to xNek9 since purified Flag-hNek9 hardly contained contaminant proteins (Figure 13A). Adding back Flag-hNek9 at around endogenous concentrations however also caused dominant-negative effects similar to those induced by Flag-xNek9.

4.2.3. Flag-hNek9 addback at 10nM final concentration rescues xNek9 depletion phenotype and bipolar spindle characteristics

While repeating the addback experiments with different concentrations of Flag-hNek9 we found that lowering the concentration of purified Flag-hNek9 (Fh9) to 10nM final concentration in the egg extract rescued the xNek9 depletion phenotype (Figure 13B). Indeed, the number of bipolar spindles was restored to close to control levels (control: 54%; ΔxNek9: 38%; addback Flag-hNek9: 51,3%) while the number of monopolar spindles was reduced (control: 22%; ΔxNek9: 30%; addback Flag-hNek9: 18%) (Figure 13C). The number of multipolar structures returned to control levels (control: 12%; ΔxNek9: 9,3%; addback Flag-hNek9: 12%). The split pole phenotype was only partially rescued by Flag-hNek9 addition (control: 10,6%; ΔxNek9: 18,6%; addback Flag-hNek9: 17,3%) suggesting that this phenotype may be a side effect of xNek9 depletion.

Finally, the proportion of aberrant structures did not change in any of the conditions (Figure 13C).

We next investigated whether bipolar spindle microtubule density was rescued by addition of 10nM Flag-hNek9. Unexpectedly, microtubule density was only slightly reduced in these experiments compared to previous ones (control: 100%; ΔxNek9: 96.2%; addback Flag-hNek9: 94,6%) (Figure 13D). This may be due to the fact that two out of 3 experiments showed only a mild reduction in microtubule density. However, combining all experimental data on microtubule density (Figure 12B and 13D), xNek9 depletion caused a significant decrease of microtubule density in bipolar spindles (control: 100%; ΔxNek9: 89.1%). No conclusion can be drawn yet whether Flag-hNek9 rescues microtubule density decrease.

We then examined the spindle length and width in the different conditions. Bipolar spindle length was not different in depletion and addback conditions compared to control (control: 34,0 μM; ΔxNek9: 35,2 μM; addback Flag-hNek9: 33,5 μM) (Figure 13E). Spindle width however significantly increased in xNek9 depleted extract and could be partially rescued by addition of Flag-hNek9 (control: 15,9 μM; ΔxNek9: 17,9 μM; addback Flag-hNek9: 15,0 μM) (Figure 13F).

Altogether, these results suggest that Flag-hNek9 addback at 10nM final concentration rescues xNek9 depletion phenotypes and restores spindle width. Whether microtubule density decrease is rescued remains to be shown.

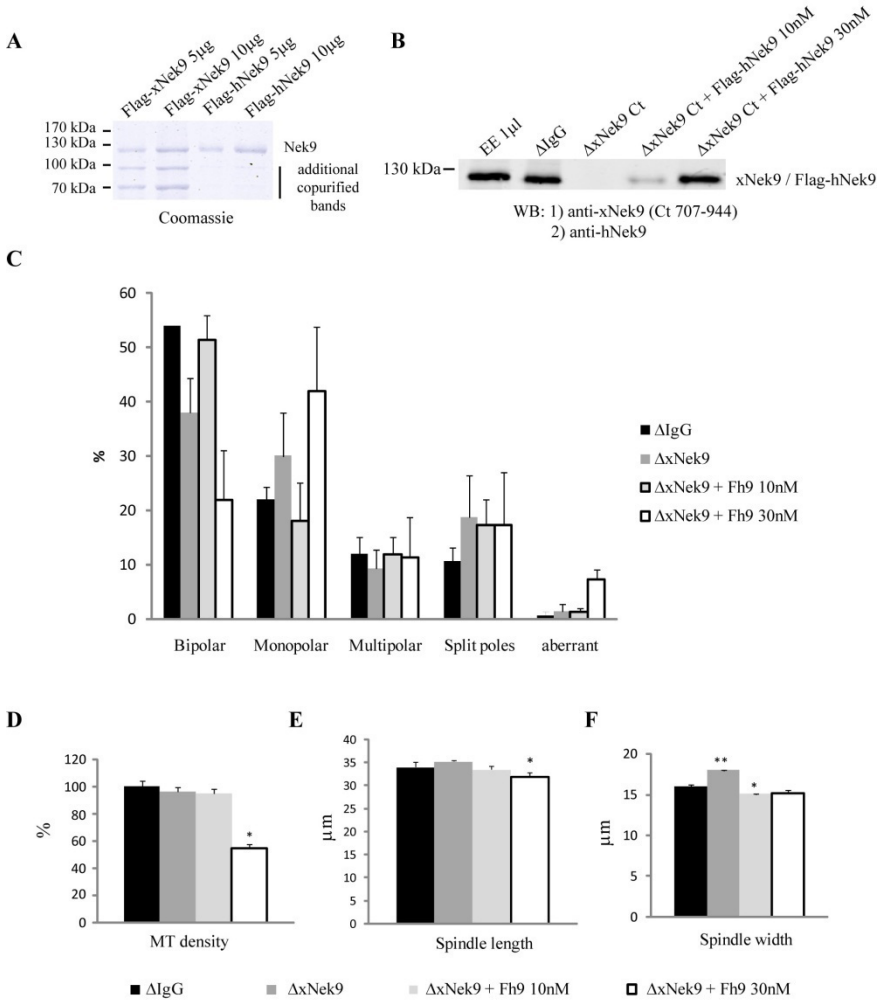

Figure 13: Addback of 10nM exogenous Flag-hNek9 rescues spindle assembly defects

(A) Coomassie gel of Flag-hNek9 and Flag-xNek9 protein purified from Hek293T cells showing additional co-purified protein bands at around 70kDa and 100kDa. **(B)** Western blot showing a representative depletion and addback of Flag-hNek9 after immunoblotting with anti-xNek9 (Ct 707-944) to detect endogenous xNek9 protein and anti-hNek9 antibody to detect exogenous Flag-hNek9 protein. **(C)** Graph representing the average percentage of phenotypes in control and xNek9 depleted egg extract from 3 independent experiments. 50 structures were analyzed in each experiment. Immunodepletion was done using rabbit IgG and anti-xNek9 (Ct 707-944) antibodies. Fh9, Flag-hNek9. **(D)**,**(E)**,**(F)**

Graphs representing the average microtubule (MT) density (in %), spindle length and spindle width (in μm) in control, xNek9 depleted and addback conditions.

Increasing Flag-hNek9 concentration interferes with bipolar spindle assembly and bipolar spindle characteristics

To further assess the importance of xNek9 concentration we also performed other rescue experiments with slightly increased concentration of Flag-hNek9. Only a slight increase to 30nM final concentration of Flag-hNek9 already showed a dominant-negative effect similar to the first rescue experiments at 150nM final concentration. Bipolarity was strongly reduced to 22% whereas monopolarity and aberrant structures strongly increased compared to control (42% and 7,3% respectively). The percentage of split pole structures remained high compared to control whereas multipolar structures slightly decreased (Figure 13C). The strong increase in monopolar and aberrant structures after addition of Flag-hNek9 to 30nM final concentration was highly reminiscent to the effect seen in previous xNek9 depletion studies (Figure 12A and 13C) strongly suggesting that monopolar and aberrant structures are the main phenotypes when xNek9 function is impaired. In addition, monopolarity and aberrant structures were also the main phenotypes in CSF – arrested egg extract previously depleted with the anti-xNek9 (Nt 3-18) antibody (data not shown). The rescue experiments strongly suggest that a tight regulation of xNek9 concentration and activity are essential for proper bipolar spindle assembly.

We next investigated the importance of xNek9 concentration on microtubule density, spindle length and width. Addition of 30nM Flag-hNek9 to xNek9 depleted extract strongly reduced microtubule density in bipolar spindles (control: 100%; Flag-hNek9 30nM: 54,9%) (Figure 13D).

Spindle length measurements showed a small but significant decrease compared to control (control: 34,0 μm; Flag-hNek9 30nM: 31,9 μm) whereas spindle width did not change (control: 15,9 μm; Flag-hNek9 30nM: 15,1 μm) (Figure 13E, F).

These results indicate that xNek9 concentration is highly determinant for microtubule assembly and also for spindle length.

4.3. Addition of GST-xNek9 Ct causes dominant-negative effects on bipolar spindle assembly but not bipolar spindle characteristics

As another approach to investigate the role of xNek9 on spindle assembly we tested whether GST-xNek9 Ct addition at high concentration to CSF – arrested egg extract could act as a dominant negative reagent as previously reported for other protein fragments (Boleti et al., 1996; Hannak and Heald, 2006). The C-terminus of Nek9 was previously reported to be the region of protein-protein interaction, to be essential for transactivation of Nek9 kinase and therefore a good candidate for a dominant-negative (Roig et al., 2002). CSF – arrested egg extract was depleted from xNek9, sent to interphase by calcium addition and driven back to mitosis by addition of a volume of the initially depleted egg extract kept on ice. At this moment also GST-xNek9 Ct was added at 2μM final concentration to the extract to create a concentration of GST-xNek9 Ct compared to endogenous xNek9. Mitotic structures were fixed after 60 minutes and processed for immunofluorescence.

Similar to bipolar spindle formation in xNek9 depleted extract, we obtained almost identical results in GST-xNek9 Ct addition experiments. The percentage of bipolar structures strongly decreased (39,0% versus

66,3% in control) whereas monopolar structures and aberrant structures increased (20,6% versus 11,6% in control and 20,6% versus 8,3% in control, respectively). Structures with split poles increased slightly (5,3% versus 2% in control) and multipolar structures remained stable (Figure 14A).

These results, very similar to xNek9 depletion, suggest that GST-xNek9 Ct acts as a dominant-negative and perturbs the function of endogenous xNek9.

We next measured microtubule density, spindle length and width in bipolar spindles assembled after GST or GST-xNek9 Ct addition. No differences were detected in any of the three factors (Figure 14B). Furthermore, spindle length (33,6 μM) and spindle width (15,4 μM) in egg extract containing GST-xNek9 Ct were almost identical to xNek9 depletion results and in the range of already published data (Cha et al., 1999) (Figure 14C, D).

These results suggest that the GST-xNek9 Ct fragment functions as dominant-negative and perturbs spindle organisation. Furthermore, the phenotypical changes upon GST-xNek9 Ct addition strongly resemble the effect of xNek9 depletion strengthening these results and again suggesting that xNek9 indeed is important for bipolar spindle organisation.

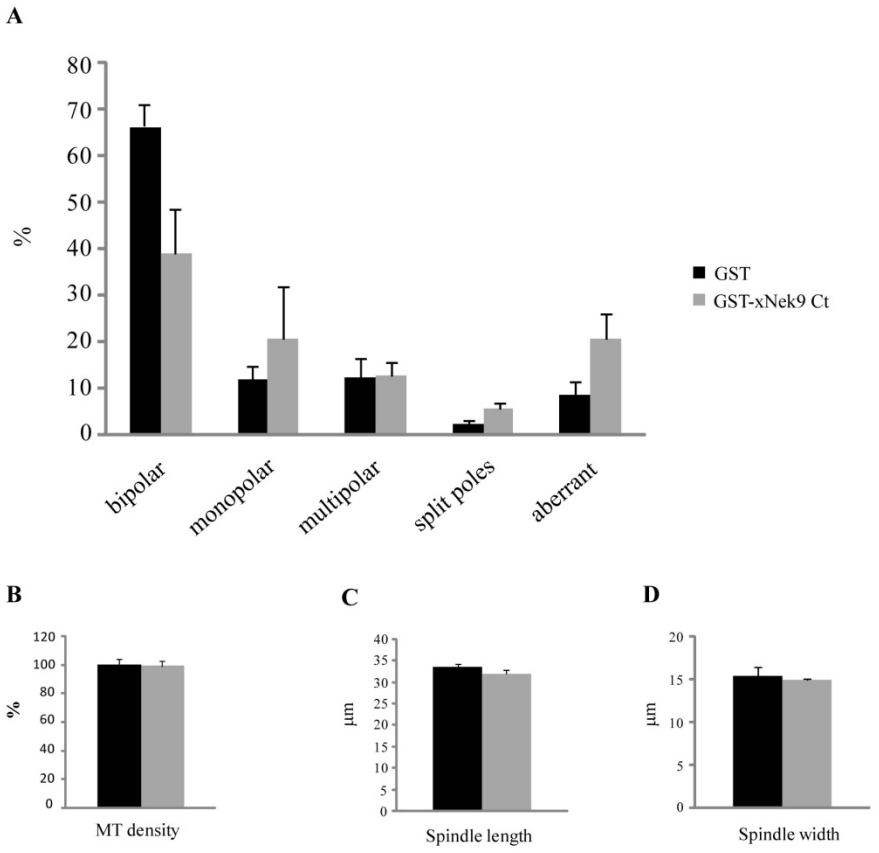

Figure 14: Addition of GST-xNek9 C-terminal (GST-xNek9 Ct) fragment impairs bipolar spindle formation

(A) Graph representing the average percentage of phenotypes in cycled egg extract previously supplemented with 2µM GST or GST-xNek9 Ct from 3 independent experiments. At least 30 structures were analyzed in each experiment. **(B)**,**(C)**,**(D)** Graphs representing the average microtubule (MT) density (in %), spindle length and spindle width (in µm) from 3 independent experiments in egg extract previously supplemented with 2µM GST or GST-xNek9 Ct.

5. The role of xNek9 in microtubule assembly

The phenotypes caused by xNek9 depletion and GST-xNek9 Ct addition may be attributed to a problem of microtubule assembly. This is supported by a decrease in microtubule density of bipolar structures upon xNek9

depletion. Therefore, we decided to examine the effect of xNek9 depletion on the two pathways of microtubule assembly.

5.1. xNek9 function in the centrosomal pathway of microtubule assembly

To examine the role of xNek9 in microtubule assembly at the centrosome we performed experiments looking at aster formation by sperm nuclei. Purified sperm nuclei consist of chromatin and an immature centrosome. Upon addition to egg extract the immature centrosome recruits proteins essential for microtubule nucleation, a process called maturation (Gomez-Ferreria and Sharp, 2008). The mature centrosome then nucleates and stabilizes microtubules and forms a microtubule aster that is also influenced by the RanGTP gradient that forms around the condensed chromatin.

Therefore, we added purified sperm nuclei to control or xNek9 depleted egg extract and incubated for 15 minutes to allow centrosome maturation and microtubule assembly. Subsequently, the samples were fixed and processed for immunofluorescence. We found that microtubule assembly was not abolished upon xNek9 depletion but asters had less microtubules and appeared smaller compared to control (Figure 15A). Indeed, xNek9 depletion caused a slight but significant 12% decrease in microtubule density (Figure 15B). In addition, aster microtubules were significantly shorter (10,1 μm versus 11,3 μm in control). These findings indicated a defect in microtubule formation due to the absence of xNek9.

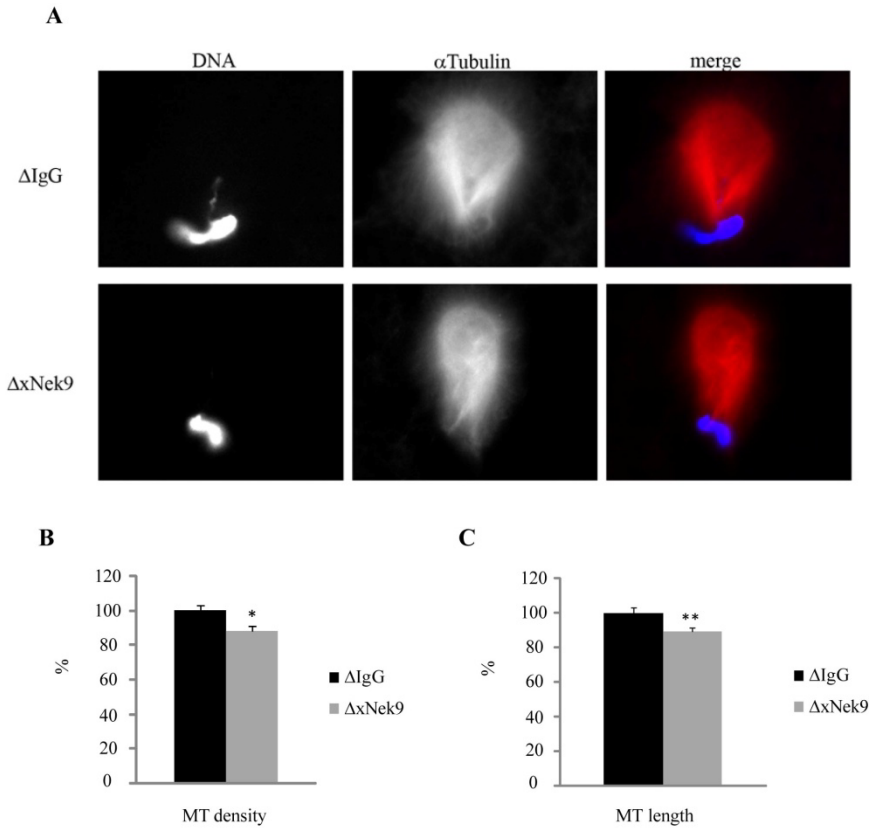

Figure 15: Depletion of xNek9 affects centrosome maturation

(A) Representative fluorescence images of sperm nuclei induced asters in egg extract previously depleted using IgG or anti-xNek9 (Ct 707-944) antibodies. DNA, blue; Tubulin, red; **(B)** Graph representing the average percentage of microtubule (MT) density in control and xNek9 depleted egg extract; results are from 5 independent experiments, each with at least 30 analyzed asters analyzed; **(C)** Graph representing the microtubule length in control and xNek9 depleted egg extract; results are from 5 independent experiments, each with at least 30 analyzed asters analyzed; length is visualized in percentage to enable the comparison between extracts.

5.2. xNek9 function in the RanGTP dependent pathway of microtubule assembly

To determine whether Nek9 has a role in the RanGTP dependent microtubule assembly pathway, RanGTP at a final concentration of 15μM was added to control or xNek9 depleted egg extract. We observed RanGTP induced aster formation over time in both conditions by taking representative samples each five minutes. Therefore, one microliter of extract was fixed and spotted between a slide and a coverslip and the number of microtubule asters recorded. Representative images of each time point are shown in figure 16A**.** In control depleted extract the first asters appeared at 10 minutes after RanGTP addition. Asters grew in number of recruited microtubules and reached their maximum length at 15 minutes. Subsequently, at 20 minutes asters progressively clumped forming connections between each other. These connections may consist of antiparallel microtubules. With time the connected asters became smaller, with shorter microtubules. At 25 minutes asters appeared small, with many short microtubules. In addition, minispindles, a bipolar structure based on two interconnected asters, appeared as pointed out by the white arrow (Figure 16B). Interestingly, RanGTP induced asters that were formed in xNek9 depleted egg extract showed the same morphology as control with the exception of a delay in timing. Whereas in control the first asters appeared at 10 minutes, asters in xNek9 depleted extract only appeared at 15 minutes. The aster morphology was identical to control and also minispindles were observed in xNek9 depleted extract at later time points. To confirm the delay in aster formation seen by fluorescence microscopy, we counted the number of asters at each time point (Figure 16B). The first asters appeared at 10 minutes with a strong increase in total aster number at 15 minutes entering into a plateau phase after 20 – 25 minutes. Aster formation in xNek9 depleted egg extract was delayed and

did not exhibit a strong increase but a steady growth of aster number. At our last time point (25 minutes) we counted 56,9% less asters in xNek9 depleted egg extract. Other RanGTP induced aster experiments showed similar timings (data not shown). In addition, RanGTP asters assembled in xNek9 depleted egg extract formed minispindles similar to the ones in control egg extract suggesting no impairment of aster formation. Therefore our data suggest a delay of RanGTP induced aster assembly in the absence of xNek9 and support a role for xNek9 in microtubule assembly during mitosis.

These experiments were performed in egg extract depleted from xNek9 by using anti-xNek9 (Nt3-18) antibodies. Mass spectrometry analysis of the double band appearing in the immunoprecipitation showed later that the higher band was indeed xNek9 (Figure 16C). The lower band was identified as Heat shock protein 105 and 110 (Hsp105/Hsp110). Therefore the egg extract was depleted from xNek9 and also from Hsp105 and Hsp110. As a consequence, the results on RanGTP aster formation must be interpreted with caution. However results are in agreement with previously published results on xNek9 function in the RanGTP pathway (Roig et al., 2005).

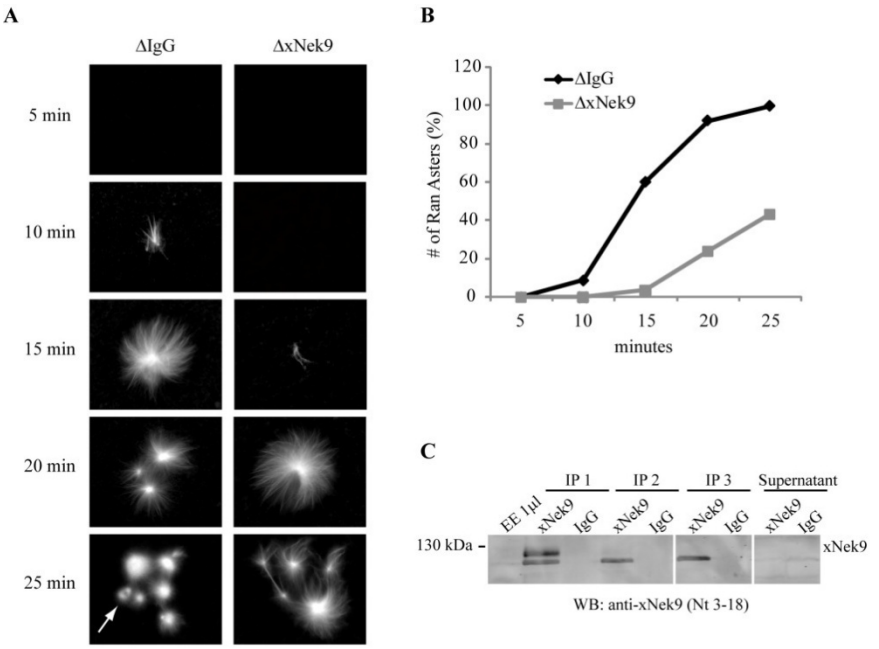

Figure 16: Depletion of xNek9 slows down RanGTP induced aster formation
(A) Representative time course of RanGTP induced aster formation in control and xNek9 depleted egg extract; asters are visualized by incorporation of Rhodamin-Tubulin in growing microtubules. The white arrow marks a minispindle. **(B)** Representative quantification of RanGTP induced aster experiment, shown in A. **(C)** Western blot analysis for xNek9 depletion. Anti-xNek9 (Nt 3-18) immunoprecipitates two bands with the higher one being xNek9 and the lower one later identified by mass spectrometry as Hsp105/110.

6. Mass spectrometry analysis identifies xNek9 interactors

The mitotic phenotypes observed upon xNek9 depletion or GST-xNek9 Ct addition, the decrease in microtubule density in sperm nuclei induced asters and the delay in RanGTP induced aster formation strongly suggested that microtubule assembly was partially impaired in the absence of xNek9. Thus, we sought to identify proteins important for microtubule assembly that simultaneously interacted with xNek9.

Therefore we performed immunoprecipitation experiments using anti-xNek9 (Ct 707-944) antibodies and analysed the samples by mass spectrometry analysis. Amongst the identified xNek9 interaction partners we found several γTubulin complex proteins (GCP) already known as interaction partners, several centrosomal proteins (Cep63, Cep152, POC5, Ninein, PCM1), both tubulin subunits, and chromosomal related proteins (Cenp-E, Kif4) (Table 1).

anti-xNek 9 (Ct 707-944)	anti-xNek9 (Nt 3-18)
xNek9	xNek9
GCP 2	GCP 2
GCP 3	GCP 3
GCP 4	GCP 4
GCP 6	GCP 6
Nedd 1	Nedd 1
Cep 63	
Cep 152	
POC 5	
Ninein	
PCM-1	PCM-1
α-Tubulin	
β-Tubulin	
Importin β	Importin β
Importin α	
Cenp-E	Cenp-E
Kif 4	
NUP 107	
	Clasp 1
Rac Gap 1	
Kif 1A	
Kif 3C	
	Clathrin
PP1A subunit 12	
	Nucleolar GTP-BP 1

Table 1: Mass spectrometry identifies various xNek9 interaction partners
Magnetic beads coated with antibodies anti-xNek9 (Ct 707-944) or anti-xNek9 (Nt 3-18) were incubated in CSF-arrested egg extract for 1h. Then the beads were retrieved, immunoprecipitated proteins were eluted and subjected to mass spectrometry analysis. A selected list of proteins is depicted in the table.

7. xNek9 is a possible regulator of the γTubulin Ring Complex (γTuRC)

7.1. xNedd1 is interaction partner of xNek9

One novel partner of xNek9 identified by mass spectrometry was xNedd1, also called GCP-WD. Using our three different anti-xNek9 antibodies we consistently found xNedd1 in the co-immunoprecipitate (Figure 17A, B, C). xNedd1 is proposed to function as the adaptor protein of the γTuRC, a complex crucial for microtubule nucleation (Luders et al., 2006). Using the anti-xNek9 (Nt 3-18) peptide antibody for immunoprecipitation xNedd1 was co-immunoprecipitated to up to 70% of total xNedd1 protein in CSF – arrested egg extract suggesting that xNek9 – xNedd1 interaction may not only be transient but may have also a structural role (Figure 17A). Using the anti-xNek9 (Ct 707-944) antibody the interaction was weaker which may be due to a partial competition of binding by the antibody (Figure 17C). Furthermore we also found γTubulin, the major component of the γTuRC in the co-immunoprecipitation strengthening the possibility of xNek9 having a role in the regulation of microtubule nucleation (Figure 17A, B, C).

7.2. xNek9 – xNedd1 – γTubulin interaction may be regulated by RanGTP

To examine whether the interaction of xNek9, xNedd1and γTubulin exists both in mitosis and interphase, we performed immunoprecipitation experiments in mitotic and interphase egg extract using polyclonal anti-xNedd1 antibodies. To obtain interphase egg extract, CSF – arrested egg extract was sent into interphase by calcium addition and supplemented with 100 μg/ml cycloheximide to inhibit novel protein synthesis. We found that xNedd1 co-immunoprecipitates xNek9 and γTubulin in both cell cycle stages suggesting that the ternary complex not only exists in mitosis but also in interphase (Figure 17D). As previously reported, xNedd1 is phosphorylated in mitosis and therefore exhibits a slower mobility in SDS-Page of the mitotic but not the interphase sample (Luders et al., 2006).

To shed further light onto the xNek9 – xNedd1 – γTubulin complex and its regulation we next tested whether their interaction is regulated during mitosis by RanGTP. Therefore we immunoprecipitated xNek9 from CSF – arrested egg extract previously incubated with RanGTP for 10 minutes to induce the release of microtubule assembly factors. We found that xNek9 interacts with xNedd1 both in the presence and absence of RanGTP. Importantly, xNek9 – xNedd1 interaction appears stronger in the presence of RanGTP, indicating that this interaction may be regulated by RanGTP (Figure 17E). This is in agreement with our results regarding RanGTP induced aster formation being delayed in the absence of xNek9. xNek9 also co-immunoprecipitated γTubulin but IgG control antibodies also pulled down this protein. Further experiments will be needed to determine whether the interaction between xNek9 and γTubulin is regulated by RanGTP.

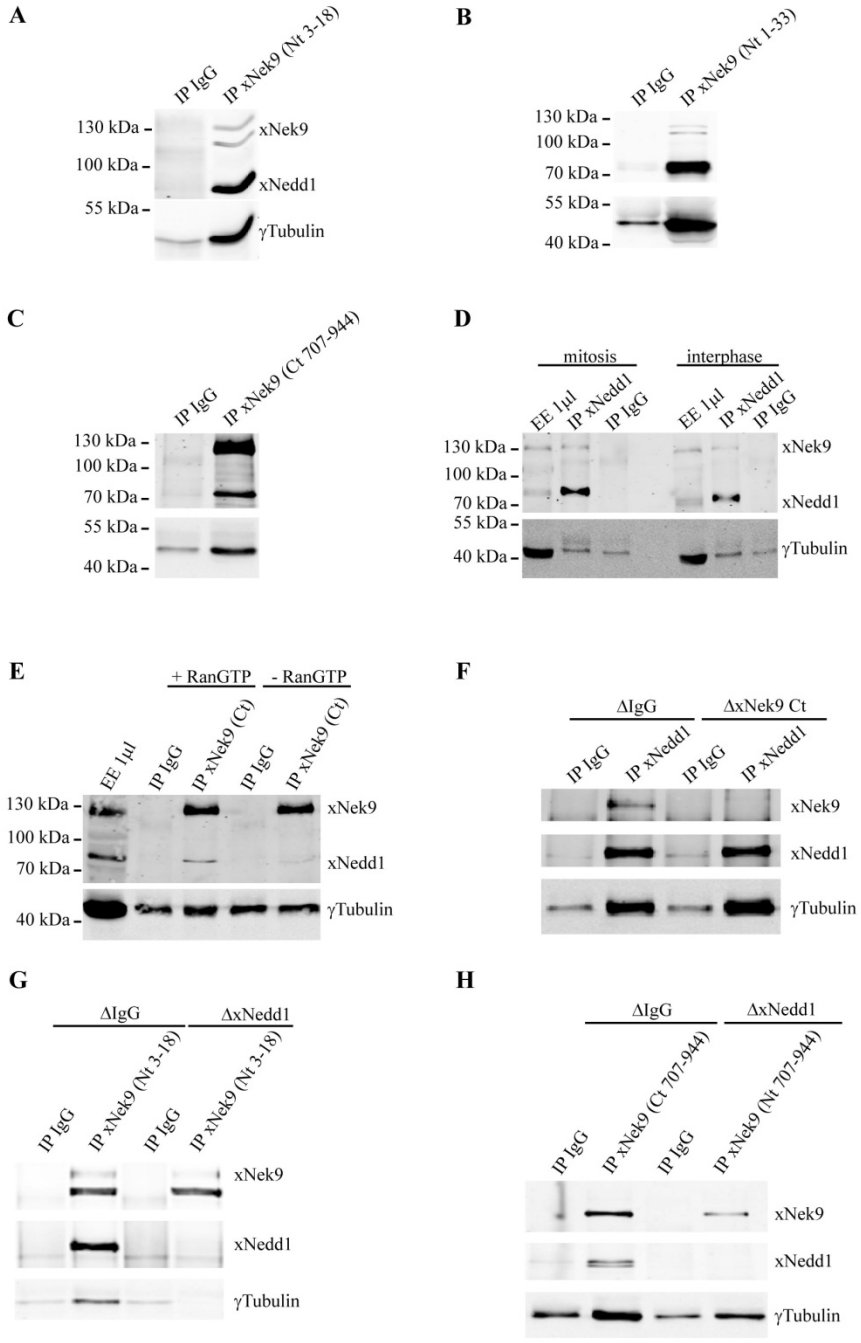

Figure 17: The γTuRC adaptor protein xNedd1 is interactor of xNek9

(A), **(B)**, **(C)** Western blot of an immunoprecipitation experiment from egg extract using three different anti-xNek9 antibodies (anti-xNek9 Nt 3-18; anti-xNek9 Nt 1-33; anti-xNek9 Ct 707-944); all three antibodies co-immunoprecipitate xNedd1 and γTubulin; both anti-xNek9 Nt antibodies show a doublet at around 130kDa that mass spectrometry analysis later identified as xNek9 (upper band) and as Hsp105/110 (lower band). **(D)** Western blot of xNedd1immunoprecipitation from CSF-arrested and interphasic egg extract. xNek9 and γTubulin co-immunoprecipitate. **(E)** Western blot of an immunoprecipitation experiment from egg extract in presence or absence of 15μM RanGTP. xNek9 co-immunoprecipitates xNedd1 stronger in presence of RanGTP. **(F)** Western blot of an immunoprecipitation experiment from control or xNek9 depleted egg extract. γTubulin co-immunoprecipitates with xNedd1 also in absence of xNek9. **(G)** Western blot of an immunoprecipitation experiment from control or xNedd1 depleted egg extract. In absence of xNedd1, xNek9 does not co-immunoprecipitate γTubulin. **(H)** Western blot of an immunoprecipitation experiment from control or xNedd1 depleted egg extract. γTubulin co-immunoprecipitates with xNek9 in absence of xNedd1.

7.3. xNek9 and xNedd1 can bind γTubulin independently

To examine whether the interaction of xNek9 with xNedd1 – γTubulin exists both in mitosis and interphase, we performed immunoprecipitation experiments in mitotic and interphase egg extract using polyclonal anti-xNedd1 antibodies. To obtain interphase egg extract, CSF – arrested egg extract was sent into interphase by calcium addition and supplemented with 100 μg/ml cycloheximide to inhibit novel protein synthesis. We found that xNedd1 co-immunoprecipitates xNek9 and γTubulin in both cell cycle stages suggesting that the ternary complex not only exists in mitosis but also in interphase (Figure 17D). As previously reported, xNedd1 is phosphorylated in mitosis and therefore exhibits a slower mobility in SDS-Page of the mitotic but not the interphase sample (Luders et al., 2006).

To shed further light onto the xNek9 – xNedd1 – γTubulin complex and its regulation we next tested whether their interaction is regulated by

RanGTP. Therefore we immunoprecipitated xNek9 from CSF – arrested egg extract previously incubated with RanGTP for 10 minutes to induce the release of microtubule assembly factors. We found that xNek9 interacts with xNedd1 both in the presence and absence of RanGTP. Importantly, xNek9 – xNedd1 interaction appears stronger in the presence of RanGTP, indicating that this interaction may be regulated by RanGTP (Figure 17E). This is in agreement with our results regarding RanGTP induced aster formation being delayed in the absence of xNek9. xNek9 also co-immunoprecipitated γTubulin but IgG control antibodies also pulled down this protein. Further experiments will be needed to determine whether the interaction between xNek9 and γTubulin is regulated by RanGTP.

8. The γTuRC adaptor protein xNedd1 is a substrate of xNek9

Nek9 is a mitotically active kinase (Roig et al., 2005). To examine whether xNedd1 is also a substrate of xNek9 we performed in vitro kinase assays with Flag-xNek9 and recombinant GST-xNedd1 C-terminus (Ct), purified from bacteria. Flag-xNek9 strongly phosphorylated recombinant GST-xNedd1 Ct but not GST alone (Figure 18A). We obtained the sameresult with the human proteins. Flag-hNek9 readily phosphorylated the C-terminus of hNedd1 (Figure 18B). We next sought to identify the specific sites of xNedd1 that were phosphorylated by Flag-xNek9. Therefore we repeated the kinase assay, subsequently immunoprecipitated GST-xNedd1 Ct and sent the samples for analysis of phosphorylated peptides by mass spectrometry. Two different peptides in GST-xNedd1 Ct were found to be phosphorylated by Flag-xNek9 with serine 378 and serine 440 being the proposed targets of phosphorylation. To test whether these amino acids are also phosphorylated “in vivo” we

immunoprecipitated endogenous xNedd1 from CSF – arrested egg extract and repeated the Phospho-mass spectrometry analysis. Indeed, these sites were also phosphorylated "in vivo". Site directed mutagenesis of these two serines to alanine however did not abolish the in vitro phosphorylation detected by radiography, suggesting that xNek9 was able to phosphorylate other sites (data not shown).

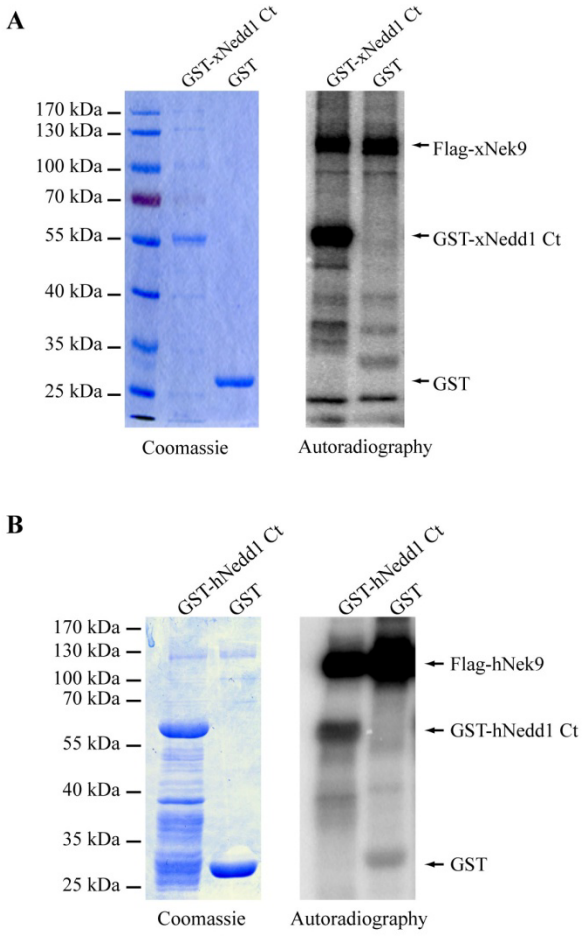

Figure 18: The γTuRC adaptor protein xNedd1 is substrate of xNek9
(A) Coomassie stained gel and corresponding autoradiography of a kinase assay using purified Flag-xNek9 and GST-xNedd1 Ct or GST as substrate. Flag-xNek9

phosphorylates GST-xNedd1 but not GST. **(B)** Coomassie stained gel and corresponding autoradiography of a kinase assay using purified Flag-hNek9 and GST-hNedd1 Ct or GST as substrate. Flag-hNek9 phosphorylates GST-hNedd1 but not GST.

9. xNek9 depletion interferes with the recruitment of xNedd1 to the immature sperm centrosome

Previous experiments have shown that xNek9 depletion causes a decrease in microtubule density and microtubule length in sperm nuclei induced asters. To assess whether these effects may be due to a misregulation of the newly identified interactor and substrate xNedd1, we took advantage again of the sperm nuclei induced aster formation assay and observed xNedd1 recruitment to the aster. We added purified sperm nuclei to control or xNek9 depleted egg extract and incubated for 15 minutes to allow centrosome maturation and microtubule assembly. Subsequently, the samples were fixed and processed for immunofluorescence.

Although xNek9 depletion did not abolish xNedd1 recruitment to the asters, xNedd1 signal appeared slightly reduced by immunofluorescence (Figure 19A). Indeed, xNedd1/αTubulin ratio was significantly lower (24%) in asters formed in xNek9 depleted egg extract (Figure 19B). These results suggest that xNedd1 recruitment to the sperm nuclei induced asters is less efficient in the absence of xNek9. This effect on xNedd1 recruitment may explain at least in part the decrease in microtubule density and length observed in xNek9 depleted egg extract.

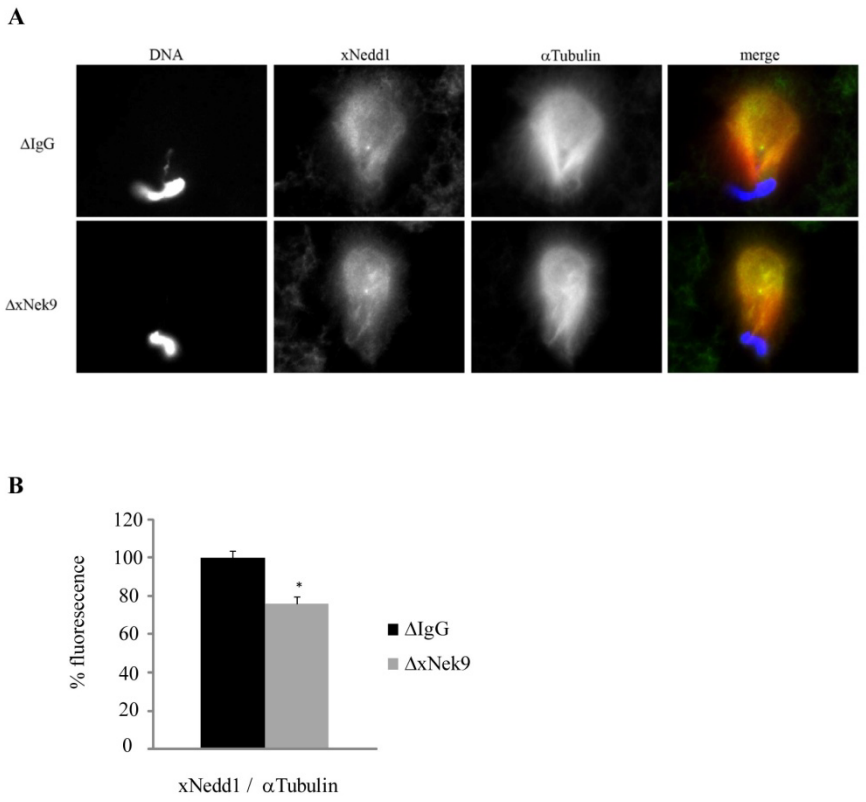

Figure 19: Depletion of xNek9 affects xNedd1 recruitment to sperm nuclei induced asters

(A) Representative fluorescence images of sperm nuclei induced asters in egg extract that was previously depleted using IgG or anti-xNek9 (Ct 707-944) antibodies. Tubulin, red; xNedd1, green; DNA, blue; **(B)** Graph representing the average percentage of xNedd1 fluorescence on microtubule asters in IgG control and xNek9 depleted egg extract; results are from 5 independent experiments, each with at least 30 analyzed asters;

10. xNek9 and its interaction partners do not promote microtubule assembly in pure tubulin

xNek9 depletion impairs microtubule assembly, possibly through its interaction with xNedd1 and the γTuRC. To directly test whether xNek9 and its interaction partners have microtubule nucleation capacity we

performed a bead assay. Therefore, anti-xNek9 antibody coated magnetic beads were incubated in CSF – arrested egg extract to recruit its interaction partners. Subsequently the beads were retrieved and washed. To check that indeed the endogenous protein was immunoprecipitated by the antibody coated beads, a fraction of beads were subjected to Western blotting. Figure 20A shows that XMap215, a known microtubule stabilizer used as positive control, and xNek9 were indeed concentrated on the corresponding beads. The remaining beads were incubated in pure tubulin for 15 minutes at 37ºC. Beads coated with anti-xNek9 (Ct 707-944) or anti-xNek9 (Nt 1-33) antibodies were not able to form microtubules in pure tubulin (Figure 20B). In contrast, beads coated with anti-XMap215 antibodies formed an array of microtubules (Figure 20B). These results suggest that the xNek9 complex is not sufficient to trigger microtubule nucleation despite the presence of γTubulin.

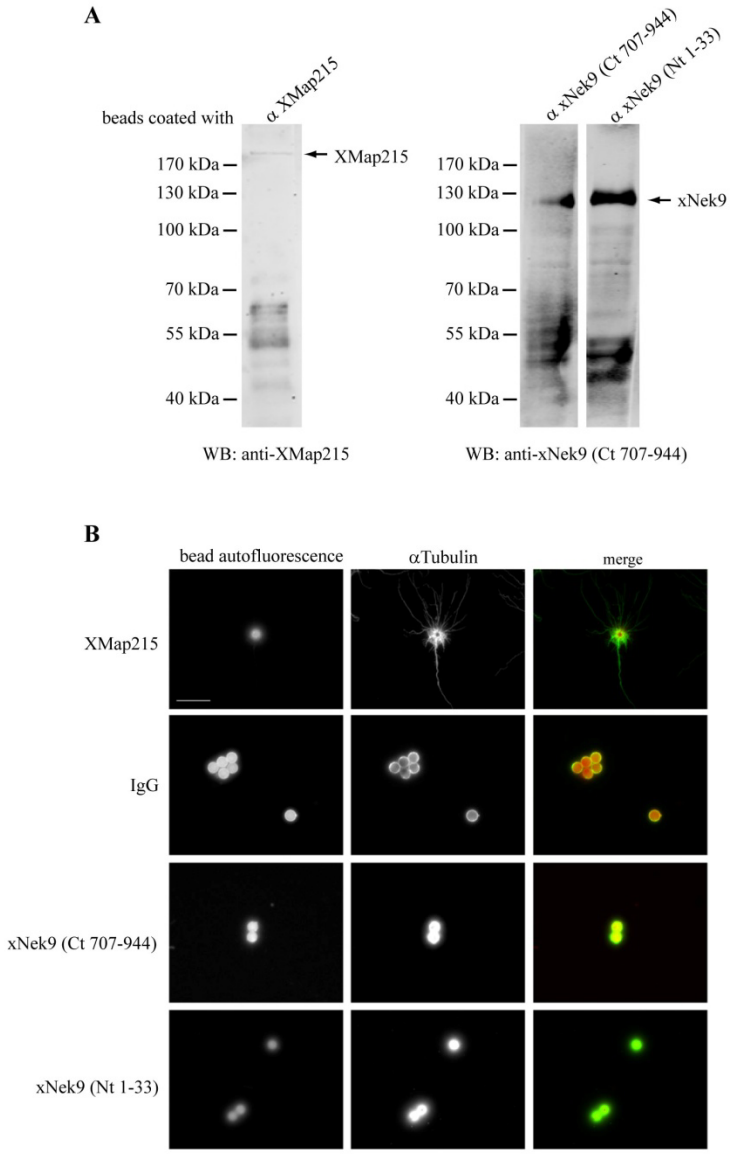

Figure 20: xNek9 and its interaction partners are not able to form microtubules in pure tubulin

(A) Western blot of a small fraction of magnetic beads. Immunoblotting with corresponding antibodies to check for presence of endogenous protein. **(B)** Representative fluorescence images of magnetic beads previously coated with IgG antibodies, XMap215 and xNek9 antibodies, incubated in egg extract and then transferred in pure tubulin. Bar 10μm.

Discussion

V. Discussion

The entry into mitosis marks for a cell a key timeframe during which it undergoes major changes at the molecular level. Proteins levels change, new protein-protein interactions form and post-translational modifications lead to changes in protein activity. In these processes, the Aurora-kinase family as well as the Polo-like kinase family are highly implicated. However, a third family is recently emerging as another important player in protein regulation.

NIMA-like kinase family members fulfil a variety of regulatory functions during the cell cycle reaching from DNA-damage response to cilia formation. They all have in common a highly conserved kinase domain at the N-terminus. It is thought that the divergent C-terminal tail "codes" for the specific function of each kinase. Some NIMA family kinases were found to play a crucial role during mitosis. Nek2 is essential for centrosome disjunction (Fry et al., 1998), Nek6 and Nek7 involved in mitotic progression (O'Regan and Fry, 2009) and Nek9 important for proper bipolar spindle assembly (Roig et al., 2005).

We started the project to shed light on the specific role of the *Xenopus* ortholog of Nek9, xNek9, during bipolar spindle assembly. Here, we showed that xNek9 may not function through a kinase cascade involving xNek6 during meiosis and it may not regulate the same substrates as in mitotic cells. Furthermore we confirmed a role of xNek9 in bipolar spindle assembly through an additional experimental setup and identified a previously unknown interaction between xNek9 and the γTubulin Ring Complex (γTuRC) adaptor protein xNedd1. In fact, xNedd1 is also substrate of xNek9. Finally, we characterized the function xNek9 in the centrosomal and RanGTP dependent pathway of spindle formation.

Our results lead us to propose a model of interaction between xNek9 and xNedd1 and a possible mode of action for their contribution to bipolar spindle assembly.

1. xNek9 function in meiosis may be different than in mitosis

In human cells Nek9 was found to be the upstream kinase of hNek6 and hNek7 and to act through them on downstream targets such as hEg5 (Belham et al., 2003; Rapley et al., 2008). Our results suggest that this interaction and kinase cascade may not exist in a meiotic system such as the *Xenopus* egg extract. Using two different polyclonal antibodies and one peptide antibody (gift from Joan Roig) against xNek6, we were not able to identify xNek6 in *Xenopus* egg extract. However, a polyclonal antibody did indeed specifically recognise xNek6 in XL177 cell lysate, a cell line from *Xenopus* laevis tadpoles.

1.1. xNek6 and xNek7 may be translationally regulated but not xNek9

Xenopus egg extract derives from unfertilized *Xenopus* eggs that are naturally arrested in metaphase of meiosis II with large amounts of protein and translationally regulated mRNA stored for the first twelve embryonic divisions after fertilisation. Within these twelve divisions, no transcription takes place. Therefore, the absence of xNek6 in *Xenopus* egg extract (but presence in XL177 cells) raised the question whether the xNek6 gene is transcribed only after fertilisation, at later stages in development or whether xNek6 mRNA has been transcribed already before and is present in the egg extract as a translationally regulated mRNA. Several proteins with a function in spindle assembly such as TPX2 or xKid are known to

be encoded by translationally regulated mRNAs (Eliscovich et al., 2008). This regulation involves translational repressor proteins such as CPE binding protein (CPEB) and Maskin that bind to specific motifs at the 3'UTR of the mRNA and thus form an mRNA-protein loop structure that inhibits ribosome binding and therefore translation (Radford et al., 2008; Stebbins-Boaz et al., 1999). Indeed, xNek6 mRNA exhibits CPE motifs strongly suggesting a translational regulation. Interestingly, the translational repression of TPX2 or Xkid mRNA is released upon progesterone induction enabling their translation during oocyte maturation with protein accumulation until metaphase of meiosis II (Eliscovich et al., 2008). xNek6 mRNA, if present, would remain in a repressed state during oocyte maturation since xNek6 protein is not present at metaphase of meiosis II. However, xNek6 mRNA would be translated at the earliest after fertilisation by the entering sperm when embryogenesis starts.

We also checked the 3' UTR mRNA sequence of xNek9 and xNek7. xNek7 also shows one regulatory motif suggesting a translational regulation. We did not detect xNek7 in the egg extract, however our antibody may not be reliable because we did not detect xNek7 in *Xenopus* XL177 cell lysate either. Published data suggest that Nek6 and Nek7 are expressed only in early embryogenesis (Feige and Motro, 2002). In contrast to xNek6 and xNek7, xNek9 mRNA does not show any sequences required for translational regulation. This is in line with the fact that xNek9 protein indeed exists in the meiotic egg extract.

1.2. xNek6 and xNek7 may not be needed in meiosis

The absence of xNek6 and xNek7 protein in the meiotic egg extract raised also another question: which function of xNek6 and xNek7 is not needed in meiosis but then required in mitosis?

Meiosis and mitosis have in common various processes but exhibit also major differences. One of these differences is the acentrosomal segregation of genetic material. Whereas in mitosis two centrosomes participate in bipolar spindle assembly and faithful segregation of chromosomes, in meiosis bipolar spindle formation is based on chromosomal microtubule formation and the concerted action of motor proteins and other spindle assembly factors. Thus, an anastral spindle forms in absence of centrosomes (Loughlin et al., 2010; Theurkauf, 2001). In fact, Nek6 and Nek7 localisation has been reported as centrosomal by several authors (Kim et al., 2007; O'Regan and Fry, 2009; Rapley et al., 2008; Yin et al., 2003; Yissachar et al., 2006). Interestingly, both kinases have been proposed recently to regulate microtubule organisation from the poles and within the spindle (O'Regan and Fry, 2009). Both, their localisation and their implication in microtubule organisation from the poles are controversial for meiotic spindle formation. Therefore, it may indeed be possible that xNek6 and xNek7 protein are only essential after fertilisation when the sperm contributes to embryogenesis by providing a centrosome.

Future experiments such as RT-PCR on *Xenopus* egg extract will reveal whether xNek6 and xNek7 mRNAs are indeed present. Furthermore, a time course of progesterone stimulated oocytes will enable us to collect oocytes in different developmental stages and to examine if xNek6 and xNek7 are present.

1.3. xNek9 may have different substrates

The absence of xNek6 in the egg extract raised the question whether xNek9 may directly bind and phosphorylate xEg5 instead of xNek6. However, we could not detect any interaction between xNek9 and xEg5

by immunoprecipitation. Although we cannot exclude that the interaction indeed exists, we could not find any evidence for this. The question remains whether later on in development the cascade may form. Interestingly, preliminary experiments indicate that exogenous GST-xNek6 but not GST is able to pull down endogenous xNek9 in meiotic egg extract suggesting that indeed this interaction also may exist later in early embryogenesis (data not shown).

Altogether we propose that xNek9 functions may be different in meiosis and that it may have different substrates compared to mitotic systems.

2. Localisation of xNek9

Nek9 localisation was reported to be cytoplasmic in human cells. At the entry into mitosis a small proportion of total Nek9 is activated through phosphorylation at threonine 210 (T210) and concentrated at the centrosomes in G2 / M. Similarly, xNek9 was reported to localise at the poles of bipolar spindles assembled in *Xenopus* egg extract (Roig et al., 2005). Our results only partially confirm this as we did not detect any xNek9 localisation in *Xenopus* egg extract spindles. One explanation for our negative result may be that the centrosomal region is not as accessible for the antibodies due to high presence of other proteins and microtubule focusing in that area. In agreement, we could detect xNek9 in centrosomal asters in egg extract. Maybe the reduced number of microtubules allowed a better accessibility of the antibody. Since only around 5% of total Nek9 is phosphorylated during mitosis (Roig et al., 2005) it is possible that very specific detection methods are needed to visualize this pool of localised xNek9 (preextraction, different antibodies, antibody concentration and fixation methods). Interestingly, we also detect increased xNek9 staining

around the chromatin in the metaphase plate. This may indicate that xNek9 not only has a function at the centrosome but also at the chromatin.

Altogether, we find xNek9 localising at the centrosome both in centrosomal asters and XL177 cells. In addition, we visualize xNek9 accumulation around the chromatin in XL177 cells.

3. Function of xNek9

Previous studies proposed that Nek9 has a role in mitotic progression. Microinjection of anti-Nek9 antibodies causes various phenotypes in different cell types reaching from prometaphase arrest to spindle abnormalities and aberrant chromosome segregation (Roig et al., 2002). In addition, experiments in *Xenopus* egg extract showed a delay in bipolar spindle assembly and the appearance of aberrant microtubule structures (Roig et al., 2005).

Using various approaches we aimed at getting a better understanding of xNek9 function in bipolar spindle formation.

3.1. xNek9 has a role in bipolar spindle assembly

We observed bipolar spindle assembly upon xNek9 depletion, addback of increased amount of Flag-hNek9 (30nM) and addition of recombinant GST-xNek9 Ct. We consistently found a substantial decrease of bipolar spindles and a high increase in monopolar spindles and aberrant structures. These results indicate that those phenotypes are specific for the loss / impairment of xNek9 function and strongly suggest a role of xNek9 in bipolar spindle assembly. Moreover, the depletion experiments were performed with two different antibodies, anti-xNek9 (Ct 707-944) or anti-

xNek9 (Nt 3-18) antibody. Although this antibody co-depletes unspecifically Hsp105 and Hsp110, it showed the same result. Therefore we conclude that co-depletion did not affect the experimental outcome. Moreover, the specificity of the phenotypes observed after depleting xNek9 could be proven by adding back Flag-hNek9 at a final concentration of 10nM. In addition, our results are in agreement with previous studies (Roig et al., 2005).

However, three questions remain to be solved:

a) Why the addback of Flag-hNek9 at 10nM final concentration rescues xNek9 depletion while the endogenous concentration is around 150nM?
b) Why does Flag-hNek9 at 30nM final concentration impair bipolar spindle assembly?
c) Why does GST-xNek9 Ct act as a dominant-negative?

Three possibilities may explain the requirement of this low concentration of 10nM Flag-hNek9 to rescue: (1) an increased kinase activity of exogenous Flag-hNek9 compared to endogenous xNek9. We do not favour this explanation since exogenous Flag-hNek9 is added directly after xNek9 depletion to the egg extract. Therefore, Flag-hNek9 cycles through interphase before entering mitosis again and should get into the same regulatory events as the endogenous kinase. (2) Flag-hNek9 encounters an activator in the egg extract. It has very recently been published that hNek9 interacts with Dynein light chain / LC8 which acts as a hub for hNek9, enables its oligomerization and favours its autoactivation (Regue et al., 2011). hNek9 – LC8 binding depends on previous hNek9 autophosphorylation at serine 944. Interestingly, neither this serine nor the binding domain required for LC8 binding exist in xNek9 kinase. It may be possible that Flag-hNek9 kinase, once added to

the egg extract, forms a complex with LC8 and gets activated. However, this is unlikely because we could obtain a rescue by addition of 50nM Flag-xNek9 (preliminary data). (3) the co-depletion of regulators together with xNek9 from the extract. Without these regulators, Flag-hNek9 kinase activity may not be regulated accordingly and small amounts of Flag-hNek9 may be sufficient to fulfil the role of endogenous xNek9. Since no candidate inhibitory protein is known immunoprecipitation experiments and subsequent mass spectrometry analysis may be required for preliminary candidate identification.

While addback of Flag-hNek9 at 10nM final concentration rescues xNek9 depletion, Flag-hNek9 at 30nM impairs bipolar spindle assembly similar to xNek9 depletion. Three possibilities may account for this effect. (1) as discussed above, an increased kinase activity or missing interaction partners that regulate kinase activity. Increasing amounts of Flag-hNek9 may act as dominant-negative on substrates. (2) Flag-hNek9 forms inactive complexes. Increasing amounts of Flag-hNek9 may induce the formation of oligomerization of Flag-hNek9 without stimulating the kinase activity. As a consequence, Flag-hNek9 addition is without effect on bipolar spindle assembly and mimics the xNek9 depletion condition. (3) the addback of additional proteins alongside with Flag-hNek9 that may also cause a dominant-negative phenotype when added to the egg extract. Indeed, a coomassie analysis of purified Flag-hNek9 for interaction partners shows two faint bands at the size of around 100kDa and 70kDa. Compared to the Flag-hNek9 at 130kDa, these two bands seem negligible. Still, those two bands and possibly other non visible bands represent proteins that are added to the egg extract concomitantly to Flag-hNek9 addition. We checked for hAurA and hNek6 since hAurA was proposed as hNek9 interactor by “Mitocheck”, a European research consortium on cell cycle control (www.mitocheck.org) and hNek6 as part of the kinase

cascade hNek9 – hNek6. Being kinases both proteins were good candidates to influence Flag-hNek9 action after addback. However, none of these kinases were detected in Western blot analysis of Flag-hNek9 pull downs.

GST-xNek9 Ct induces similar phenotypes to xNek9 depletion. How does this xNek9 fragment cause the effect? Three modes of action seem possible. (1) GST-xNek9 Ct dimerizes with endogenous xNek9. Previously it was proposed that Nek9 transactivates upon dimerization through the coiled coil domain (Regue et al., 2011; Roig et al., 2002). GST-xNek9 Ct dimerization with endogenous xNek9 would inhibit activation since it lacks the kinase domain. Endogenous xNek9 would then remain inactive and therefore could not perform its tasks in spindle assembly. By Western blot we did not find endogenous xNek9 in a pull down of GST-xNek9 Ct which was previously incubated in *Xenopus* egg extract suggesting that GST-xNek9 Ct does not dimerize with endogenous xNek9. However, we cannot rule out that the interaction indeed exists. Further pull down experiments and subsequent mass spectrometry analysis are ongoing. (2) GST-xNek9 Ct competes with endogenous xNek9 for its interaction partners. Nek9 binds Nek6 and Nek7 through the C-terminus. In addition, coiled-coil domains favour protein interaction as shown by Nek9 – Nek9 dimerization through this domain. Therefore, addition of GST-xNek9 Ct may sequester interaction partners and therefore inhibit xNek9 kinase function or xNek9 structural function through mere interactions. However, a GST-xNek9 Ct pull down was surprisingly “clean” on a coomassie stained SDS-PAGE so that no candidate interactor could be identified by mass spectrometry analysis. Further experiments may be required to identify possible interactors.

Altogether we conclude that xNek9 plays a major role in bipolar spindle assembly. Furthermore our results show that xNek9 concentration requires tight regulation for proper spindle assembly. In addition, we find that GST-xNek9 Ct acts as a dominant-negative and may be used in the future as a new tool to study xNek9 function in spindle assembly. Its way of action remains to be elucidated.

3.2. xNek9 has a role in microtubule formation from the centrosome and at the chromatin

Previously it was shown that xNek9 interacts with γTubulin and γTuRC members (Roig et al., 2005). We confirmed these interactions and in addition, identified xNedd1 as a novel interactor. xNedd1 was reported to be required for centrosomal and chromatin-mediated microtubule nucleation. Interestingly, RNAi of Nedd1 causes the formation of monopolar structures (Haren et al., 2006; Luders et al., 2006) similar to those seen by us suggesting an xNek9 – xNedd1 interplay in microtubule nucleation. Monopolar structures can be the consequence of impaired microtubule nucleation from the centrosome. The reduced number of nucleated microtubules may bind a limited number of motors that eventually would not be sufficient to induce initial centrosome separation. Therefore, the centrosomes may remain close together and form a monopolar aster (Boleti et al., 1996; Kapitein et al., 2005; Tanenbaum and Medema, 2010). Therefore, the increase in monopolar structures that we observe under various conditions (xNek9 depletion, increased Flag-hNek9 addback to 30nM final concentration and GST-xNek9 Ct addition) suggests a function for xNek9 in microtubule nucleation and/or centrosome separation. Indeed, a combination of all our depletion experiments results in a significant 11% decrease of microtubule density

in bipolar spindles (data not shown). Moreover, increasing addback of Flag-hNek9 to 30nM to the egg extract decreases microtubule density of 45%. However, this effect on bipolar spindle formation is not exclusively due to the centrosomal pathway of microtubule formation but includes also the RanGTP pathway. Our experiments on sperm nuclei induced asters were performed to get a closer look on the centrosomal effect of microtubule nucleation even though the RanGTP induced effect cannot be totally excluded. Indeed, similar to the overall effect on bipolar spindles, xNek9 depletion affects also the sperm nuclei induced aster formation by decreasing microtubule density and microtubule length. It is noteworthy that microtubules are located mostly around the centrosome and not around the chromatin suggesting that the nucleated microtubules mainly are due to centrosomal activity.

Our results also support a role of xNek9 in microtubule nucleation at the chromatin. We found that RanGTP induced aster formation is delayed upon xNek9 depletion which is in agreement with previously published data (Roig et al., 2005). However, in our hands, RanGTP asters formed in xNek9 depleted egg extract are not different in morphology compared to control. Our data suggest that xNek9 delays but does not impair the formation of asters since at later timepoints in both conditions so called "minispindles" are formed. One possibility to explain the delay of aster formation may arise from the observation that RanGTP strengthen the interaction between xNek9 and xNedd1. Therefore, xNek9 depletion may decrease substantially the microtubule nucleation capacity of xNedd1 and the γTuRC in the egg extract and thus delay aster formation. Indeed, several other hints support the idea that xNek9 is regulated by RanGTP. Previously it was reported that Nek9 is able to bind Ran in both forms, RanGDP or RanGTP with preference for RanGDP. Furthermore, Nek9 exhibits an RCC1-like domain although crucial amino acids are missing or

mutated within and therefore has no GEF activity (Roig et al., 2002). Moreover, Nek9 has two classical nuclear localisation signals (NLS), stretches of basic aminoacids, which are essential for the binding of the importin complex (Roig et al., 2005). Although not entirely conserved, xNek9 exhibits similar basic amino acid stretches suggesting that these sequences may function as NLS. Indeed, in mass spectrometry analysis we find the importin complex as an xNek9 interaction partner supporting the idea that xNek9 may be regulated by RanGTP and partially be involved in microtubule formation at the chromatin. Also our confocal imaging data which localises xNek9 close to chromatin in the metaphase plate argues in this line.

Further data supports the idea that xNek9 functions in microtubule assembly possibly through xNedd1. Inhibition of xNek9 causes only partial xNedd1 recruitment to sperm nuclei induced asters and therefore decreased microtubule nucleation from the centrosome. Whether the recruitment signal is dependent on xNedd1 phosphorylation by xNek9 remains to be shown. xNek9 phosphorylates xNedd1 but the site and the role of phosphorylation remain to be elucidated.

Altogether, we find that xNek9 has an important role in microtubule formation from the centrosome and at the chromatin. As a potential effector of this role we identify xNedd1 as a novel xNek9 interactor and substrate. Furthermore we show that xNek9 is at least partially responsible for xNedd1 recruitment to the centrosome and exert its function at least in part through xNedd1. The role of xNedd1 phosphorylation in this process remains to be shown

Interestingly, Nedd1 is known to be phosphorylated by Cdk1 and Plk1 (Luders et al., 2006; Zhang et al., 2009). Their sequential phosphorylation is necessary to target Nedd1 and thereby the γTuRC to the centrosome

(Zhang et al., 2009). Zhang et al also propose that Nedd1 and thus γTuRC recruitment is not due to Nedd1 phosphorylation by Plk1 or the direct interaction between Plk1 and Nedd1. This is due to the fact that a Plk1 Phospho-site mimicking mutant of Nedd1 is not recruited to the centrosome. Thus, they propose that Plk1 regulates Nedd1 recruitment to the centrosome by regulating other centrosomal proteins. Under our conditions we have not detected an xPlk1-xNek9 interaction in immunoprecipitation experiments using any of our anti-xNek9 antibodies or anti-xPlk1 antibodies nor GST-xNek9 Ct for pull down experiments. However, we know through collaboration that Plk1 is not only interacting but also phosphorylating and activating hNek9 (Joan Roig, personal communication). Taking into account this knowledge and combining it with our data and published data by Zhang et al, we may establish the following model cascade (Figure 21). The Nek9 –Nedd1 – γTubulin complex exists in interphase as shown by our immunoprecipitation studies. At the onset of mitosis Cdk1 primes Nedd1 to enable phosphorylation by Plk1 (Zhang et al., 2009). Simultaneously, Plk1 activates the Cdk1 primed Nek9 kinase (Joan Roig, personal communication). Plk1 phosphorylation activates Nek9 which then induces Nedd1 phosphorylation. This may function as a recruitment signal for the Nek9 –Nedd1 – γTubulin complex to concentrate at the centrosome where the γTuRC nucleates microtubules that are necessary to push apart the duplicated centrosomes and to eventually assemble a bipolar spindle.

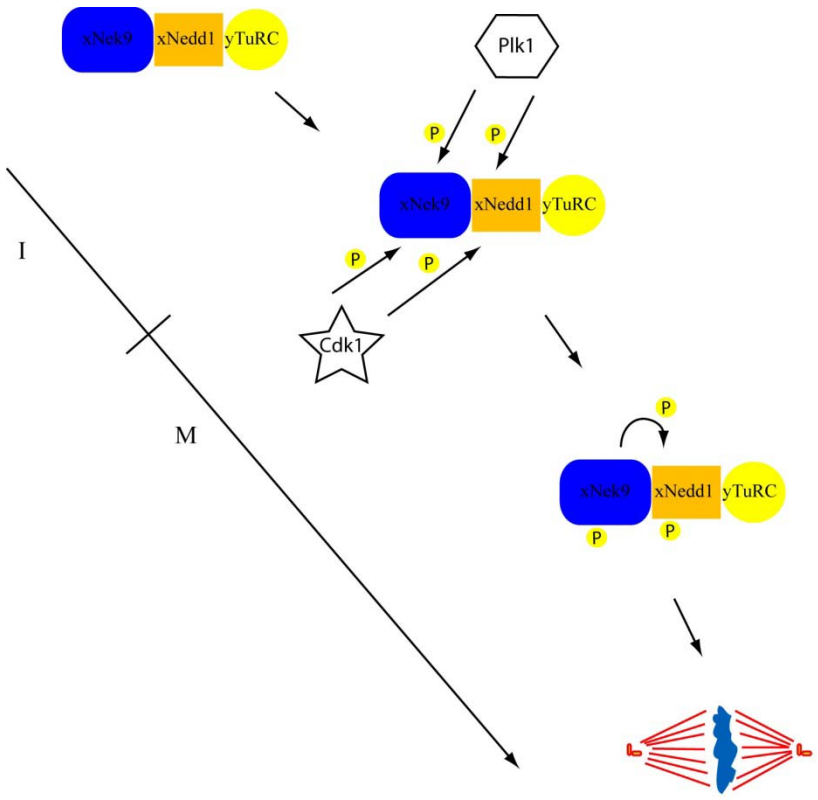

Figure 21: Model for xNek9 - xNedd1 recruitment to the mitotic spindle
xNek9, xNedd1 and γTubulin form a ternary complex during interphase. At the onset of mitosis, both xNek9 and xNedd1 are substrates for the priming kinase Cdk1 followed by Plk1 phosphorylation (Zhang et al, 2009; personal communication, Joan Roig,IRB); Nek9 phosphorylation activates the kinase activity which allows Nedd1 phosphorylation. The phosphorylation may be a recruitment signal to the spindle for microtubule nucleation during mitosis.

Indeed, external regulation of the Nek9 – Nedd1 – γTubulin complex is likely. By contrast to XMap215, a microtubule stabilizer, the xNek9 – xNedd1 – γTubulin complex on its own is not able to nucleate microtubules as shown in our bead assay results in pure tubulin. It remains

the question whether xNek9 and interaction partners are able to nucleate microtubules in egg extract. Concentration of γTubulin on beads in egg extract is not inducing microtubule nucleation (Popov et al., 2002). It is possible that through the interaction with xNek9 and xNedd1 and proper regulation in egg extract, γTubulin may gain this capacity.

Altogether, we propose a kinase cascade involving Cdk1 and Plk1 that activates the ternary complex Nek9 – Nedd1 – γTubulin and trigger their recruitment to the centrosome at the onset of mitosis.

4. Regulation of xNek9 – xNedd1 – γTubulin interaction

Several indications give a hint on how xNek9 may bind xNedd1 (Figure 22). Previously it was found that Nek9 forms a dimer through the coiled coil domain in its C-terminus (Roig et al., 2002). In addition, recent findings suggest that RCC1-like repeats form beta-propeller domains and act as interaction domains with other beta-propeller domains (Smith, 2008; Stevens and Paoli, 2008). Knowing that xNedd1 exhibits a WD40 domain which forms a beta propeller, this provides a possible model for the region of interaction and a possible binding orientation of Nek9 – Nedd1 (Manning and Kumar, 2007; Smith et al., 1999). Interaction through the RCC1 like repeats and WD40 domain of Nedd1 could cause proximity between Nek9 kinase domain and the C-terminus of Nedd1. We show that Nedd1 C-tail is indeed phosphorylated by Nek9 supporting our model of interaction. In addition, this binding orientation would allow both Nek9 and Nedd1 to bind γTubulin as shown in immunoprecipitation experiments. Interestingly, this model may also explain the at first sight controversial results on xNek9 – xNedd1 – γTubulin binding experiments using different anti-xNek9 antibodies. The model visualizes a possible

explanation why γTubulin is not found in an immunoprecipitate of xNek9 using anti-xNek9 (Nt 3-18) antibodies after xNedd1 depletion. The anti-xNek9 (Nt 3-18) antibody reacts against xNek9 exactly at the binding region of γTubulin causing a steric hindrance for γTubulin protein binding and therefore no signal in the Western blot. Finally, this model would also fit with the results of pull down experiments where GST-xNek9 Nt does pull down xNedd1, GST-xNek9 Ct however does not (data not shown).

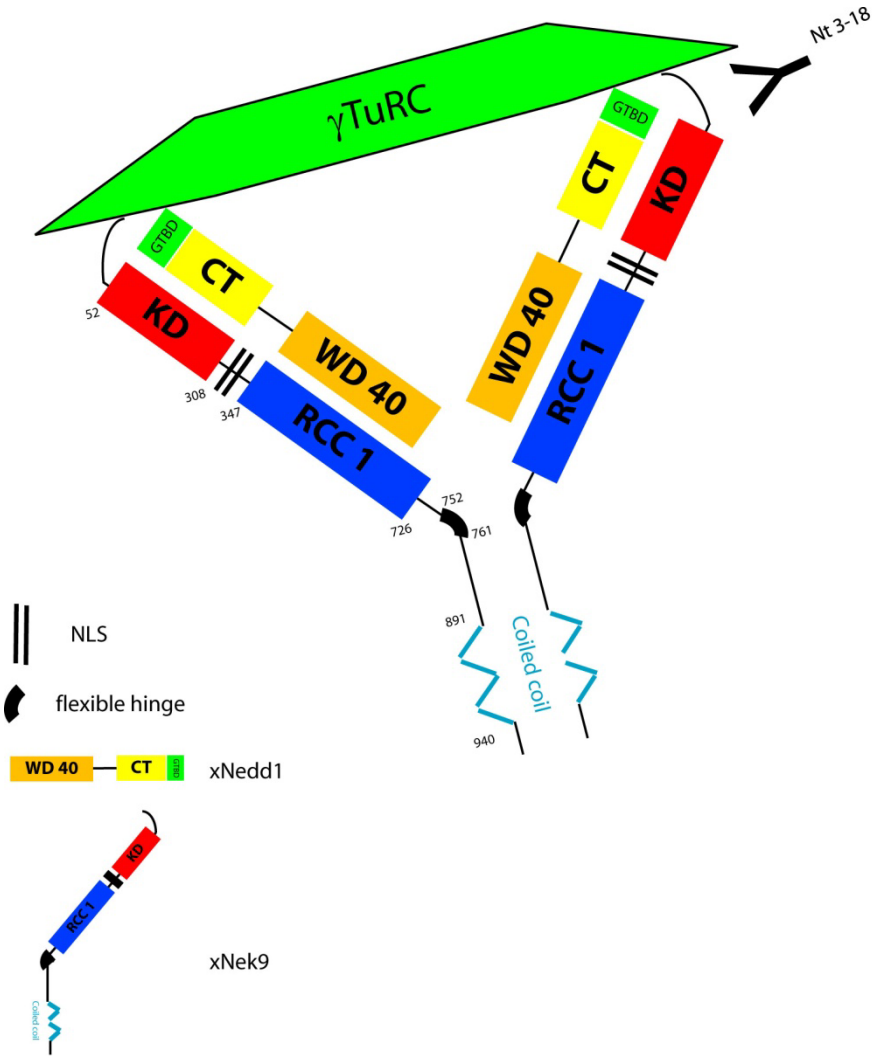

Figure 22: Model for xNek9 - xNedd1 interaction
Nek9 is known to dimerize through the C-terminus; recent publications suggest binding between RCC1 and WD domains, both being β-propeller domains; this orientation allows phosphorylation of Nedd1 C-terminus and concomitant binding of γTubulin; anti-xNek9 (Nt 3-18) antibody competes with γTubulin for Nek9 binding; numbers stand for amino acids in xNek9 full length protein (RCC1, Regulator of Chromosome Condensation 1; KD, Kinase Domain; CT, C-Terminus; GTBD, Gamma-Tubulin Binding Domain; NLS, Nuclear Localisation Signal)

5. Open questions

5.1. Does xNek9 alter chromosome structure?

The addback of Flag-hNek9 to 30nM final concentration strongly increased the appearance of aberrant structures with very condensed chromatin. This finding suggests that Flag-hNek9 may induce changes in chromosome structure or regulate chromosome condensation. Interestingly, NIMA kinase, the founder of the NIMA kinase family causes chromosome condensation when overexpressed in Aspergillus, fission yeast or human cells (O'Connell et al., 1994); similarly, the overexpression of fin1, the NIMA homologue in fission yeast, induces chromosome condensation from any point of the cell cycle (Krien et al., 1998). Previously it has also been suggested that the various functions of NIMA may be distributed among the different NIMA-like kinases in human cells (O'Connell et al., 2003). However, until now no NIMA-like kinase was proposed to function in chromosome condensation. Our data suggest that xNek9 may fulfil this role. Interestingly, NIMA was reported to phosphorylate histone H3 serine 10, a site which was previously correlated with chromosome condensation when phosphorylated (De Souza et al., 2000; Goto et al., 1999). Indeed, both Flag-hNek9 and Flag-xNek9 phosphorylate histone H3 in vitro (data not shown). Intriguingly, xNek9 exhibits an RCC1-like domain (RCC1, Regulator of Chromosome

Condensation). Although the name could suggest that RCC1 is required for chromatin condensation, experiments in *Xenopus* egg extract however have shown that RCC1 is important for the replication of sperm DNA and more importantly acts as the GTP exchange factor (GEF) for the small GTPase Ran (Dasso, 1993; Dasso et al., 1992; Hadjebi et al., 2008).

Therefore we propose that xNek9 may fulfil one role of the founder kinase NIMA in regulating chromosome condensation. Further experimental data are required to strengthen this idea.

5.2. Does xNek9 regulate spindle width?

Pooling all xNek9 depletion data, spindle width increases slightly but statistically significant (data not shown). Using mass spectrometry we found Kif4, the human homolog of Xklp1 as interaction partner. Xklp1, localised at the chromatin, was previously found to increase spindle width when depleted from *Xenopus* egg extract (Castoldi and Vernos, 2006).These results suggest that xNek9 may interact with and phosphorylate Xklp1. Indeed, in immunoprecipitation experiments we have confirmed an interaction between xNek9 and Xklp1 indicating a functional relationship. Interestingly, xNek9 depletion causes microtubule density decrease whereas Xklp1 depletion was reported to increase microtubule mass suggesting that xNek9 may negatively regulate Xklp1 localisation at the chromatin (Castoldi and Vernos, 2006). However, in preliminary experiments we have found that xNek9 depletion does not change Xklp1 localisation in *Xenopus* egg extract spindles.

More experiments will be required to understand that interesting interaction between xNek9 and Xklp1.

Conclusions

VI. Conclusions

1) There is no evidence for xNek6 or xNek7 presence in the meiotic *Xenopus* egg extract system. Therefore in meiosis xNek9 may not act through a kinase cascade as proposed for hNek9 in mitosis

2) xNek9 may have different substrates in meiosis. No interaction has been found with xEg5 which was previously proposed to be interaction partner and substrate of hNek9-hNek6 signalling module in mitosis

3) xNek9 putative role in spindle assembly is the regulation of microtubule assembly from the centrosome and at the chromatin

4) GST-xNek9 Ct acts as a dominant-negative and is a new tool to analyze xNek9 function;

5) xNek9 interacts with and phosphorylates xNedd1. This interaction is regulated by RanGTP

6) xNek9 is partially responsible for the recruitment of xNedd1 to sperm nuclei induced asters

7) xNek9 and interaction partners do not promote microtubule assembly in pure tubulin

VII. Bibliography

Akhmanova, A., and M.O. Steinmetz. 2008. Tracking the ends: a dynamic protein network controls the fate of microtubule tips. *Nat Rev Mol Cell Biol*. 9:309-22.

Alberts, B. 2008. Molecular biology of the cell. Garland Science, New York. 1725.

Amos, L.A., and D. Schlieper. 2005. Microtubules and maps. *Adv Protein Chem*. 71:257-98.

Andersen, J.S., C.J. Wilkinson, T. Mayor, P. Mortensen, E.A. Nigg, and M. Mann. 2003. Proteomic characterization of the human centrosome by protein correlation profiling. *Nature*. 426:570-4.

Baas, P.W., A. Karabay, and L. Qiang. 2005. Microtubules cut and run. *Trends Cell Biol*. 15:518-24.

Basto, R., J. Lau, T. Vinogradova, A. Gardiol, C.G. Woods, A. Khodjakov, and J.W. Raff. 2006. Flies without centrioles. *Cell*. 125:1375-86.

Belham, C., J. Roig, J.A. Caldwell, Y. Aoyama, B.E. Kemp, M. Comb, and J. Avruch. 2003. A mitotic cascade of NIMA family kinases. Nercc1/Nek9 activates the Nek6 and Nek7 kinases. *J Biol Chem*. 278:34897-909.

Bobinnec, Y., A. Khodjakov, L.M. Mir, C.L. Rieder, B. Edde, and M. Bornens. 1998. Centriole disassembly in vivo and its effect on centrosome structure and function in vertebrate cells. *J Cell Biol*. 143:1575-89.

Boleti, H., E. Karsenti, and I. Vernos. 1996. Xklp2, a novel Xenopus centrosomal kinesin-like protein required for centrosome separation during mitosis. *Cell*. 84:49-59.

Bornens, M. 2002. Centrosome composition and microtubule anchoring mechanisms. *Curr Opin Cell Biol*. 14:25-34.

Carazo-Salas, R.E., G. Guarguaglini, O.J. Gruss, A. Segref, E. Karsenti, and I.W. Mattaj. 1999. Generation of GTP-bound Ran by RCC1 is required for chromatin-induced mitotic spindle formation. *Nature*. 400:178-81.

Casenghi, M., P. Meraldi, U. Weinhart, P.I. Duncan, R. Korner, and E.A. Nigg. 2003. Polo-like kinase 1 regulates Nlp, a centrosome protein involved in microtubule nucleation. *Dev Cell*. 5:113-25.

Castoldi, M., and I. Vernos. 2006. Chromokinesin Xklp1 contributes to the regulation of microtubule density and organisation during spindle assembly. *Mol Biol Cell*. 17:1451-60.

Caudron, M., G. Bunt, P. Bastiaens, and E. Karsenti. 2005. Spatial coordination of spindle assembly by chromosome-mediated signaling gradients. *Science*. 309:1373-6.

Compton, D.A. 2000. Spindle assembly in animal cells. *Annu Rev Biochem*. 69:95-114.

Cha, B., L. Cassimeris, and D.L. Gard. 1999. XMAP230 is required for normal spindle assembly in vivo and in vitro. *J Cell Sci*. 112 (Pt 23):4337-46.

Chang, J., R.H. Baloh, and J. Milbrandt. 2009. The NIMA-family kinase Nek3 regulates microtubule acetylation in neurons. *J Cell Sci*. 122:2274-82.

Chen, Y., C.F. Chen, D.J. Riley, and P.L. Chen. 2011. Nek1 kinase functions in DNA damage response and checkpoint control through a pathway independent of ATM and ATR. *Cell Cycle*. 10:655-63.

Chretien, D., S.D. Fuller, and E. Karsenti. 1995. Structure of growing microtubule ends: two-dimensional sheets close into tubes at variable rates. *J Cell Biol*. 129:1311-28.

Dasso, M. 1993. RCC1 in the cell cycle: the regulator of chromosome condensation takes on new roles. *Trends Biochem Sci*. 18:96-101.

Dasso, M., H. Nishitani, S. Kornbluth, T. Nishimoto, and J.W. Newport. 1992. RCC1, a regulator of mitosis, is essential for DNA replication. *Mol Cell Biol*. 12:3337-45.

De Souza, C.P., A.H. Osmani, L.P. Wu, J.L. Spotts, and S.A. Osmani. 2000. Mitotic histone H3 phosphorylation by the NIMA kinase in Aspergillus nidulans. *Cell*. 102:293-302.

Delgehyr, N., J. Sillibourne, and M. Bornens. 2005. Microtubule nucleation and anchoring at the centrosome are independent processes linked by ninein function. *J Cell Sci*. 118:1565-75.

Desai, A., and T.J. Mitchison. 1997. Microtubule polymerization dynamics. *Annu Rev Cell Dev Biol*. 13:83-117.

Doles, J., and M.T. Hemann. 2010. Nek4 status differentially alters sensitivity to distinct microtubule poisons. *Cancer Res*. 70:1033-41.

Doree, M., and S. Galas. 1994. The cyclin-dependent protein kinases and the control of cell division. *FASEB J*. 8:1114-21.

Du, J., X. Cai, J. Yao, X. Ding, Q. Wu, S. Pei, K. Jiang, Y. Zhang, W. Wang, Y. Shi, Y. Lai, J. Shen, M. Teng, H. Huang, Q. Fei, E.S. Reddy, J. Zhu, C. Jin, and X. Yao. 2008. The mitotic checkpoint kinase NEK2A

regulates kinetochore microtubule attachment stability. *Oncogene*. 27:4107-14.

Dzhindzhev, N.S., Q.D. Yu, K. Weiskopf, G. Tzolovsky, I. Cunha-Ferreira, M. Riparbelli, A. Rodrigues-Martins, M. Bettencourt-Dias, G. Callaini, and D.M. Glover. 2010. Asterless is a scaffold for the onset of centriole assembly. *Nature*. 467:714-8.

Eliscovich, C., I. Peset, I. Vernos, and R. Mendez. 2008. Spindle-localised CPE-mediated translation controls meiotic chromosome segregation. *Nat Cell Biol*. 10:858-65.

Erickson, H.P. 2000. Gamma-tubulin nucleation: template or protofilament? *Nat Cell Biol*. 2:E93-6.

Erickson, H.P., and D. Stoffler. 1996. Protofilaments and rings, two conformations of the tubulin family conserved from bacterial FtsZ to alpha/beta and gamma tubulin. *J Cell Biol*. 135:5-8.

Faragher, A.J., and A.M. Fry. 2003. Nek2A kinase stimulates centrosome disjunction and is required for formation of bipolar mitotic spindles. *Mol Biol Cell*. 14:2876-89.

Feige, E., and B. Motro. 2002. The related murine kinases, Nek6 and Nek7, display distinct patterns of expression. *Mech Dev*. 110:219-23.

Fry, A.M., P. Meraldi, and E.A. Nigg. 1998. A centrosomal function for the human Nek2 protein kinase, a member of the NIMA family of cell cycle regulators. *EMBO J*. 17:470-81.

Gadde, S., and R. Heald. 2004. Mechanisms and molecules of the mitotic spindle. *Curr Biol*. 14:R797-805.

Gomez-Ferreria, M.A., and D.J. Sharp. 2008. Cep192 and the generation of the mitotic spindle. *Cell Cycle*. 7:1507-10.

Goshima, G., M. Mayer, N. Zhang, N. Stuurman, and R.D. Vale. 2008. Augmin: a protein complex required for centrosome-independent microtubule generation within the spindle. *J Cell Biol*. 181:421-9.

Goshima, G., and J.M. Scholey. 2010. Control of mitotic spindle length. *Annu Rev Cell Dev Biol*. 26:21-57.

Goto, H., Y. Tomono, K. Ajiro, H. Kosako, M. Fujita, M. Sakurai, K. Okawa, A. Iwamatsu, T. Okigaki, T. Takahashi, and M. Inagaki. 1999. Identification of a novel phosphorylation site on histone H3 coupled with mitotic chromosome condensation. *J Biol Chem*. 274:25543-9.

Gruss, O.J., M. Wittmann, H. Yokoyama, R. Pepperkok, T. Kufer, H. Sillje, E. Karsenti, I.W. Mattaj, and I. Vernos. 2002. Chromosome-

induced microtubule assembly mediated by TPX2 is required for spindle formation in HeLa cells. *Nat Cell Biol*. 4:871-9.

Hadjebi, O., E. Casas-Terradellas, F.R. Garcia-Gonzalo, and J.L. Rosa. 2008. The RCC1 superfamily: from genes, to function, to disease. *Biochim Biophys Acta*. 1783:1467-79.

Hannak, E., and R. Heald. 2006. Xorbit/CLASP links dynamic microtubules to chromosomes in the Xenopus meiotic spindle. *J Cell Biol*. 172:19-25.

Haren, L., M.H. Remy, I. Bazin, I. Callebaut, M. Wright, and A. Merdes. 2006. NEDD1-dependent recruitment of the gamma-tubulin ring complex to the centrosome is necessary for centriole duplication and spindle assembly. *J Cell Biol*. 172:505-15.

Heald, R., R. Tournebize, T. Blank, R. Sandaltzopoulos, P. Becker, A. Hyman, and E. Karsenti. 1996. Self-organisation of microtubules into bipolar spindles around artificial chromosomes in Xenopus egg extracts. *Nature*. 382:420-5.

Hutchins, J.R., Y. Toyoda, B. Hegemann, I. Poser, J.K. Heriche, M.M. Sykora, M. Augsburg, O. Hudecz, B.A. Buschhorn, J. Bulkescher, C. Conrad, D. Comartin, A. Schleiffer, M. Sarov, A. Pozniakovsky, M.M. Slabicki, S. Schloissnig, I. Steinmacher, M. Leuschner, A. Ssykor, S. Lawo, L. Pelletier, H. Stark, K. Nasmyth, J. Ellenberg, R. Durbin, F. Buchholz, K. Mechtler, A.A. Hyman, and J.M. Peters. 2010. Systematic analysis of human protein complexes identifies chromosome segregation proteins. *Science*. 328:593-9.

Janosi, I.M., D. Chretien, and H. Flyvbjerg. 2002. Structural microtubule cap: stability, catastrophe, rescue, and third state. *Biophys J*. 83:1317-30.

Kalab, P., A. Pralle, E.Y. Isacoff, R. Heald, and K. Weis. 2006. Analysis of a RanGTP-regulated gradient in mitotic somatic cells. *Nature*. 440:697-701.

Kalab, P., R.T. Pu, and M. Dasso. 1999. The ran GTPase regulates mitotic spindle assembly. *Curr Biol*. 9:481-4.

Kalab, P., K. Weis, and R. Heald. 2002. Visualization of a Ran-GTP gradient in interphase and mitotic Xenopus egg extracts. *Science*. 295:2452-6.

Kapitein, L.C., E.J. Peterman, B.H. Kwok, J.H. Kim, T.M. Kapoor, and C.F. Schmidt. 2005. The bipolar mitotic kinesin Eg5 moves on both microtubules that it crosslinks. *Nature*. 435:114-8.

Karsenti, E., J. Newport, and M. Kirschner. 1984. Respective roles of centrosomes and chromatin in the conversion of microtubule arrays from interphase to metaphase. *J Cell Biol*. 99:47s-54s.

Keating, T.J., and G.G. Borisy. 2000. Immunostructural evidence for the template mechanism of microtubule nucleation. *Nat Cell Biol*. 2:352-7.

Keating, T.J., J.G. Peloquin, V.I. Rodionov, D. Momcilovic, and G.G. Borisy. 1997. Microtubule release from the centrosome. *Proc Natl Acad Sci U S A*. 94:5078-83.

Khodjakov, A., R.W. Cole, B.R. Oakley, and C.L. Rieder. 2000. Centrosome-independent mitotic spindle formation in vertebrates. *Curr Biol*. 10:59-67.

Kim, S., K. Lee, and K. Rhee. 2007. NEK7 is a centrosomal kinase critical for microtubule nucleation. *Biochem Biophys Res Commun*. 360:56-62.

Kollman, J.M., J.K. Polka, A. Zelter, T.N. Davis, and D.A. Agard. 2010. Microtubule nucleating gamma-TuSC assembles structures with 13-fold microtubule-like symmetry. *Nature*. 466:879-82.

Krien, M.J., S.J. Bugg, M. Palatsides, G. Asouline, M. Morimyo, and M.J. O'Connell. 1998. A NIMA homologue promotes chromatin condensation in fission yeast. *J Cell Sci*. 111 (Pt 7):967-76.

Laemmli, U.K. 1970. Cleavage of structural proteins during the assembly of the head of bacteriophage T4. *Nature*. 227:680-5.

Laurell, E., K. Beck, K. Krupina, G. Theerthagiri, B. Bodenmiller, P. Horvath, R. Aebersold, W. Antonin, and U. Kutay. 2011. Phosphorylation of Nup98 by multiple kinases is crucial for NPC disassembly during mitotic entry. *Cell*. 144:539-50.

Le Bot, N., C. Antony, J. White, E. Karsenti, and I. Vernos. 1998. Role of xklp3, a subunit of the Xenopus kinesin II heterotrimeric complex, in membrane transport between the endoplasmic reticulum and the Golgi apparatus. *J Cell Biol*. 143:1559-73.

Loughlin, R., R. Heald, and F. Nedelec. 2010. A computational model predicts Xenopus meiotic spindle organisation. *J Cell Biol*. 191:1239-49.

Luders, J., U.K. Patel, and T. Stearns. 2006. GCP-WD is a gamma-tubulin targeting factor required for centrosomal and chromatin-mediated microtubule nucleation. *Nat Cell Biol*. 8:137-47.

Maiato, H., P. Sampaio, and C.E. Sunkel. 2004. Microtubule-associated proteins and their essential roles during mitosis. *Int Rev Cytol*. 241:53-153.

Manning, J., and S. Kumar. 2007. NEDD1: function in microtubule nucleation, spindle assembly and beyond. *Int J Biochem Cell Biol*. 39:7-11.

Mardin, B.R., C. Lange, J.E. Baxter, T. Hardy, S.R. Scholz, A.M. Fry, and E. Schiebel. 2010. Components of the Hippo pathway cooperate with Nek2 kinase to regulate centrosome disjunction. *Nat Cell Biol*. 12:1166-76.

Margolis, R.L., and L. Wilson. 1978. Opposite end assembly and disassembly of microtubules at steady state in vitro. *Cell*. 13:1-8.

Melixetian, M., D.K. Klein, C.S. Sorensen, and K. Helin. 2009. NEK11 regulates CDC25A degradation and the IR-induced G2/M checkpoint. *Nat Cell Biol*. 11:1247-53.

Miller, L., and J.C. Daniel. 1977. Comparison of in vivo and in vitro ribosomal RNA synthesis in nucleolar mutants of Xenopus laevis. *In Vitro*. 13:557-63.

Miller, S.L., G. Antico, P.N. Raghunath, J.E. Tomaszewski, and C.V. Clevenger. 2007. Nek3 kinase regulates prolactin-mediated cytoskeletal reorganisation and motility of breast cancer cells. *Oncogene*. 26:4668-78.

Mitchison, T., and M. Kirschner. 1984. Dynamic instability of microtubule growth. *Nature*. 312:237-42.

Moniz, L.S., and V. Stambolic. 2011. Nek10 mediates G2/M cell cycle arrest and MEK autoactivation in response to UV irradiation. *Mol Cell Biol*. 31:30-42.

Moritz, M., and D.A. Agard. 2001. Gamma-tubulin complexes and microtubule nucleation. *Curr Opin Struct Biol*. 11:174-81.

Moritz, M., M.B. Braunfeld, V. Guenebaut, J. Heuser, and D.A. Agard. 2000. Structure of the gamma-tubulin ring complex: a template for microtubule nucleation. *Nat Cell Biol*. 2:365-70.

Morris, N.R. 1975. Mitotic mutants of Aspergillus nidulans. *Genet Res*. 26:237-54.

Murray, A.W. 1991. Cell cycle extract. *In* Methods Cell Biol. Vol. 36. 581-605.

Murray, A.W., M.J. Solomon, and M.W. Kirschner. 1989. The role of cyclin synthesis and degradation in the control of maturation promoting factor activity. *Nature*. 339:280-6.

O'Connell, C.B., and A.L. Khodjakov. 2007. Cooperative mechanisms of mitotic spindle formation. *J Cell Sci*. 120:1717-22.

O'Connell, M.J., M.J. Krien, and T. Hunter. 2003. Never say never. The NIMA-related protein kinases in mitotic control. *Trends Cell Biol*. 13:221-8.

O'Connell, M.J., C. Norbury, and P. Nurse. 1994. Premature chromatin condensation upon accumulation of NIMA. *EMBO J*. 13:4926-37.

O'Regan, L., and A.M. Fry. 2009. The Nek6 and Nek7 protein kinases are required for robust mitotic spindle formation and cytokinesis. *Mol Cell Biol*. 29:3975-90.

Oakley, B.R., and N.R. Morris. 1983. A mutation in Aspergillus nidulans that blocks the transition from interphase to prophase. *J Cell Biol*. 96:1155-8.

Osmani, A.H., K. O'Donnell, R.T. Pu, and S.A. Osmani. 1991. Activation of the nimA protein kinase plays a unique role during mitosis that cannot be bypassed by absence of the bimE checkpoint. *EMBO J*. 10:2669-79.

Osmani, S.A., R.T. Pu, and N.R. Morris. 1988. Mitotic induction and maintenance by overexpression of a G2-specific gene that encodes a potential protein kinase. *Cell*. 53:237-44.

Otto, E.A., M.L. Trapp, U.T. Schultheiss, J. Helou, L.M. Quarmby, and F. Hildebrandt. 2008. NEK8 mutations affect ciliary and centrosomal localisation and may cause nephronophthisis. *J Am Soc Nephrol*. 19:587-92.

Paintrand, M., M. Moudjou, H. Delacroix, and M. Bornens. 1992. Centrosome organisation and centriole architecture: their sensitivity to divalent cations. *J Struct Biol*. 108:107-28.

Peset, I., J. Seiler, T. Sardon, L.A. Bejarano, S. Rybina, and I. Vernos. 2005. Function and regulation of Maskin, a TACC family protein, in microtubule growth during mitosis. *J Cell Biol*. 170:1057-66.

Piel, M., P. Meyer, A. Khodjakov, C.L. Rieder, and M. Bornens. 2000. The respective contributions of the mother and daughter centrioles to centrosome activity and behavior in vertebrate cells. *J Cell Biol*. 149:317-30.

Popov, A.V., F. Severin, and E. Karsenti. 2002. XMAP215 is required for the microtubule-nucleating activity of centrosomes. *Curr Biol*. 12:1326-30.

Radford, H.E., H.A. Meijer, and C.H. de Moor. 2008. Translational control by cytoplasmic polyadenylation in Xenopus oocytes. *Biochim Biophys Acta*. 1779:217-29.

Rapley, J., M. Nicolas, A. Groen, L. Regue, M.T. Bertran, C. Caelles, J. Avruch, and J. Roig. 2008. The NIMA-family kinase Nek6 phosphorylates the kinesin Eg5 at a novel site necessary for mitotic spindle formation. *J Cell Sci*. 121:3912-21.

Regue, L., S. Sdelci, M.T. Bertran, C. Caelles, D. Reverter, and J. Roig. 2011. DYNLL/LC8 controls signal transduction through the Nek9/Nek6 signaling module by regulating Nek6 binding to Nek9. *J Biol Chem*.

Richards, M.W., L. O'Regan, C. Mas-Droux, J.M. Blot, J. Cheung, S. Hoelder, A.M. Fry, and R. Bayliss. 2009. An autoinhibitory tyrosine motif in the cell-cycle-regulated Nek7 kinase is released through binding of Nek9. *Mol Cell*. 36:560-70.

Roig, J., A. Groen, J. Caldwell, and J. Avruch. 2005. Active Nercc1 protein kinase concentrates at centrosomes early in mitosis and is necessary for proper spindle assembly. *Mol Biol Cell*. 16:4827-40.

Roig, J., A. Mikhailov, C. Belham, and J. Avruch. 2002. Nercc1, a mammalian NIMA-family kinase, binds the Ran GTPase and regulates mitotic progression. *Genes Dev*. 16:1640-58.

Rusan, N.M., U.S. Tulu, C. Fagerstrom, and P. Wadsworth. 2002. Reorganisation of the microtubule array in prophase/prometaphase requires cytoplasmic dynein-dependent microtubule transport. *J Cell Biol*. 158:997-1003.

Sawin, K.E., and T.J. Mitchison. 1991. Mitotic spindle assembly by two different pathways in vitro. *J Cell Biol*. 112:925-40.

Shalom, O., N. Shalva, Y. Altschuler, and B. Motro. 2008. The mammalian Nek1 kinase is involved in primary cilium formation. *FEBS Lett*. 582:1465-70.

Smith, T.F. 2008. Diversity of WD-repeat proteins. *Subcell Biochem*. 48:20-30.

Smith, T.F., C. Gaitatzes, K. Saxena, and E.J. Neer. 1999. The WD repeat: a common architecture for diverse functions. *Trends Biochem Sci*. 24:181-5.

Sohara, E., Y. Luo, J. Zhang, D.K. Manning, D.R. Beier, and J. Zhou. 2008. Nek8 regulates the expression and localisation of polycystin-1 and polycystin-2. *J Am Soc Nephrol*. 19:469-76.

Sorensen, C.S., M. Melixetian, D.K. Klein, and K. Helin. 2010. NEK11: linking CHK1 and CDC25A in DNA damage checkpoint signaling. *Cell Cycle*. 9:450-5.

Stebbins-Boaz, B., Q. Cao, C.H. de Moor, R. Mendez, and J.D. Richter. 1999. Maskin is a CPEB-associated factor that transiently interacts with elF-4E. *Mol Cell*. 4:1017-27.

Stevens, T.J., and M. Paoli. 2008. RCC1-like repeat proteins: a pangenomic, structurally diverse new superfamily of beta-propeller domains. *Proteins*. 70:378-87.

Tanenbaum, M.E., and R.H. Medema. 2010. Mechanisms of centrosome separation and bipolar spindle assembly. *Dev Cell*. 19:797-806.

Teixido-Travesa, N., J. Villen, C. Lacasa, M.T. Bertran, M. Archinti, S.P. Gygi, C. Caelles, J. Roig, and J. Luders. 2010. The gammaTuRC revisited: a comparative analysis of interphase and mitotic

human gammaTuRC redefines the set of core components and identifies the novel subunit GCP8. *Mol Biol Cell*. 21:3963-72.

Theurkauf, W.E. 2001. TACCing down the spindle poles. *Nat Cell Biol*. 3:E159-61.

Tulu, U.S., C. Fagerstrom, N.P. Ferenz, and P. Wadsworth. 2006. Molecular requirements for kinetochore-associated microtubule formation in mammalian cells. *Curr Biol*. 16:536-41.

Walczak, C.E., and R. Heald. 2008. Mechanisms of mitotic spindle assembly and function. *Int Rev Cytol*. 265:111-58.

Walczak, C.E., T.J. Mitchison, and A. Desai. 1996. XKCM1: a Xenopus kinesin-related protein that regulates microtubule dynamics during mitotic spindle assembly. *Cell*. 84:37-47.

White, M.C., and L.M. Quarmby. 2008. The NIMA-family kinase, Nek1 affects the stability of centrosomes and ciliogenesis. *BMC Cell Biol*. 9:29.

Wiese, C., and Y. Zheng. 2000. A new function for the gamma-tubulin ring complex as a microtubule minus-end cap. *Nat Cell Biol*. 2:358-64.

Wollman, R., E.N. Cytrynbaum, J.T. Jones, T. Meyer, J.M. Scholey, and A. Mogilner. 2005. Efficient chromosome capture requires a bias in the 'search-and-capture' process during mitotic-spindle assembly. *Curr Biol*. 15:828-32.

Yin, M.J., L. Shao, D. Voehringer, T. Smeal, and B. Jallal. 2003. The serine/threonine kinase Nek6 is required for cell cycle progression through mitosis. *J Biol Chem*. 278:52454-60.

Yissachar, N., H. Salem, T. Tennenbaum, and B. Motro. 2006. Nek7 kinase is enriched at the centrosome, and is required for proper spindle assembly and mitotic progression. *FEBS Lett*. 580:6489-95.

Zhang, C., M. Hughes, and P.R. Clarke. 1999. Ran-GTP stabilises microtubule asters and inhibits nuclear assembly in Xenopus egg extracts. *J Cell Sci*. 112 (Pt 14):2453-61.

Zhang, X., Q. Chen, J. Feng, J. Hou, F. Yang, J. Liu, Q. Jiang, and C. Zhang. 2009. Sequential phosphorylation of Nedd1 by Cdk1 and Plk1 is required for targeting of the gammaTuRC to the centrosome. *J Cell Sci*. 122:2240-51.

Zheng, Y., M.L. Wong, B. Alberts, and T. Mitchison. 1995. Nucleation of microtubule assembly by a gamma-tubulin-containing ring complex. *Nature*. 378:578-83.

Zhu, F., S. Lawo, A. Bird, D. Pinchev, A. Ralph, C. Richter, T. Muller-Reichert, R. Kittler, A.A. Hyman, and L. Pelletier. 2008. The mammalian SPD-2 ortholog Cep192 regulates centrosome biogenesis. *Curr Biol*. 18:136-41.

Acknowledgements

.. aquí estoy, de repente parece que he terminado de escribir la tesis, juntado todos los resultados, discutido todo.. todo está escrito.. de repente miro atrás todos estos años..

Mucha gente me ha ayudado a lo largo de mi tiempo del doctorado y me apetece muchísimo de decir gracias aunque creo que palabras no serán suficientes de exprimir lo que siento ahora..

Isabelle, merci danke gracias thank you!! Who could have known that my interview with you at the end of February 2006 for a 1 year research assistant position would actually be my interview for a PhD position?! Isabelle, I'm deeply grateful for all the energy, time and effort that you have invested in me during the last five years. Thank you for your constant help, your presence whenever I wanted to talk to you, your constructive criticism and for making me feel the spirit of the (scientific) discoverer! Outside of science, thank you for your humanity and understanding at all times. There may not be many like you!

Joan, a big thank you also goes to you. It always has been a pleasure to meet with you and to discuss my results. Thank you for the motivation that you transmitted me throughout the years. Also you made me experience how interesting science can be!! Thanks a lot!

Los Vernosinhos… mi familia…

Rosy, Rosewood, Rose, Bunyols,.. cuantos apodos me he inventado para ti durante estos años?! Cuantos horas hemos estado en la esquina ahi sonriendo, riéndonos por cualquier tontería?! No sé exprimirlo en palabras como de importante eres para mi vida.. espero que puedes sentir mi

gratitud cada dia por todo lo que me ayudas, enseñas, haces reir,…! Gracias por tu energía, tu positivismo, tu sencillez, tu altruismo! Gracias por los chicles, pan duro, los clones, los kinase assays que hacemos juntos, los consejos.. gracias por contestarme a todos las preguntas.. gracias por estar!

"Crazy Corner" reloaded - David, Maria, Nuri, Marti... no cabe duda que mereceis de estar ahi :) !! David, ha sido un placer durante estos años de verte bailar, escucharte cantar, y vivir tu manera de expresar tu insatisfacción sobre la política belga o algunos resultados en el labo. Muchas gracias por todos estos momentos. David CAMPEON! Maria, gracias por todas las risas que nos echamos con Rosewood! A parte, desayunar contigo en la terraza de la quinta a las seis de la mañana junto al amanecer.. un momento inolvidable. Gracias por todo y animo!!

Nuri, mi database! Me encantas!! Gracias por tu felicidad, tu sonrisa de cada dia, tu apoyo no solo a mí pero a todo el labo! Eres un sol!! Marti, creo que los del Barça son todos zombies.. o como hacen entonces que ganan siempre??!! Gracias por compartir el análisis diario de Barça, Cep192, Madrid, Pep, incidencias en el tráfico en las autopistas alemanas, Mourinho, ImageJ, … gracias!!!

"Chaos Corner" – Teresa, Isa, Sylvain! Teresa, gracias por tu ayuda durante todos estos años. El "venga, vamos, animo" ha sido muy útil para mí! Isa, al final no estuve tu estudiante personal jaja! Pero poco importa.. mas importante, gracias a ti por todos los abrazos y Viva Poble Sec! Te echo de menos!! Sylvinho, gracias por tu disponibilidad en el labo, todos los consejos por cualquier duda, gracias por las cenas en tu casa, anualmente las plantas de verdura.. y esperemos que los sueños se cumplen!

“C…. Corner” – o ya tiene nombre?! Vanesinha y Adonis! Vanesinha, gracias por dejarme participar en tu vida, en los cambios que lleva el doctorado! Estoy orgulloso del resultado :)!! Adonis, el griego, me encantan tu respuestas directas!! Un dia lo conseguiré también!! A parte, gracias por las risas durante los cafés, tu ayuda en el labo y la informatica!

Por fin, Luis y Leo, gracias a vosotros dos por haber llevado orden en el labo. Y gracias también a “los nuevos”.. Jacopo, Tommaso y Violeta!! Estoy seguro que vais a tener un tiempo increíble aquí en el labo, un apoyo que va mas allá que solo colegas del trabajo!! Gracias Vernos Lab!!!!

Gaki und Josch, ihr könnt hier natürlich auf keinen Fall fehlen! Danke an euch für all die Verschwörungstheorien, politischen und auch wissenschaftliche Diskussionen. Mit euch lernt man nie aus! Danke für’s zuhören wenn auch anderer Rat gefragt ist! Ihr habt grossen Anteil an meinem Wohlbefinden!! Danke!!

Thanks also to my Thesis Committee Panel members Cristina, James and Manuel! You have been very helpful throughout these years! Thanks for all your questions and advice!

“Los Madrileños” – que bonito es la vida!!!

Gracias por acogerme un vuestra casa, gracias para enseñarme vuestro idioma (me falta, Manu!), gracias para integrarme en la vida española, gracias por integrarme en la vuestra!!! Bea, gracias por hacerlo posible! Marta, un gracias especial a ti.. gracias por todo el tiempo que pasamos juntos! Lo pienso muchas veces! Santi se va, Santi se viene ;) gracias por todo!! Estoy contento de haber ocupado vuestro piso y de haberos conocido! Manu y Mel, para mi sois inseparables! Me habeis cambiado la

vida! Gracias por enseñarme tantos canciones y de reíros de mi! Nunca podré!! Fernan, anda, pronto nos vamos de viaje otra vez! Gracias por las horas que pasamos juntos!! Un gracias enorme a Bego, Pipi, Alfred, Gerard, Juanjo, Bebi, Joaquin, Alfonso, Numa, Taty Vicen y Barbara (espero de no haber olvidado nadie) por todas las fiestas en las playas, parques, noches de baile en el BeGood!! Muchas muchas gracias!!!

"Casa Bobila" – una soap opera

Gracias a todos los compañeros de piso que tengo/tenia! Baldu, son casi 4 años que vivimos juntos! Gracias por ser un pilar, un constante, un respalde en mi vida aqui, más que nada durante los últimos meses! Gracias por tu energía positiva, tus opiniones fuertes, las discusiones, los vinos,.. gracias por cuidarme!! Fra, y Rao, porque os habeis ido?! Os echo de menos! Gracias a vosotros por vuestro espíritu que me transmite una tranquilidad enorme! Chiara, gracias también a ti por todo! Me has influenciado mucho, me has dejado sentir vivo! Gracias por todos los sentimientos que viví! Mil gracias! Virginie, Pau, Hui, Mete, Leon, Valentin, Fede, Irene, Stefano, José.. gracias por todas las cenas y demás! Merci!!

"Zeitlhof" – meine Ferien

Jungs, a wenn'ds es ned wirklich an direkten Einfluss af mei Oabad habt's, ihr habt's mi imma wieda zum lacha brocht, und gebt's ma des Gfui vo heimat! I woass dass i eich imma oruafa konn und i werd's ma heiffa und des gibt ma unglaublich vui sicherheit! I dank eich wirklich vo herzem!! Merci Paze, Jost, Knotti, Uli, Mora, Fes und Hiwi! Danke danke danke!!

Muchas gracias a todos los Face Pelotazos (Ignasi, Ali, Sonia, Ari, Sergi, Andrea, Kriszti, Esteban,..); estos partidos con vosotros me han dado un monton de energía!! Gracias también a los futbolistas de los viernes y los Darwins (James, Holger, Hagen, Jesus, Phil, Antoine, Thomas, Ema, Luciano,….); ha sido un placer de jugar con y contra vosotros!!

Gracias a la gente de la seguridad del PRBB.. no me sentí solo nunca en horas avanzadas! Merci a las mujeres de la frutería bajo de mi casa por su fruta y verdura súper buena, fresca y por su amabilidad! Merci a la Cañada por quintos frescos! Gracias al restaurante Montalban para el pulpo y las navajas como no lo he encontrado en ningún otro sitio más! Gracias a Fede y Lorenzo, Cedrik, Paka, Paco y Alvaro para todas las cenas y hacerme reír siempre cuando nos veamos!!

Tiki tiki, merci por ser un ejemplo de realizar las ideas que uno tiene!! Eres un ejemplo por la vida en general!! Gracias!!

Mein grösstes Dankeschön geht an Euch:

Mama, Papa, Christian, Reinhard und Roland!

Auch nach sechs Jahren im Ausland,

Ihr seid mein Grundfest, meine Pfeiler, die mich stützen,

Danke an Euch für die Vergangenheit und für die Zukunft!

Dank Euch fühle ich dass ich alles erreichen kann!